

I-MISSED: INTERDISCIPLINARY MISSION FOR IMAGING SATELLITES AND SPACE DEBRIS

ASHLEY BARNES, JORDAN BROWN, ADELLE INGRID DIMITUI,
HENRY HA, TERESA IRIGOYEN-LOPEZ, BARTEK KACZMARSKI,
WILLIAM KITTLER, CURTIS MERRILL, JOSEPH PURYEAR III,
VIVEQUE RAMJI, COLIN REILLY, JUAN SEPULVEDA VARON,
OMKAR SHENDE, JEREMY SPIEZIO, SOUMYA SUDHAKAR, AND
DAVID WU

FINAL REPORT

MAY 9, 2018



MAE 342
175 PAGES

© Copyright by Ashley Barnes, Jordan Brown, Adelle Ingrid Dimitui, Henry Ha,
Teresa Irigoyen-Lopez, Bartek Kaczmarski, William Kittler, Curtis Merrill, Joseph
Puryear III, Viveque Ramji, Colin Reilly, Juan Sepulveda Varon, Omkar Shende,
Jeremy Spiezio, Soumya Sudhakar, and David Wu; 2018.

All Rights Reserved

This report represents our own work in accordance with University regulations.

Mission Concept

Name	I-MISSED
Sponsor	NOAA/NASA
Orbit	GEO (35786×35786) km
Subject	GOES-T
Primary Mission	Space surveillance of GOES satellite to provide on-station physical information
Secondary Mission	Tracking of ephemerides of debris crossing imager FOV while trained on subject
Equipment	Casegrain telescope with a visual CMOS imager
Configuration	CubeSat (6U)
Propulsion	EP for large ΔV maneuvers and ACDS, reaction wheels
Power	4 deployable solar arrays, batteries
Lifetime	10 years
Mass	20 kg
Launch vehicle and delivery	ESPA ring on board Atlas V launch of STP-3
Timeline	GOES-T and STP-3 will be launched in 2019
Data delivery	Image data will be compressed and sent to a ground station. TT&C will be relayed via direct ground link.

Executive Summary

The primary goal of I-MISSED is the design of a 6U sized cubesat that can be launched into GEO for the imaging of a subject satellite, GOES-T, on schedule to launch in 2020. This follower cubesat can perform on-station, on-demand visual imaging of the multi-billion dollar subject satellite, providing operating information on mechanism deployments and damage assessments after potential collision events. A secondary objective will be performing basic space debris analysis that can provide feedback on potential impacts.

I-MISSED will be in an elliptic, nominally geosynchronous orbit that fully orbits the leader satellite. This orbit will be attained after a phasing transfer from a GEO injection from a NASA rideshare. The mission will seek to transmit image data down to Earth directly via a high-gain UHF/VHF link and will allow for three-dimensional reconstruction of the leader satellite on the ground, while telemetry relayed down to Earth can provide on-demand scheduling, mission planning, and assist with digital twinning of assets.

Should the Cubesat operate successfully with the GOES-T satellite, the same system would be easily adapted for commercial customers, namely communications companies such as SiriusXM or DirecTV, who launch large satellites worth between \$25 and \$170 million in revenue per year. Other customers could include DoD or NASA payloads heading to Earth-Sun Lagrange points, such as the James Webb Space Telescope. Extending operational lifetimes of these satellites by even one year would provide immense value to stakeholders, demonstrating an existing market for the I-MISSED mission.

Contents

Mission Concept	iii
Executive Summary	iv
List of Tables	viii
List of Figures	ix
List of Symbols and Acronyms	xiii
1 Project Details	1
1.1 Mission	1
1.2 Project Management	2
1.2.1 Organization	3
1.2.2 Work Breakdown Structure	4
1.2.3 Gantt Chart and Schedule	8
1.3 Technical Requirements	9
2 Trajectory and Environment	12
2.1 Space Environment	12
2.1.1 Radiation	12
2.1.2 Debris	14
2.1.3 Space Charge	16
2.1.4 Communication	17
2.2 Launch Vehicle and Loads	19
2.2.1 Analysis of Launching with GOES-T	19
2.2.2 NASA Rideshare	21
2.2.3 Launch Load Data	22
2.3 Longitude Shifting Procedure	24
2.3.1 Overview and Motivation of the Maneuver	24
2.3.2 STK Analysis	24
2.4 Regulations	31
2.4.1 Component Regulations	31

2.4.2	Communications Frequency Regulations	31
2.4.3	Mechanical Regulations	31
2.4.4	Required Testing Before Launch	32
2.4.5	Waivers	33
2.4.6	Requirements for End of Life	33
3	Guidance, Navigation, and Control	34
3.1	Orbital Elements for I-MISSED	34
3.2	Perturbations and Disturbances	35
3.3	Orbit Maintenance	39
3.4	Scheduling	39
3.5	Attitude Determination and Control System	40
3.6	Thruster Selection	44
3.7	GPS Orbit Determination	45
3.7.1	Using GPS in MEO for Orbit Determination in GEO	46
3.7.2	Using Payload Imager	47
3.8	Detumbling	48
3.9	Control Simulation	49
4	Payload	54
4.1	Imager	54
4.1.1	Imager Selection	54
4.1.2	STARE Imager	56
4.2	Telecommunications, including telemetry and Control	57
4.2.1	Antenna Selection	57
4.2.2	Ground Stations	58
4.2.3	Link Budgets	59
4.2.4	Transceiver Frequencies	60
4.3	Data	63
4.3.1	Data Handling	63
4.3.2	Size of Data	64
4.3.3	Scheduling for Data	65
5	Power and Thermal Control	67
5.1	Power Loadings	67
5.2	Power Storage	69
5.2.1	Secondary Battery	69

5.2.2	Primary Battery	71
5.3	Power Generation	72
5.3.1	Sizing the Solar Array	72
5.3.2	Off-the-Shelf Solar Array	73
5.4	Power Regulation and Distribution	74
5.4.1	Charging	75
5.4.2	Regulation and Distribution	75
5.5	Thermal Loadings	78
5.5.1	Steady State Thermal Analysis	78
5.5.2	Transient Thermal Analysis	80
5.6	Thermal Control	80
5.6.1	Temperature Range	81
5.6.2	Spacecraft Thermal Control	82
5.6.3	Thruster Thermal Control	83
5.6.4	Solar Array Thermal Control	85
6	Structure	87
6.1	Mass Breakdown	88
6.2	Deployment Interface and Constraints	88
6.3	Configurations and Analysis	89
6.4	Structural Validation	97
6.5	Failure Tree Analysis	100
7	Conclusions	106
7.1	Potential Improvements	106
7.2	Evaluating Success	108
Bibliography		109
A	Code	114
B	Simulation Results	132
B.1	Frequency Analysis	132
B.2	Stress Analysis	142

List of Tables

2.1	Total Thickness Equivalence	15
3.1	Actuator Information	41
4.1	Cypress IBIS5-B-1300 Imager	56
5.1	Power Budget	68
5.2	Secondary Battery Trade Study	69
5.3	Sunlight, Penumbra, and Umbra Times	69
5.4	Electrical Component Voltages	77
5.5	Operating Temperatures of Electrical Components	82
6.1	Total mass breakdown of all satellite components and their average densities	88
6.2	Probability of Failure of Components	102

List of Figures

1.1	Organization Chart for I-MISSED	3
1.2	Gantt Chart	8
2.1	SPENVIS ionizing dose model for radiation against aluminum thickness.	13
2.2	Measured radiation in geosynchronous orbit.	14
2.3	Each graph depicts variance of radiation with aluminum ratio.	15
2.4	SPENVIS model for debris density with altitude.	16
2.5	SPENVIS model for debris flux at GEO.	17
2.6	Electron density for low altitudes. The maximum at 300 km limits communication frequencies.	18
2.13	STK Snapshots of the most representative moments during the longitude shifting procedure	27
2.14	STK Snapshot of the GOES-T rendezvous on September 1st, 2020, 16:00:00 UTC	28
3.1	IGRF Field Model in 2020	37
3.2	Simulation of Single Orbit in STK	38
3.3	List of Reaction Wheels	42
3.4	Thruster Trade Study	45
3.5	Method of Orbit Determination Using GPS for GEO	46
3.6	Access to GPS satellites in MEO in one orbit of I-MISSED in GEO .	47
3.7	Orbit determination using imager	48
3.8	Change in Rotation Rate for the First 40 Seconds	49
3.9	Initial Condition Response	51
3.10	Control Effort for Initial Condition Response	52
3.11	Response to Step Input	53
4.1	Imager Trade Study	55
4.2	STARE Cassegrain Telescope	57

4.3	Ground Stations	58
4.4	I-MISSED’s UHF Downlink Link Budget	59
4.5	I-MISSED’s VHF Uplink Link Budget	60
4.6	Friis Transmission Equation	60
4.7	Signal to Noise Ratio Equation	60
4.8	VHF Downlink Link Budget	61
4.9	Northrop Grumman High Gain, Deployable, UHF, Helical Antenna .	62
4.10	Directive Gain of I-MISSED’s Antenna	62
4.11	Directivity and Gain of I-MISSED’s Antenna	63
4.12	ISIS UHF Full Duplex Transceiver	63
4.13	I-MISSED Ground Track and Kauai Community College Ground Station	64
4.14	Ground Station Access during Longitude Shift	66
5.1	Cycle Life of GOMspace BPX	70
5.2	eHawk Deployment Sequence	74
5.3	NanoPower P60 Dock	75
5.4	NanoPower P60 ACU-200	76
5.5	NanoPower P60 PDU-200	76
5.6	Power Bus Schematic	77
5.7	Minimum and Maximum Solar Flux Orbital Trajectories	78
5.8	Transient Thermal Analysis During Eclipse	81
5.9	Louver Mechanism	84
6.1	Attachment between the ESPA ring and the orbital deployment mechanism	89
6.2	Payload mass and dimensional requirements of the orbital deployment mechanism	90
6.3	The XYZ coordinate system used to verify the COM of the stowed configuration.	90
6.4	Dimensions of I-MISSED in its stowed configuration	91
6.5	Layout of the components in I-MISSED	92
6.6	I-MISSED in its stowed and deployed configurations	93
6.7	Stowed COM and Moments of Inertia	94
6.8	COM and Moments of Inertia	95
6.9	Rotated COM and Moments of Inertia	96
6.10	The XYZ coordinate systems used to calculate the COM of the deployed configurations.	97

6.11	Acoustic Levels for Atlas V	98
6.12	Vibration Levels for Atlas V	98
6.13	Modal Frequency Analysis Results	99
6.14	Atlas V Limit Load Factors	100
6.15	Axial Static Stress Analysis Results	101
6.16	Axial Displacement Graphic Results	102
6.17	Major Axis Lateral Displacement Graphic Results	103
6.18	Minor Axis Lateral Displacement Graphic Results	103
6.19	FTA Model	103
6.20	FTA Component Contributions	104
6.21	FTA Results	104
6.22	FTA Unreliability	105

List of Symbols and Acronyms

GEO	Geostationary Orbit	1
NASA	National Aeronautics and Space Administration	2
NOAA	National Oceanic and Atmospheric Administration	2
GOES	Geostationary Operational Environmental Satellite	2
TRL	Technology Readiness Level	2
COTS	Commercial, Off The Shelf	2
ΔV	Velocity increment	5
ESPA	EELV Secondary Payload Adapter	11
EELV	Evolved Expendable Launch Vehicle	11
A	Effective area	15
T	Time in orbit	15
F	Weighted cross-sectional area flux	15
P_c	Probability of collision	15
ϵ_0	Permittivity of free space	16
k_B	Boltzmann constant	16
T_e	Electron temperature	16
n_e	Electron density	16
e	Electron Charge	16
n_e	Electron Density	17
e	Electron Charge	17
ϵ_0	Permittivity of free space	17
m_e	Mass of Electron	17
GTO	Geosynchronous Transfer Orbit	20
STP	The Space Test Program	21
ESPA	Expendable Launch Vehicle Secondary Payload Adapter	21
STK	Systems Tool Kit	24
UTC	Coordinated Universal Time	25
GNC	Guidance, Navigation, and Control	34

IGRF	International Geomagnetic Reference Field	37
ADCS	Attitude Determination and Control System	40
FEEP	Field Emission Electric Propulsion	44
GPS	Global Positioning System	45
MEO	Middle Earth Orbit	46
STARE	Space-based Telescopes for the Actionable Refinement of Ephemeris	56
CSD	Canisterized Satellite Dispenser	88
COM	Center of Mass	89
BECO	Booster Engine Cutoff	99

Chapter 1

Project Details

In this chapter, an overview of the intended mission will be given, project management details pertinent to the development of this white paper will be provided, and the high level technical requirements of the mission will be enumerated.

1.1 Mission

The mission designed by the Red Team is named I-MISSED, the Interdisciplinary Mission for Imaging Satellites and SpacE Debris. The primary goal of I-MISSED is the design of a 6U sized cubesat that can be launched into geostationary orbit for the imaging of a subject satellite, GOES-T, on schedule to launch in 2020. This follower cubesat can perform on-station, on-demand visual imaging of the multi-billion dollar subject satellite, providing operating information on mechanism deployments and damage assessments after potential collision events. A secondary objective will be performing basic space debris analysis that can provide feedback on potential impacts. The mission is designed to last for around 10 years, the approximate design lifetime of many satellites currently in geostationary orbit.

To achieve this primary mission, there are a few overarching goals for I-MISSED:

- Design a cubesat that can operate in GEO through end-of-life
- Design a cubesat can inform mission operations for a larger subject satellite
- Design a cubesat can help with debris tracking in GEO
- Design a cubesat for GEO with a life-cycle on par with a larger subject satellite

One may question why such a mission needs to exist; the answer lies in the enormous costs of going to space. The James Webb Space Telescope, for example, is a multi-billion dollar NASA project that has been in development for decades. Complex missions such as James Webb are large investments, and many of their failure and contingency modes rely on accurate understandings of what components are functional. A follower cubesat can be injected onto trajectories with such large satellites, and provide mission-critical information.

For the GOES platform, each satellite costs around \$25 billion through its lifetime, and sometimes errors happen, such as in 2013, when a meteorite struck a GOES satellite and put it out of commission for three weeks [1]. A follower cubesat could have helped diagnose the issue earlier and improved outcomes for stakeholders, such as the taxpayers under NOAA’s forecast zone. The I-MISSED cubesat is expected to cost around \$250,000, orders of magnitude lower than the total mission cost of a GEO satellite.

To maximize the return on investment, there are three guiding principles of this program:

- Commercial, Off the Shelf (COTS)
- Durability
- Extensibility

Using a cubesat as a surveillance platform provides inherent benefits, including a wealth of existing knowledge and freedom to use COTS hardware with existing high technology readiness levels (TRL). Designing a system that can last for 10 years justifies its higher costs compared to smaller 3U missions, and the ability to work in GEO allows it to be applied to a wide range of commercial and government launches.

1.2 Project Management

In preparation for weekly presentations, coordination sessions were held prior to presentations to course staff, and all-hand debriefs were held immediately following. In addition, all-hands progress meetings were held between weekly presentations to update status.

1.2.1 Organization

In addition to the project manager and chief engineer, there were five sub-teams, each focused on a specific aspect of I-MISSED.

The Trajectory Subteam was focused on detailed accounting of space environmental effects, orbit and launch design, and the regulations required to operate in GEO. The GNC Subteam was focused on designing the actuators, sensors, and manual/automatic control required to fulfill the prime mission, which the Payload Subteam focused on accomplishing through design of an imaging and data transmission system to examine the target satellite. The PTC Subteam provided the power and thermal control needed to maintain component viability, while the Structures Subteam validated system reliability and created computer models to test system response to loads and stresses, and ensured its integrity.

Figure 1.1 shows overall team structure.

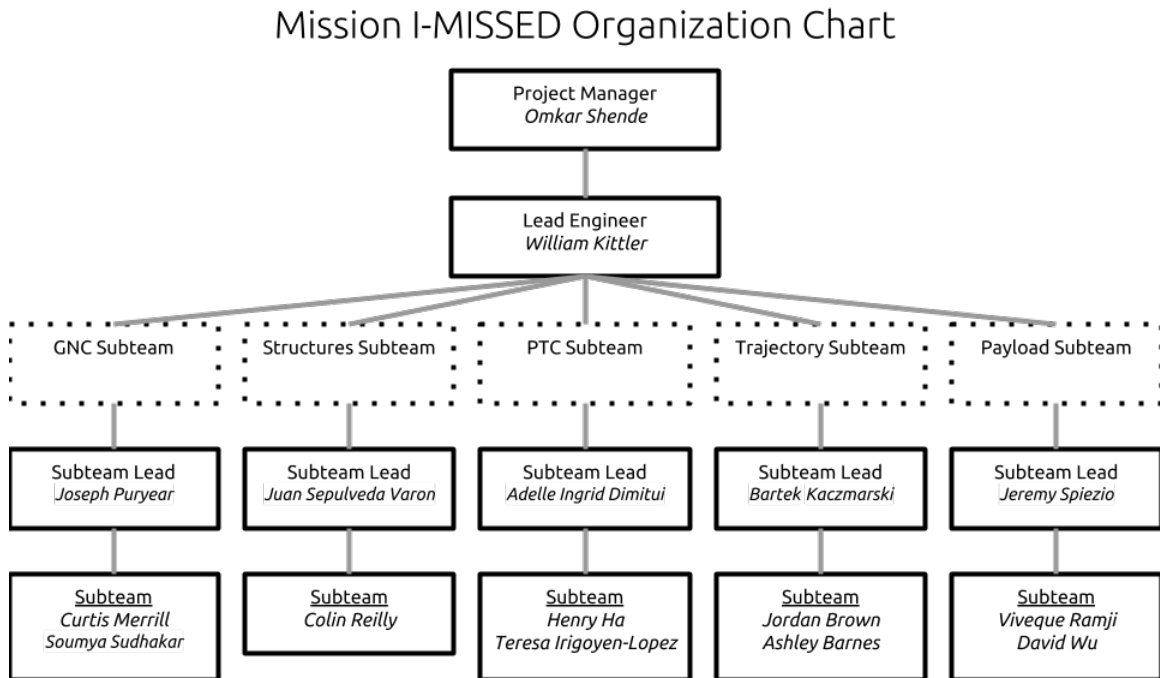


Figure 1.1: The organization chart for I-MISSED

1.2.2 Work Breakdown Structure

The work breakdown structure for the project follows, as broken down by sub-team.

1. Project Administration
 - 1.1. Ensure weekly progress goals are met and weekly deliverables are created
 - 1.2. Prepare CDR presentation
 - 1.3. Prepare final deliverables
2. Trajectory Sub-team
 - 2.1. Space Environment
 - 2.1.1. Determine radiation levels in GEO
 - 2.1.2. Calculation of electronic effects on structure and communications
 - 2.1.3. Accounting for space debris
 - 2.1.4. Determine the shielding needed on the spacecraft
 - 2.2. Launch Analysis
 - 2.2.1. Select launch vehicle for rideshare
 - 2.2.2. Determine launch loads
 - 2.2.3. Determine rideshare canister
 - 2.2.4. Create master STK file for analysis
 - 2.2.5. Determine ΔV for phase shift following GEO orbit injection
 - 2.3. STK Analysis
 - 2.3.1. Run an analysis on Sunlight and Eclipse times
 - 2.3.2. Determine antenna access time based on antenna data from Payload
 - 2.4. Regulatory Compliance
 - 2.4.1. Define cubesat general requirements
 - 2.4.2. Determine constraints on satellites based on GEO orbit research
 - 2.4.3. Research regulations on communication frequencies
3. Guidance, Navigation, and Control Sub-team
 - 3.1. Guidance
 - 3.1.1. Determine magnitude of perturbations and disturbance torques in GEO

- 3.1.2. Determine passive control actuators and modes
- 3.1.3. Select reaction processing unit
- 3.1.4. Select stationkeeping control system
- 3.1.5. Schedule attitude maneuvers to meet imaging requirements

3.2. Navigation

- 3.2.1. Determine required navigation precision
- 3.2.2. Determine scheduling for maneuvers and data transfer
- 3.2.3. Select attitude sensor systems
- 3.2.4. Select inertial measurement sensor system
- 3.2.5. Select avionics package
- 3.2.6. Determine formation flying orbital parameters

3.3. Propulsion Requirements

- 3.3.1. Determine ΔV requirements for stationkeeping
- 3.3.2. Determine ΔV for pointing of imager and antenna
- 3.3.3. Determine propulsion system for required ΔV budget
 - 3.3.3.1. Conduct a trade study

3.4. Control

- 3.4.1. Determine required control precision and slew rates
 - 3.4.1.1. Retrieve data from Payload Team about imaging resolution and ground pointing requirements
- 3.4.2. Select attitude control system actuators
- 3.4.3. Design Bdot control laws

4. Payload Sub-team

4.1. Scientific Payload

- 4.1.1. Imager selection
 - 4.1.1.1. Perform trade study on optical imager
 - 4.1.2. Determine imager angular resolution and field of view
 - 4.1.3. Determine processing hardware requirements

4.2. Communications

- 4.2.1. Research communication options

- 4.2.1.1. Determine range of usable frequencies from Trajectory Sub-team
- 4.2.1.2. Determine acceptable signal-to-noise ratio
- 4.2.2. Determine Ground Station locations / requirements
 - 4.2.2.1. Research ground stations near desired position over Earth
 - 4.2.2.2. Perform trade study for best transceiver
 - 4.2.2.3. Select data encoding scheme based on ground station
- 4.2.3. Determine onboard communication equipment
 - 4.2.3.1. Start link budget
 - 4.2.3.2. Perform antenna trade-study
 - 4.2.3.3. Finalize specifications of telecommunication equipment
 - 4.2.3.4. Finalize link budget

4.3. Integration

- 4.3.1. Create observation and communication schedule
- 4.3.2. Select data processing computer
- 4.3.3. Compile full mass, power and thermal requirements

5. Power and Thermal Control

5.1. Identify requirements

- 5.1.1. Research power usage of selected spacecraft and payload
- 5.1.2. Quantify average/peak electrical power demand

5.2. Power source selection

- 5.2.1. Research power source options based on power needs
- 5.2.2. Select power source

5.3. Power supply/distribution design

- 5.3.1. Size power source to provide sufficient electrical supply
- 5.3.2. Select primary/secondary power storage methods
- 5.3.3. Select power distribution architecture
- 5.3.4. Design power bus

5.4. Thermal control

- 5.4.1. Compile operating temperature ranges for components
- 5.4.2. Estimate incident/internal heat fluxes through steady-state analysis

5.4.3. Select methods of passive thermal control

5.4.4. Perform transient thermal analysis

6. Structures

6.1. Gather component specifications

6.1.1. Gather dimensions, weight, and material properties of each component

6.1.2. Gather all available computer-aided-design (CAD) files for the components

6.1.3. Define mass and volume allocations for components

6.2. Identify orbital deployment mechanism

6.2.1. Identify orbital deployment mechanism for the cubesat

6.2.2. Identify attachment points between the structure and orbital deployment mechanism

6.2.3. Identify design constraints associated with the orbital deployment mechanism

6.3. Model PTC components

6.3.1. Determine position and orientation of solar panels and deployment mechanism

6.3.2. Determine locations of thermal sinks/sources

6.4. System integration and reliability analysis

6.4.1. Compile all components into a CAD file

6.4.2. Determine the model mass, center-of-mass, and moments of inertia

6.4.3. Iterate over component placements until volume and center-of-mass requirements are met

6.4.4. Create a fault tree and analyze reliability

6.5. Run FEA simulations and validate structural limits

6.5.1. Run modal frequency simulation

6.5.2. Run forces/moments simulation

6.5.3. Generate component renders

6.5.4. Build scale models for demonstration

1.2.3 Gantt Chart and Schedule

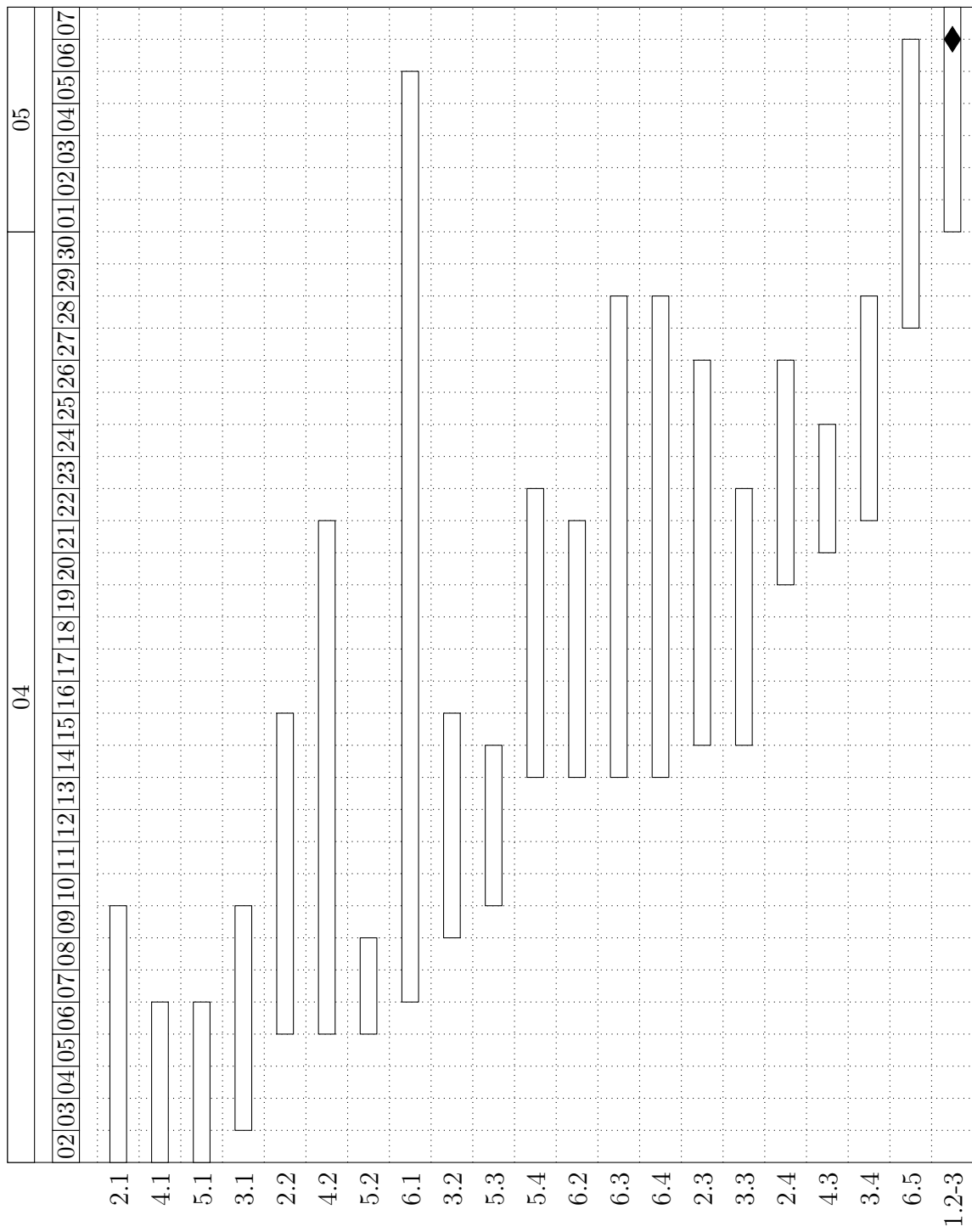


Figure 1.2: I-MISSED Gantt Chart to CDR with tasks corresponding to §1.2.2

Figure 1.2 is the Gantt chart for this project. It shows the schedule for the project, using the task listings given in the previous subsection as short codes.

1.3 Technical Requirements

To conclude this chapter, the high-level technical requirements that were generated throughout mission planning for I-MISSED are collated below.

1. Performance
 - 1.1. Primary objective is imaging the GOES-T satellite for maintenance
 - 1.2. Secondary objective is imaging space debris in the field of view
 - 1.3. Payload must fit in 6U spacecraft bus
 - 1.4. Pointing accuracy must be +/- 0.72 degrees
 - 1.5. Typical maximum power required of 6U CubeSat is 40 W
2. Coverage
 - 2.1. Orbital eccentricity is 0.00017
 - 2.2. Semimajor axis of nominally GEO orbit is 42,164 km
 - 2.3. Range of approach to GOES-T is between 7.17 and 14.8 km
 - 2.4. Data transmission occurs during less than 10% of orbit period
 - 2.5. Imaging should occur for at least 75% of orbit period
3. Responsiveness
 - 3.1. Communications architecture should support conventional cubesat standards and be up to NASA/NOAA standards
 - 3.2. Ground stations during phase shift of the orbit should be part of the Near Earth Network
 - 3.3. Ground stations need to be in UHF/VHF
4. Duration
 - 4.1. Design life of 10 years
5. Survivability

- 5.1. Expected debris density of 1e-10 objects/ km^3
- 5.2. Electronics should be appropriately shielded against radiation effects, assuming a solar maximum
- 5.3. Shielding should reduce radiation to around 10e-3 rads
- 5.4. Temperature must be regulated between 0-25 degrees C
6. Data Distribution, Content, and Format
 - 6.1. Data must be sent directly to Earth as essentially raw image files that will be transmitted to Earth for post-processing
 - 6.2. Must match PCM and encoding of ground stations
 - 6.3. Link margin in either direction of 1+ dB
 - 6.4. Downlink in UHF and uplink in VHF
7. Cost
 - 7.1. Cost is not a constraint or mission driver for the purposes of this project
8. Schedule
 - 8.1. As we are using a cubesat bus and using almost exclusively COTS components, there will be fairly high technical readiness levels for all components
 - 8.2. Rideshare with STP-3 Mission to GEO has best opportunity in 2019
 - 8.3. Launching on Atlas V 551
 - 8.4. Mission must be able to perform orbital transfer from injection orbit to target orbit
9. Regulations
 - 9.1. Satellite must be able to deorbit at end of life
 - 9.2. Ensurance of cessation of radio emissions
 - 9.3. Must maintain 0.05 degrees of assigned E/W longitude
 - 9.4. Satellite must comply with orbital deployment mechanism constraints
 - 9.5. Must follow general cubesat requirements or have a waiver
10. Political Considerations

10.1. Should allow the mission to work with other NASA missions

11. Launch Environment

11.1. The cubesat must withstand 3 minutes of Random Noise and Sinusoidal vibrations of MPE + 6dB in all three axes

11.2. The cubesat must withstand three 6dB shocks in all three axes

11.3. The dispenser must withstand thermal vacuum cycling from MPE² +/- 10 degrees C

11.4. Maximum acceleration of 6 g during launch

11.5. Maximum shock of 1000 - 4500 g, depending on payload adapter

11.6. Vibration frequencies between 0 - 100 Hz

11.7. Max temperature in payload fairing 88 degrees C

12. Interfacing

12.1. System must be primarily autonomous

12.2. Override instructions must be able to be given so that the cubesat can respond to unforeseen circumstances

12.3. The ESPA ring that our cubesat will be cantilevered from during launch requires dimensional and mass requirements on the cubesat-dispenser system

12.4. The total mass of the cubesat and its dispenser must be less than 180 kg to be carried by ESPA

12.5. The dimensions of the cubesat and its dispenser must be less than 24" x 28" x 38"

13. Developmental Constraints

13.1. Must work with existing NASA space infrastructure

Chapter 2

Trajectory and Environment

The Trajectory sub-team will deal with selection of proper shielding to survive and mitigate radiation effects in orbit, after calculating for and selecting the necessary launch vehicle to launch the constellation. This includes analyzing any maneuvers required to get the spacecraft to its final orbit. It will also ensure that the designed mission is in accordance with regulations for GEO satellites, including end-of-life decommissioning. Lastly, the Trajectory sub-team completed various STK analyses related to the longitude shift period of the launch of the I-Missed, such as antenna access and sunlight and eclipse timings during the longitude shift maneuver.

2.1 Space Environment

2.1.1 Radiation

The 10 year GEO mission will subject the spacecraft to multiple sources of radiation. This radiation has the potential to damage non-hardened electronic devices. To determine the amount of protective shielding required, the Space Environment Information System (SPENVIS) was utilized. The half period to reach GEO amounts to roughly 5.25 hours, which is entirely negligible compared to the 10 year mission lifespan. The following studies detail the effect of radiation while in GEO.

The AP-8 and AE-8 models were used to determine the threshold flux exposure for a period of 10 years. For the same duration, the NASA ESP-PSYCHIC model calculated the effect of solar protons, while the ISO-15390 model calculated the radiation from galactic cosmic rays. The results of each of these models were combined for the

ionizing dose models, depicted in figure 2.1. This models determined the radiation dose in the center of an aluminum sphere of variable wall thicknesses.

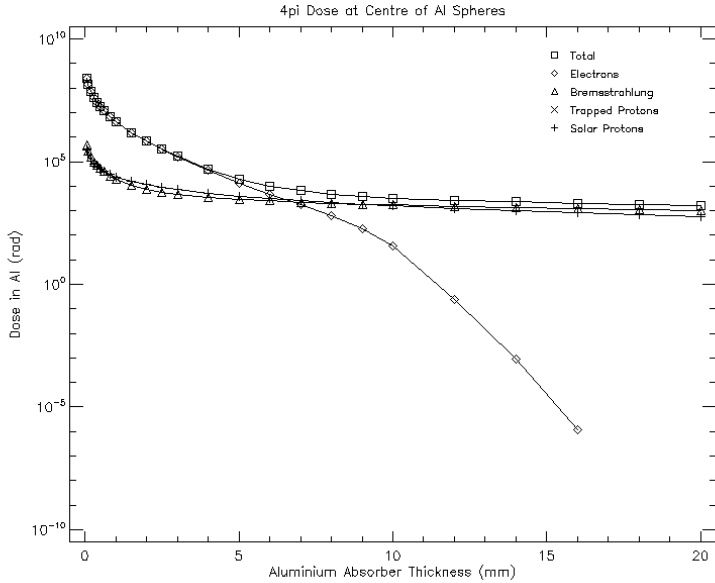


Figure 2.1: SPENVIS ionizing dose model for radiation against aluminum thickness.

The threshold radiation dose for most electronic hardware is between 10^3 and 10^4 rad. From the ionizing does model, it was decided that at least 15 mm of shielding was required to meet this criteria. To confirm the validity of the SPENVIS results, GEO radiation conditions were further researched. A study performed by the Indian Space Research Organization measured the radiation levels in GEO [2]. The results for the one year study are showcased in Figure 2.2. Extrapolating these results for a 10 year period yields comparable results to the SPENVIS predictions, to within an order of magnitude. Any discrepancies can be attributed to the maximum flux assumptions of the SPENVIS model.

However, the 15 mm shielding provided a significant restriction to mass and space on the cubesat. Table 2.1 lists equivalent shielding thicknesses for aluminum, tantalum, and lead. An alternative shielding material was required. Of the three materials, tantalum was the chosen alternative. Interpolating the listed values suggests that the equivalent for 15 mm of aluminum would be around 2.44 mm of tantalum [3]. It was also discovered layered aluminum and tantalum performed better than tantalum alone. Figure 2.3 show a global minimum radiation for around 20% aluminum, by thickness. A 4:1 tantalum-aluminum ratio was determined of total thickness 2.5 mm. This would provide more shielding than tantalum alone, and slightly more than the 15 mm of pure aluminum [3].

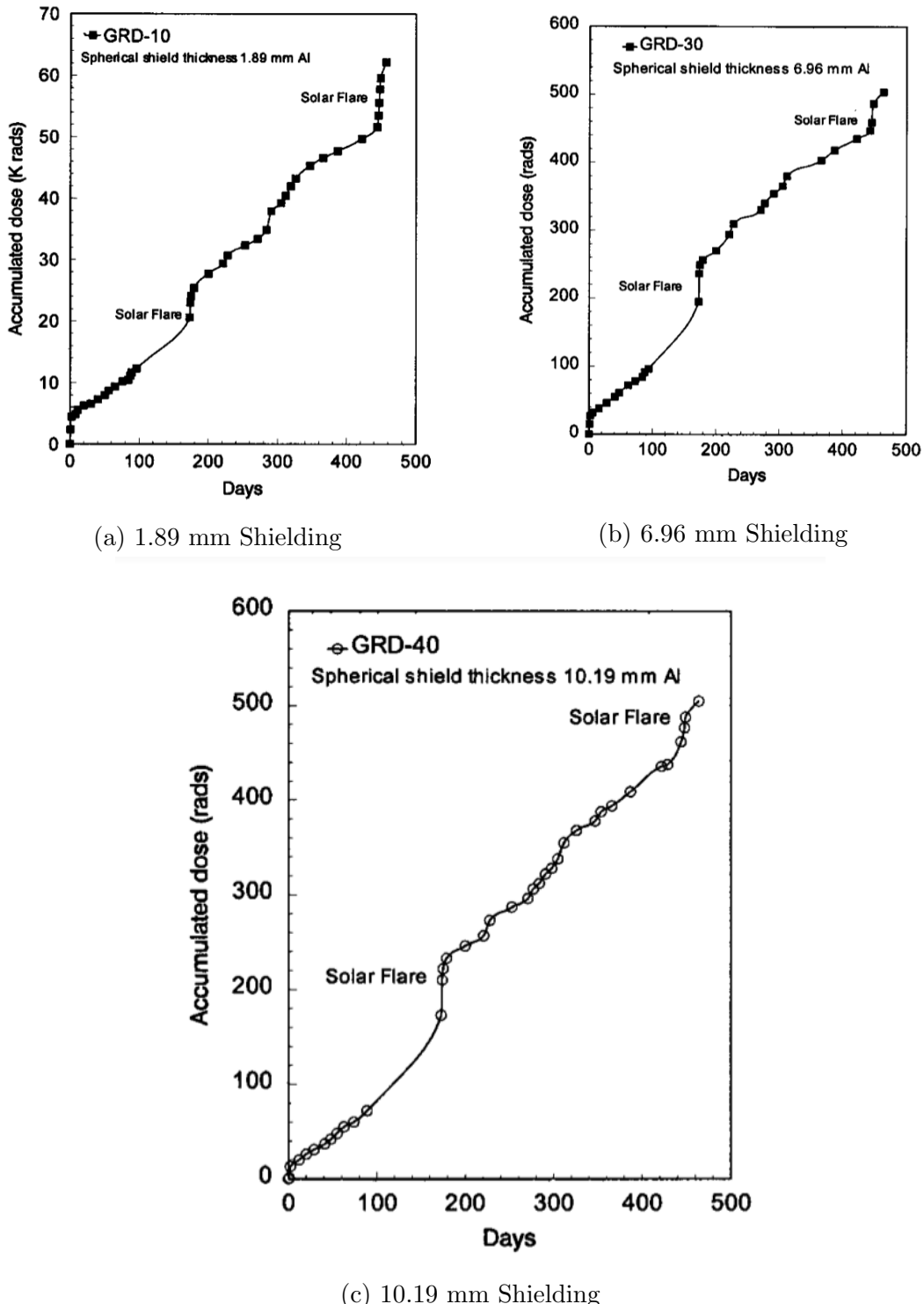


Figure 2.2: Measured radiation in geosynchronous orbit.

2.1.2 Debris

In addition to radiation, SPENVIS was also used to model the debris in GEO. Figures 2.4 and 2.5 categorize the debris density and magnitudes at GEO. Due to its

Areal thickness [g/cm ²]	pure Al [mm]	pure Ta [mm]	pure Pb [mm]
.81	3	.49	.71
2.70	10	1.63	2.38
5.40	20	3.25	4.76
8.10	30	4.88	7.14

Table 2.1: Total Thickness Equivalence

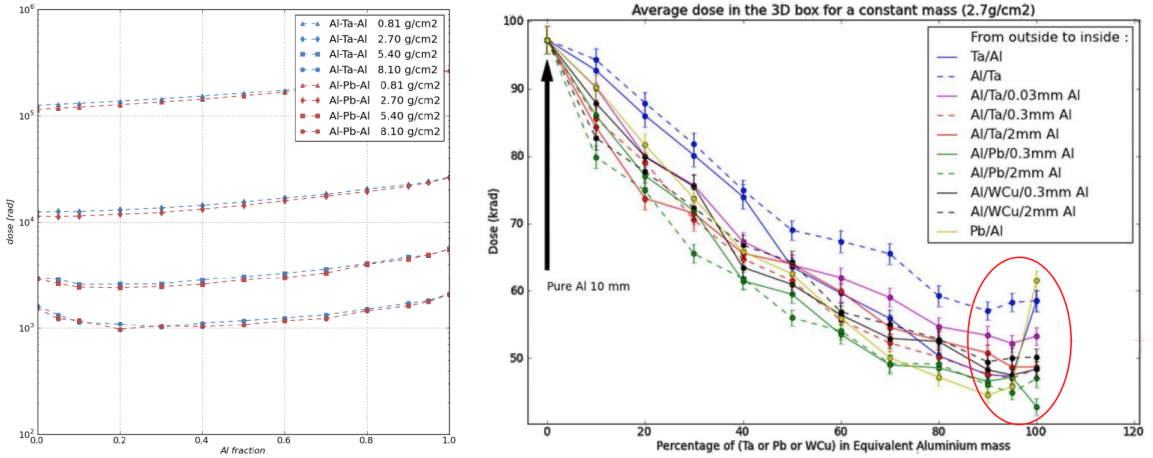


Figure 2.3: Each graph depicts variance of radiation with aluminum ratio.

common use, the debris density is at a local maximum in GEO. NASA regulations state that potential missions should demonstrate that the probability of collision with a sufficiently massed object is less than .01 [4]. The magnitude of this mass is determined by the collision required to disrupt post-mission disposal requirements. For this mission, the mass was chosen to be a conservative .01 grams. The equation to calculate the probability is

$$P_c = 1 - e^{FAT} \quad (2.1.1)$$

where F is the weighted cross-sectional area flux for the orbital debris environment exposure, A is the effective cross-sectional area of the spacecraft, and T is the time of orbit. Using Figure 2.5, the approximate flux is $10^{-4} \text{ m}^{-2}\text{yr}^{-2}$. Assuming the solar panels constitute the largest contribution to the area, the probability of collision is .0007. This value falls well below the .01 margin set by NASA, indicating that the mission would meet any debris related regulations.

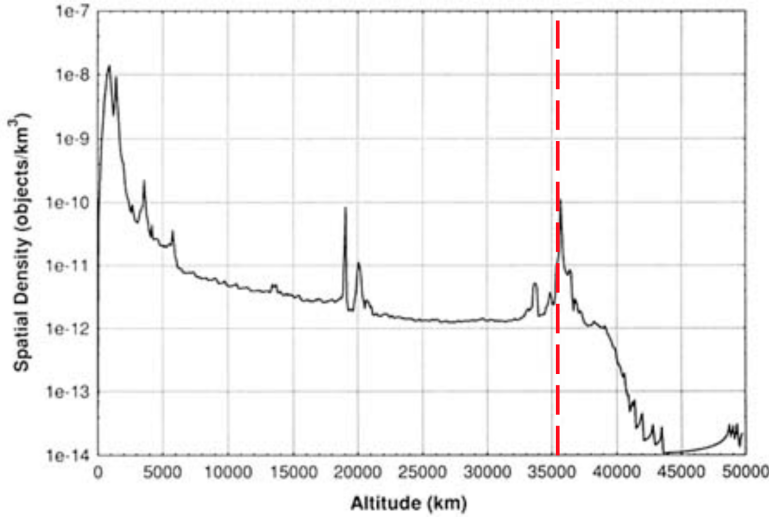


Figure 2.4: SPENVIS model for debris density with altitude.

2.1.3 Space Charge

The conditions of GEO are not favorable for space charge. While in space, the sun will excite electrons on exposed spacecraft surfaces. This will cause some electrons to be emitted from the spacecraft. The exposed side develops a positive charge, while the other develops a negative charge. If great enough, this potential difference can cause arcing, which can damage the spacecraft. These issues are exacerbated in GEO, where the large electron temperature, T_e , and low electron density, n_e , result in a large Debye length:

$$\lambda_D = \frac{\epsilon_0 k_B T_e}{n_e e^2} \quad (2.1.2)$$

where ϵ_0 is the permittivity of free space, k_B is the Boltzmann constant, and e is the electron charge. The Debye length is effectively the distance over which a spacecraft can attract atmospheric electrons. Within GEO the Debye length can reach several hundred meters, depending on the time of day. This results in increased probabilities for arcing, necessitating multiple preventative measures. The spacecraft body should be made out of conductive metals to transfer charge, and a layer of insulating Kapton should be applied to regions exposed to space.

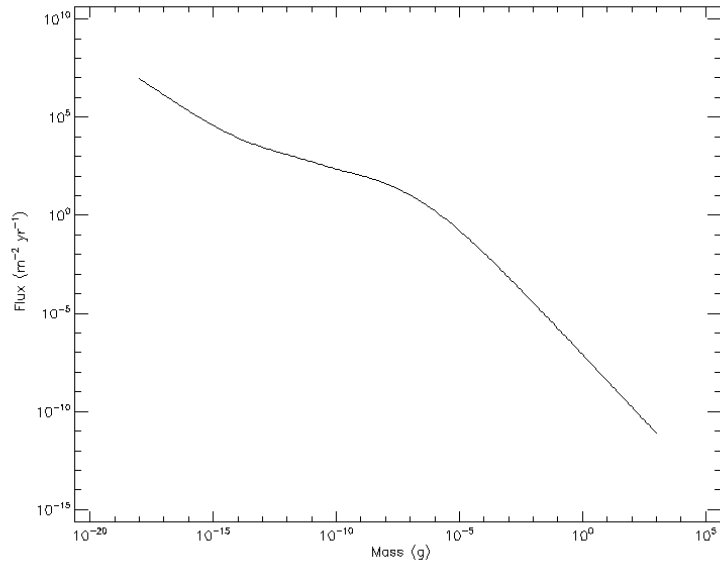


Figure 2.5: SPENVIS model for debris flux at GEO.

2.1.4 Communication

The atmosphere also has deleterious effects on satellite communication. The electrons in the atmosphere have a natural oscillation frequency called the plasma frequency:

$$\omega_p = \frac{n_e e^2}{\epsilon_0 m_e} \quad (2.1.3)$$

Here ω is the plasma frequency and m_e is the mass of an electron. These electron oscillations reflect low-frequency electromagnetic waves, limiting the possible frequencies for communication. Assuming a conservative electron density of 10^7 from Figure 2.6, the minimum communication frequency that will reach GEO is 29 MHz. This necessitates the use of the VHF/UHF satellite band or greater.

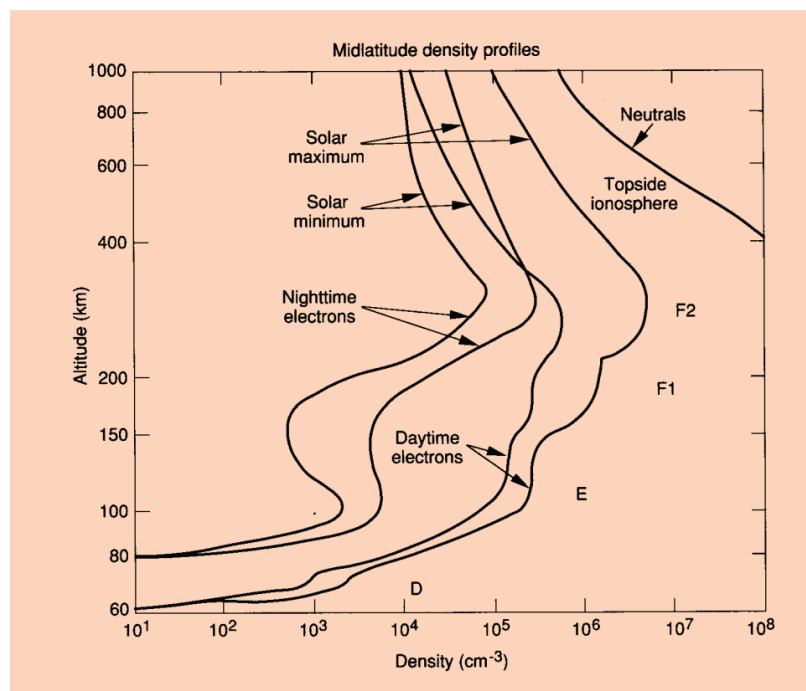


Figure 2.6: Electron density for low altitudes. The maximum at 300 km limits communication frequencies.

2.2 Launch Vehicle and Loads

One of the most important aspects of scheduling the overall time-line of the mission is the determination of the launch vehicle, as its launch availability determines the final deadline of the design and construction. There were two methods of launching the I-MISSED satellite into GEO that were considered: launching with the GOES-T, or utilizing the NASA Rideshare opportunity. A trade study of which method would be most efficient and realizable was considered.

2.2.1 Analysis of Launching with GOES-T

Since the I-MISSED will be following the GOES-T to complete its mission of imaging and watching for damage and space debris, it is most convenient for it to be launched with the GOES-T on the same launch vehicle. This was the method that was considered first. In this case, the GOES-R satellite constellation launches its installments using an Atlas V 541 rocket from the Cape Canaveral launch site. This payload of the GOES-T satellite itself is projected to be 5192 kg at launch [5], but the Atlas V 541 can carry a payload of approximately 8240 kg to a GEO transfer orbit [6], so there is more than adequate power to support the extra payload. In terms of size, the leftover space in the payload fairing will be a large constraint on the satellites design. The payload fairing for the Atlas V 541 satellite can be as long as 23.4 meters [6], and the GOES-T satellite is only 6.1 meters long [5]. The weight and size specifications can be found on the GOES-R series website.

Spacecraft Specifications

- **6.1 m x 5.6 m x 3.9 m (20.0 ft x 18.4 ft x 12.8 ft)**
- **2,857 kg (6,299 lbs) dry mass**
- **5,192 kg (11,446 lbs) at launch (fueled)**

Figure 2.7: Specifications of the GOES-R satellites [5]

Therefore, a small cube satellite would be able to fit comfortably within the constraints of the launch vehicle. In addition, all Atlas Vs are now being built to be cubesat dispenser compatible [7], so launching on the same launch vehicle as the GOES-T would not be an issue. However, once in the geostationary transfer orbit, and making the safe assumption that NASA would not allow the satellite to attach to

the GOES-T itself, the I-MISSED would need the propulsive power to transfer from GTO to GEO. Being a cubesat, the propulsive system of the I-MISSED will be electric. One of the characteristics of electric propulsion is providing very low thrust for a much longer time than chemical rocket. This makes the main concerns for completing the transfer the amount of time it would take and the ΔV . A paper detailing data from simulations of transferring from GTO to GEO using electric propulsion was a guideline for determining how intensive the transfer would be [8]. According to their calculations, the ΔV for the maneuver would be between 1.5645 and 1.8497 km/sec, as shown in Figure 2.8 [8].

Table 3. ΔV [km/s] - Results from MP-AIDEA.

	<i>w</i>	Min	Mean	Max
Strat. 1	1	1.6558	1.7263	1.8497
	10	1.6473	1.7129	1.8683
	100	1.7046	1.7580	1.8551
Strat. 2	1	1.5644	1.5668	1.5728
	10	1.5646	1.5673	1.5746
	100	1.5648	1.5685	1.5763
Strat. 3	1	1.6626	1.7144	1.8424
	10	1.6747	1.7342	1.8223
	100	1.6833	1.7538	1.8715
Strat. 4	1	1.5646	1.5665	1.5691
	10	1.5650	1.5675	1.5758
	100	1.5645	1.5673	1.5710

Figure 2.8: GTO to GEO Transfer ΔV 's Calculated with Different Computational Strategies [8]

Even the minimal calculated transfer ΔV is many times larger than the total ΔV that the I-MISSED currently undergoes over its entire lifetime. Finding an electric propulsion system that would be able to complete this maneuver and fit within a 6U cubesat would be a very difficult task. In addition, the time of flight for the transfer would be approximately 225 days [8]. It is safe to assume that the propulsion system of the GOES-T will be different than that of the I-MISSED, resulting in a time difference between when the GOES-T arrives to GEO and when the I-MISSED arrives at the same place. This would indicate that the I-MISSED will have to do another maneuver to rendezvous with the GOES-T after the transfer. The time spent transferring and then maneuvering to link with GOES-T undermines the overall mission. The GOES-T spends a lot of time unmonitored while the transfer takes place and any changes

to it during this time would not be imaged. After analysis of this option, it began to become clear that another option of launching might be more feasible for this mission. This is where NASA Rideshare comes in.

2.2.2 NASA Rideshare

The NASA Rideshare program is an initiative to integrate cubesat dispensers on NASA and Air Force launch missions [9]. In this case, a mission can be chosen that directly injects the I-MISSED into GEO at an earlier date instead of being launched into GTO with the GOES-T. The next mission that launches into GEO before the GOES-T launch is the STP-3 mission. The STP-3 mission's main payload is a nuclear blast detection satellite, and it is planning to include six smaller payloads on its launch vehicle in an Evolved Expendable Launch Vehicle Secondary Payload Adapter or ESPA ring [10].

NASA & Air Force Rideshare Opportunities



Year	LEO (mid inc)	LEO (hi inc)	MEO	GEO	Other / TLO
2017					TESS
2018	STP-2				EM-1
2019	RALI		GPS III-3	STP-3	
2020		Landsat-9 Sentinel-6 (JPL)	GPS III-4		
2021		STP-S28 SWOT (JPL) JPSS-2	GPS III-5	SBIRS/G5 (GTO)	EM-2
2022		PACE			EM-3
2023	STP-S29				EM-4

Figure 2.9: Table Showing Rideshare Opportunities in the Near Future [9]

This will all be launched on an Atlas V-551 launch vehicle [10]. Since the STP-3 is being launched directly into GEO, the only maneuver that the cubesat has to complete is a longitude shift to rendezvous with the GOES-T satellite. The planned

launch date for the Satellite Test Program satellite (STP-3) is in June of 2019 at a longitude of between 80 and 120 degrees West [11], and the planned launch date for the GOES-T is in September of 2020 [5]. In order to rendezvous with GOES-T the I-MISSED will transfer into an circular inner orbit from GEO and orbit until GOES-T arrives and it transfers back into its final orbit around GOES-T. As detailed in section 2.3, this procedure is much less intensive than that of the GTO to GEO transfer mentioned in section 2.2.1.

2.2.3 Launch Load Data

Because the I-MISSED will be launched on an Atlas V launch vehicle, the launch loads and accelerations are well documented. The main loads considered are accelerations during launch, shocks (Figure 2.12), and vibration (Figure 2.11) loading. The data from the Atlas V User's Manual is passed on to the Structure team to ensure that the I-MISSED will withstand the launch sequence. The procedure from launch to payload deployment along with the accelerations on each segment are portrayed here:

Figure 2.4.2-3: Typical Atlas V 521 Standard Short-Coast GTO Ascent Profile and Ground Trace (1 of 2)

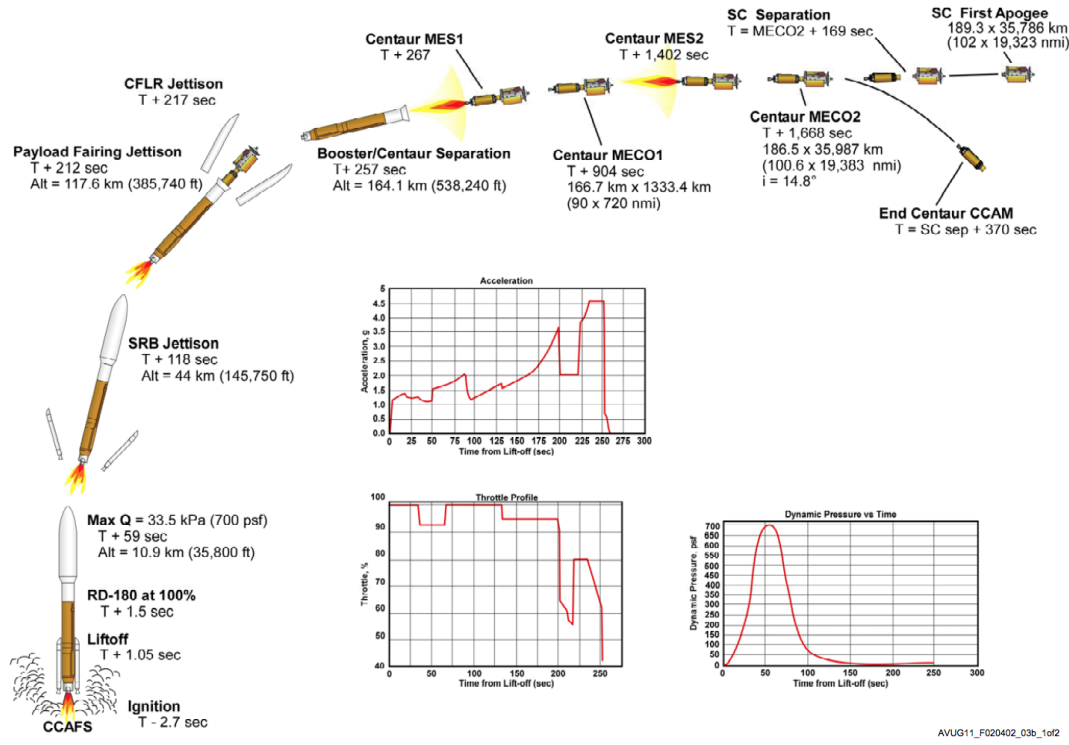


Figure 2.10: Diagram outlining the payload separation during launch [6]

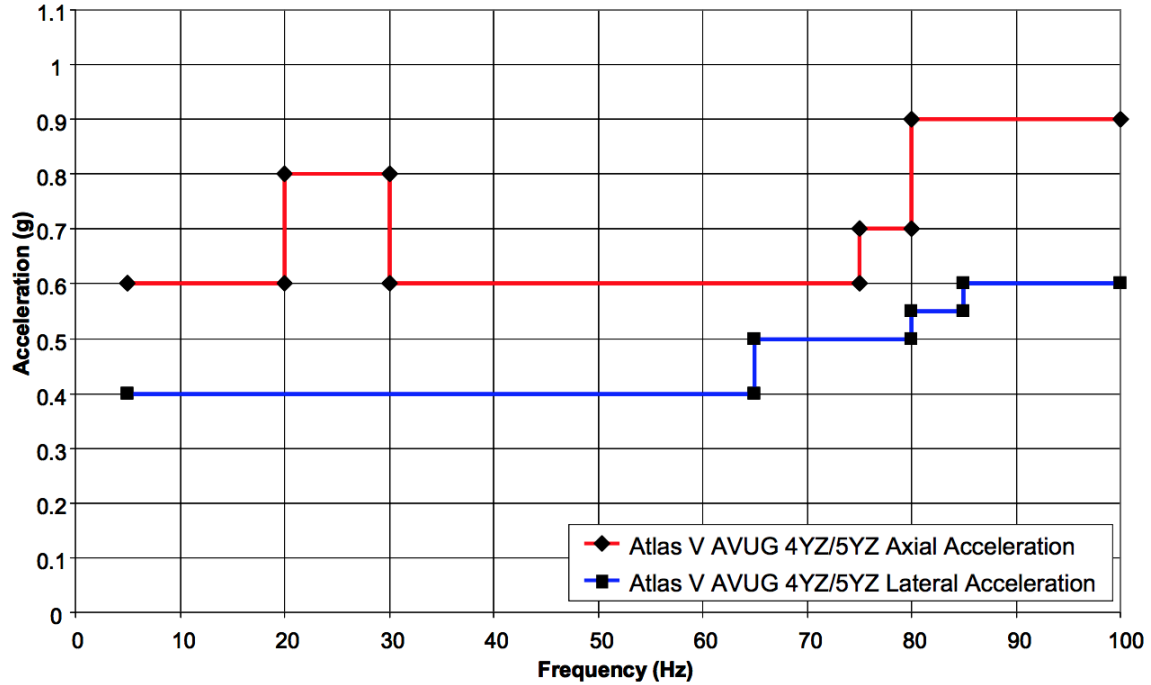


Figure 2.11: Quasi-Sinusoidal Vibration Levels for Atlas V 400 Series and Atlas V 500 Series Based on SRS with Q=20 [6]

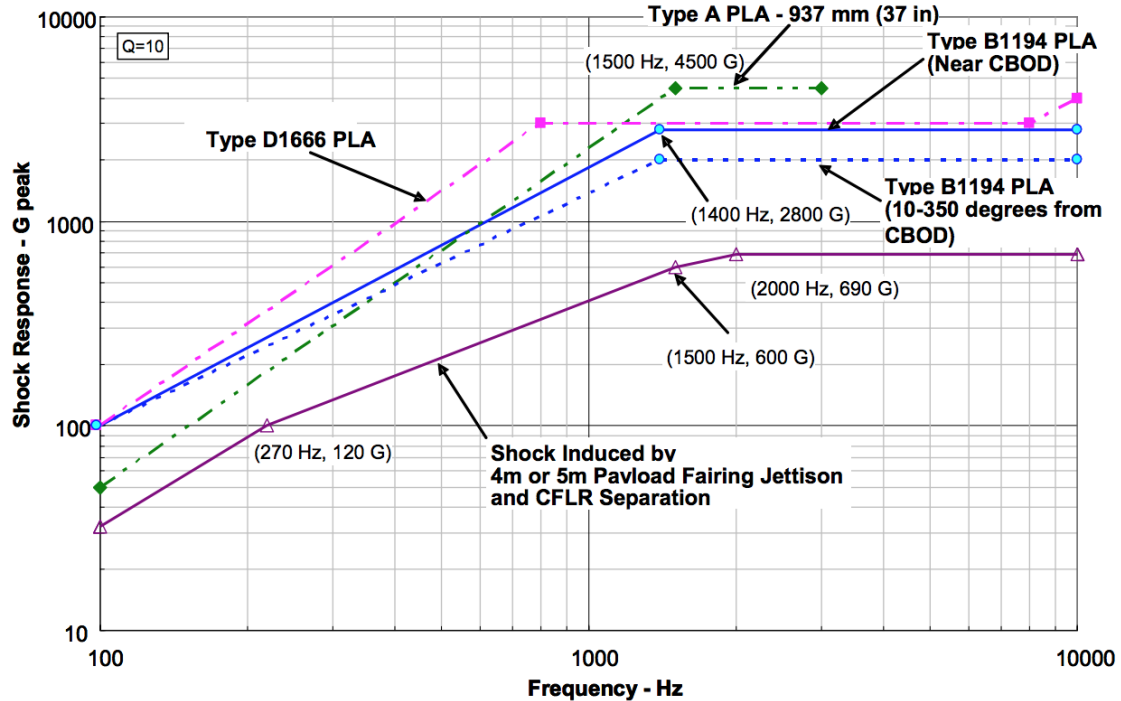


Figure 2.12: Typical Maximum Atlas Shock Levels for Atlas V Standard Payload Adapters [6]

2.3 Longitude Shifting Procedure

2.3.1 Overview and Motivation of the Maneuver

As outlined in section 2.2, the trade study of different possible methods to successfully rendezvous with GOES-T has shown that it is most efficient and desirable to launch with the STP-3 mission. The STP-3 launch vehicle will put the I-MISSED cubesat directly in GEO in June, 2019 at the longitude between 80 and 120 degrees West [11]. The GOES-T subject satellite will be injected at 137 degrees West longitude in September, 2020 [5]. Therefore, a change in longitude of I-MISSED is necessary to align with the 137 degrees West longitude of the GOES-T spacecraft. The fact that the STP-3 along with the cubesat will be launched more than a year before GOES-T is highly favorable for performing the longitude shift, because such a maneuver requires a significant amount of time to execute. A general qualitative overview of the longitude shifting procedure is outlined below (a detailed analysis will follow after the overview):

1. I-MISSED Satellite is injected directly into GEO by the STP-3 launch vehicle in June 2019.
2. The satellite transfers to a circular orbit with a lower altitude, which is no longer geosynchronous. This allows for a shift in longitude over time.
3. The satellite progressively shifts its longitude by some amount every orbital period.
4. The satellite transfers back to the GEO orbit such that its longitude exactly matches the longitude of GOES-T in September 2020.

In order to determine the exact scheduling and required ΔV values for the longitude shifting maneuver, a more detailed computational analysis was executed in STK .

2.3.2 STK Analysis

The steps outlined above were simulated in STK 11 such that the longitude of the I-MISSED cubesat matches the one of GOES-T when GOES-T is injected into GEO. Several assumptions were needed to be made in order to perform the STK analysis of the problem, because of lack of detailed information regarding scheduling and other details of the GOES-T and STP-3 missions. The assumptions are listed below:

1. It was assumed that I-MISSED (together with STP-3) will arrive at GEO on June 1st, 2019 at 16:00:00 UTC , since there is currently no further information available about the exact launch date of the STP-3 mission.
2. It was assumed that the GOES-T satellite will be injected into GEO on September 1st, 2020 at 16:00:00 UTC. No further detailed information about the exact injection time of GOES-T was found.
3. Finally, it was assumed that the STP-3 satellite will be injected into GEO at 80 degrees West longitude (the lower bound of the previously mentioned range of 80 to 120 degrees West longitude of the STP-3 spacecraft). Making this assumption is equivalent to considering the worst-case scenario of the longitude shifting maneuver (largest difference in longitudes between STP-3 and GOES-T) that results in computing the most conservative ΔV and maneuver time values.

The I-MISSED cubesat will use an electric propulsion system (described in detail in Chapter 3) to perform the longitude shifting maneuvers. The STK software was used to determine the scheduling, ΔV and other necessary details of all the maneuvers necessary to shift the longitude of I-MISSED to 137 degrees West. The specifications of the propulsion system given in Chapter 3 were used to model the electric propulsion thruster within STK. Using the Astrogator analysis module, the exact trajectories of I-MISSED required to successfully perform the longitude shifting procedure were computed. The analysis was performed with continuous electric propulsion burns. A full description of the STK analysis longitude shifting procedure is provided below in the "Electric Propulsion (Finite Burn) STK Longitude Shifting Procedure" subsection. Additionally, a description of a longitude shifting procedure analysis with an assumption of impulsive burns is also given in the "Appendix: Impulsive Case of the Longitude Shifting Procedure" in the end of this section. Even though the data obtained in the impulsive burn analysis is not as accurate as the data acquired in the "Electric Propulsion (Finite Burn)..." subsection (since it does not account for the long duration of the finite electric propulsion burns), it was proved to be of help in gaining preliminary insight into the longitude shifting problem.

Electric Propulsion (Finite Burn) Longitude Shifting Procedure

The steps of the longitude shifting procedure assuming finite burns of the electric propulsion system are enumerated and explained below:

1. I-MISSED Satellite is injected into GEO on June 1st, 2019 at 16:00:00 UTC.
 - (a) Altitude = 35,786 km
 - (b) Eccentricity = 0 (Circular)
 - (c) Longitude = 80 degrees West
2. Start the finite burn transfer to the inner orbit of lower altitude on June 2nd, 2019 at 16:00:00 UTC. The transfer trajectory is a spiral with the electric propulsion system thrusting in the anti-velocity vector direction of the cubesat.
3. Propagate the spiral transfer orbit until the lower altitude of the inner circular orbit is achieved. The altitude was chosen to be 35,072 km (714 km below GEO), since it allows for a relatively quick change in longitude, while keeping the required ΔV value low. Moreover, the altitude of the inner orbit has to be sufficiently low to have a ground track velocity fast enough, such that the I-MISSED cubesat has access to the ground stations frequently enough. As indicated later in this section, the orbit altitude of 35,072 km provides a relatively frequent communication access with the ground stations.
4. The inner orbit is reached on June 5th, 2019 at 11:45:00 UTC. The ΔV required to perform the maneuver is 24.79 m/s.
 - (a) Altitude = 35,072 km
 - (b) Eccentricity = 0 (Circular)
5. Stay in the lower-altitude orbit for 439.83 days.
6. Start the finite burn transfer back to GEO on August 18th, 2020 at 07:40:00 UTC. The electric propulsion system is set to thrust in the direction of the velocity vector of the cubesat.
7. Propagate the spiral transfer orbit until GEO is reached.
8. The I-MISSED satellite reaches the GEO orbit at the longitude of 137 degrees West on August 21st, 2020 at 03:13:00 UTC. The ΔV required to perform the maneuver is 24.76 m/s.
 - (a) Altitude = 35,786 km
 - (b) Eccentricity = 0 (Circular)

(c) Longitude = 137 degrees West

9. The GOES-T subject satellite is injected into GEO at 137 degrees West longitude on September 1st, 2020 at 16:00:00 UTC. The I-MISSED cubesat has performed a successful rendezvous with GOES-T at the desired longitude.

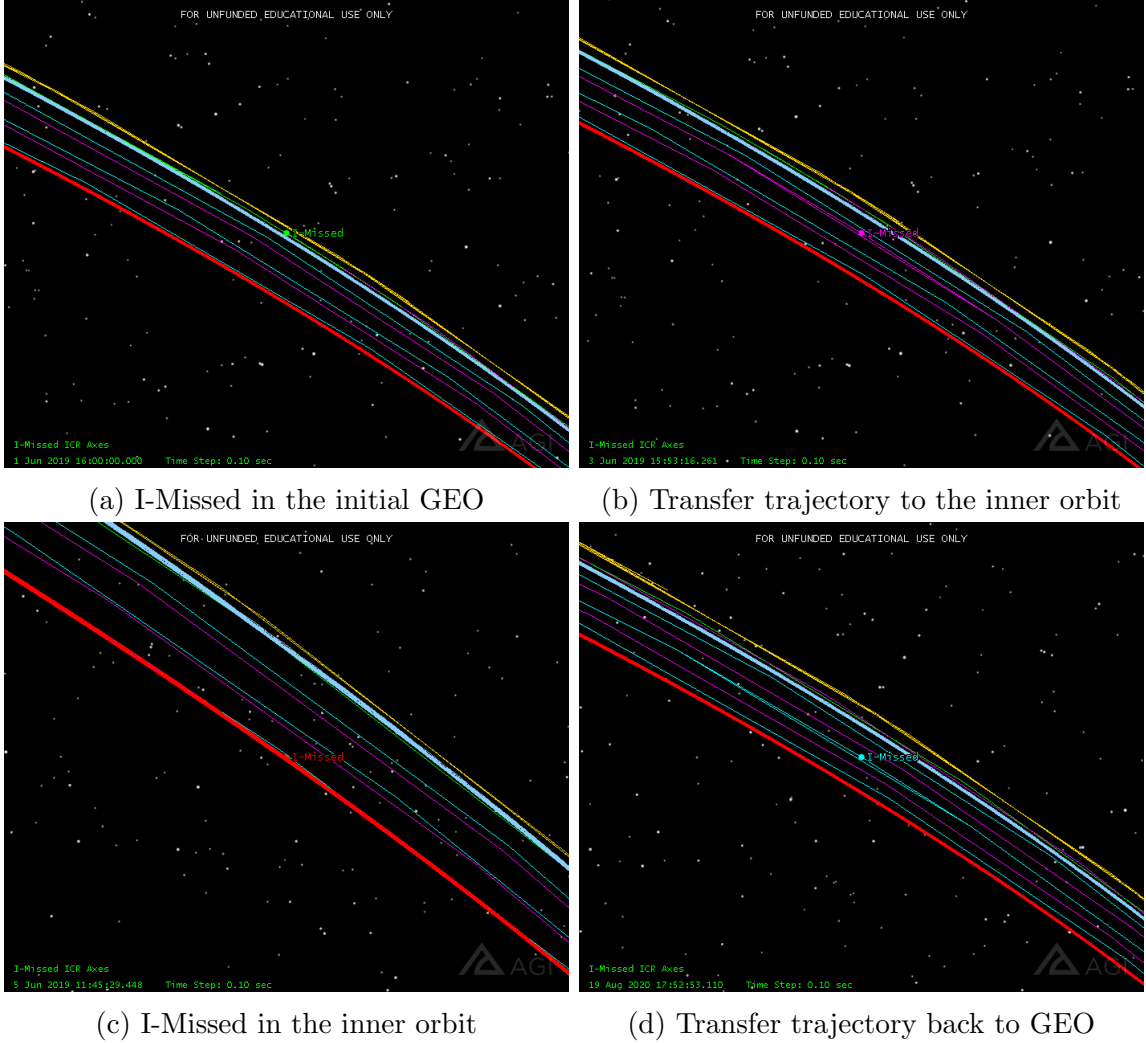


Figure 2.13: STK Snapshots of the most representative moments during the longitude shifting procedure

By utilizing the procedure outlined above, the I-MISSED cubesat will shift its longitude to match the longitude of GOES-T, such that the imaging of the GOES-T subject satellite can commence right when GOES-T starts its mission in GEO. The total ΔV of the maneuver was computed to be $\Delta V = 49.55 \text{ m/s}$, which is a relatively small ΔV value as compared to the overall available ΔV budget (see Chapter 3). The snapshots of the most representative moments during the longitude shifting procedure

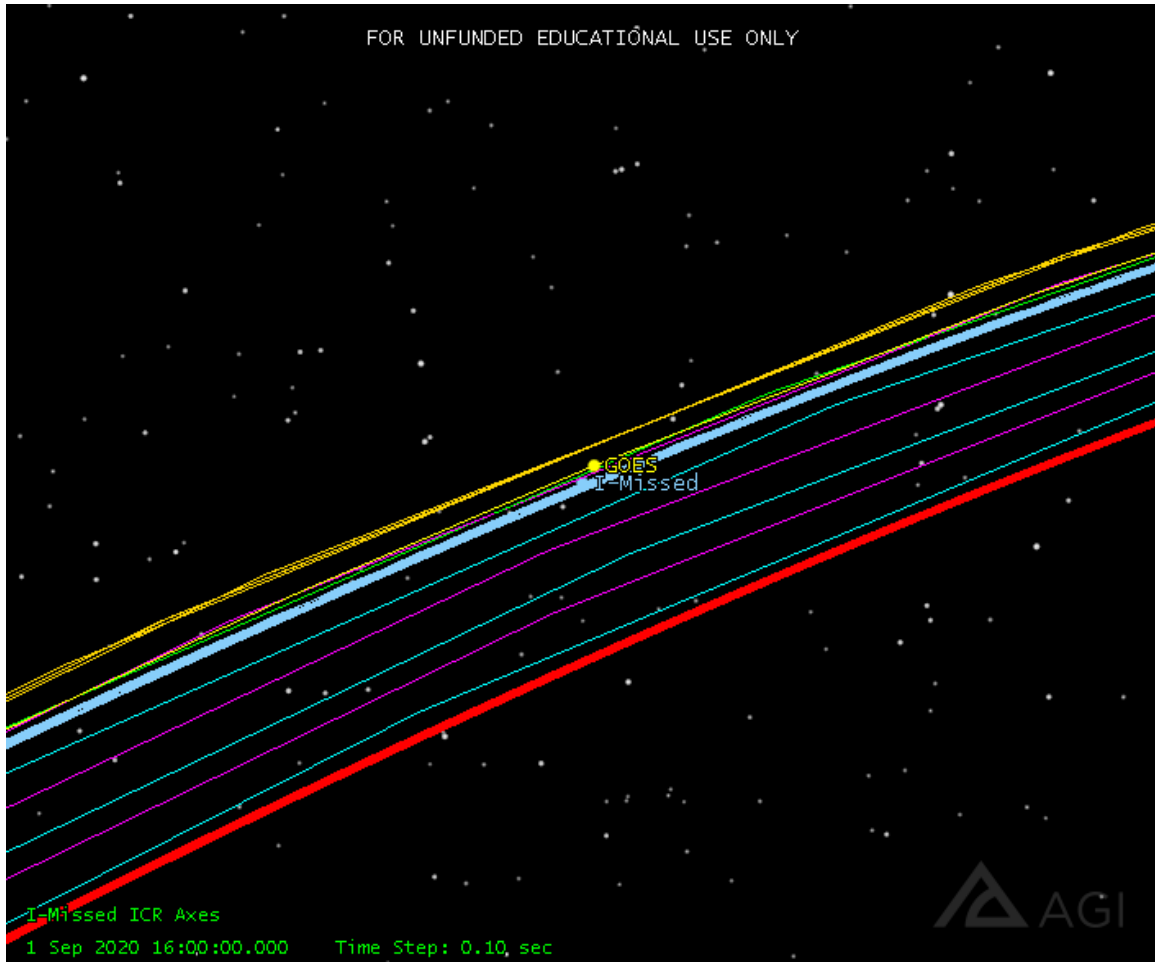


Figure 2.14: STK Snapshot of the GOES-T rendezvous on September 1st, 2020, 16:00:00 UTC

(taken from the STK 3D Graphics environment) are included in Figures 2.13 and 2.14. As mentioned in the steps of the procedure given above, the selection of the inner orbit altitude was also dependent on how often a given inner orbit trajectory will enable the I-Missed cubesat to communicate with appropriate ground stations. Figure 4.14 in Chapter 4 was generated using to determine the ground station access time periods for I-Missed. The figure indicates that I-Missed will be able to communicate with one of the main ground stations (Wallops Island or Kauai) about every 2 weeks (27 days of full access available followed by a 14 day time period with no access). This time interval between subsequent available accesses was considered to be short enough to be able to monitor the satellite in the inner orbit.

Appendix: Impulsive Case of the Longitude Shifting Procedure

As a remark, this impulsive maneuver analysis was used only to gain initial insight into the longitude shifting problem. The resultant maneuver scheduling and ΔV values do not accurately represent the longitude shifting procedure using an electric propulsion system. For accurate trajectory data for the longitude shifting procedure refer to the "Electric Propulsion (Finite Burn) Longitude Shifting Procedure" provided above.

The steps of the longitude shifting procedure assuming impulsive maneuvers are specified below¹:

1. I-MISSED Satellite is injected into GEO on June 1st, 2019 at 16:00:00 UTC (the same as for the electric propulsion case).
 - (a) Altitude = 35,786 km
 - (b) Eccentricity = 0 (Circular)
 - (c) Longitude = 80 degrees West
2. Burn into a Hohmann transfer orbit (leading to the inner orbit) on June 2nd, 2019 at 16:00:00 UTC.
 - (a) Perigee altitude = 35,072 km
 - (b) Apogee altitude = 35,786 km
 - (c) ΔV of the maneuver is 13.17 m/s.
3. Propagate the Hohmann transfer orbit until the perigee is reached.
4. Circularize the orbit to achieve the inner orbit trajectory.
 - (a) Altitude = 35,072 km
 - (b) Eccentricity = 0 (Circular)
 - (c) ΔV of the maneuver is 13.02 m/s.
5. The inner orbit trajectory is established on June 3rd, 2019 at 03:49:00 UTC.
6. Stay in the lower-altitude orbit for 456.54 days.
7. Burn into a Hohmann transfer orbit (leading to GEO) on September 1st, 2020 at 16:52:00 UTC.

¹Some steps of this STK analysis are exactly the same as for the finite burn case, since the initial orbit (GEO), the lower-altitude inner orbit, and the final orbit (GEO) have the same specifications.

- (a) Perigee altitude = 35,072 km
 - (b) Apogee altitude = 35,786 km
 - (c) ΔV of the maneuver is 13.28 m/s.
8. Propagate the Hohmann transfer orbit until the apogee is reached.
9. Circularize the orbit to attain GEO trajectory.
- (a) Altitude = 35,786 km
 - (b) Eccentricity = 0 (Circular)
 - (c) Longitude = 137 degrees West
 - (d) ΔV of the maneuver is 13.02 m/s.
10. The I-MISSED satellite reaches the GEO orbit at the longitude of 137 degrees West on September 2nd, 2020 at 04:44:00 UTC. The I-MISSED cubesat has performed a successful rendezvous with GOES-T at the desired longitude.

In the impulsive burn case, the total ΔV of the maneuver was computed to be $\Delta V = 52.48$ m/s (slightly larger than in the electric propulsion, finite burn case)

2.4 Regulations

Since the I-MISSED will be launched along with the NASA mission STP-3, much of the regulations regarding launch sites and launch conditions will already be taken care of. In addition, many of the I-MISSED's components are off-the-shelf so they meet many of the general requirements for a cubesat. Therefore, the main regulations that need to be considered are those that come into effect once the I-MISSED has reached its final orbit, regulations on the overall structure of the I-MISSED, and also regulations regarding communications frequencies.

2.4.1 Component Regulations

Regulations regarding the propulsion system such as the propulsion system needs "3 independent inhibits to activation" [12] and electrical requirements such as the deployment switch, RBF pin, and battery circuit protection [12], are requirements that are integrated into the off-the-shelf components that are made specifically for cubesats.

2.4.2 Communications Frequency Regulations

Transmission frequency is another heavily regulated field to consider once the satellite is in orbit. The National Telecommunications and Information Administration website has a full list of communications frequencies and their uses. [13] This ensures that a communications frequency is picked that will not be in interference with any other communication. Finally, a legal document must be completed to obtain a license to transmit in the chosen frequency.

2.4.3 Mechanical Regulations

Regulations on the structure of the I-MISSED include limits on the overall dimensions on the cubesat, the total weight limit, limits on the location of center of gravity, and other regulations regarding materials and railing. These are all detailed in Figure 2.15.

3.2 CubeSat Mechanical Requirements

6U CubeSats are picosatellites with dimensions and features outlined in the 6U CubeSat Specification Drawing (Appendix B). These requirements are applicable for all dispensers not utilizing the tab constraint method. CubeSats designed with tabs can find those specific requirements at the PSC website (planetarysystemscorp.com). General features of all CubeSats without tabs include:

- 3.2.1 The CubeSat shall use the coordinate system as defined in Appendix B. The origin of the CubeSat coordinate system is located at the geometric center of the CubeSat.
 - 3.2.1.1 The 6U CubeSat configuration and physical dimensions shall be per the appropriate section of Appendix B.
- 3.2.2 The -Z face of the CubeSat will be inserted first into the 6U Dispenser.
- 3.2.3 No components on the yellow shaded faces shall exceed 10 mm normal to the surface.
 - 3.2.3.1 When completing a CubeSat Acceptance Checklist (CAC), protrusions will be measured from the plane of the rails.
- 3.2.4 Deployables shall be constrained by the CubeSat, not the 6U Dispenser.
 - 3.2.4.1 **Note:** This requirement is derived from launch vehicle requirements.
- 3.2.5 Rails shall have a minimum width of 8.5mm.
- 3.2.6 Rails will have a surface roughness less than 1.6 μm .
- 3.2.7 The edges of the rails will be rounded to a radius of at least 1 mm.
- 3.2.8 At least 75% of the rail will be in contact with the 6U Dispenser rails. 25% of the rails may be recessed, and no part of the rails will exceed the specification.
- 3.2.9 The maximum mass of a 6U CubeSat shall be 12.00 kg.
 - 3.2.9.1 **Note:** Larger masses may be evaluated by the Mission Integrator on a mission specific basis.
- 3.2.10 The CubeSat center of gravity shall be located within 4.5 cm from its geometric center in the X direction, within 2 cm from its geometric center in the Y direction, and within 7 cm from its geometric center in the Z direction
- 3.2.11 Typically, Aluminum 7075, 6061, 6082, 5005, and/or 5052 are used for both the main CubeSat structure and the rails. If materials other than aluminum are used, the CubeSat Developer should contact the Mission Integrator or dispenser manufacturer.
- 3.2.12 The CubeSat rails and standoff, which contact the 6U Dispenser rails and ejector plate, shall be hard anodized aluminum to prevent any cold welding within the 6U Dispenser.

Figure 2.15: Regulations on the structural components of a cubesat
[12]

2.4.4 Required Testing Before Launch

The I-MISSED must also be tested before launching for various types of loading. Before launch the I-MISSED would have to undergo: random vibration testing, thermal testing, and shock testing. It will also have to pass a visual inspection before it is approved for launch. The general timeline for the testing of a cubesat is shown in 2.16 [12]

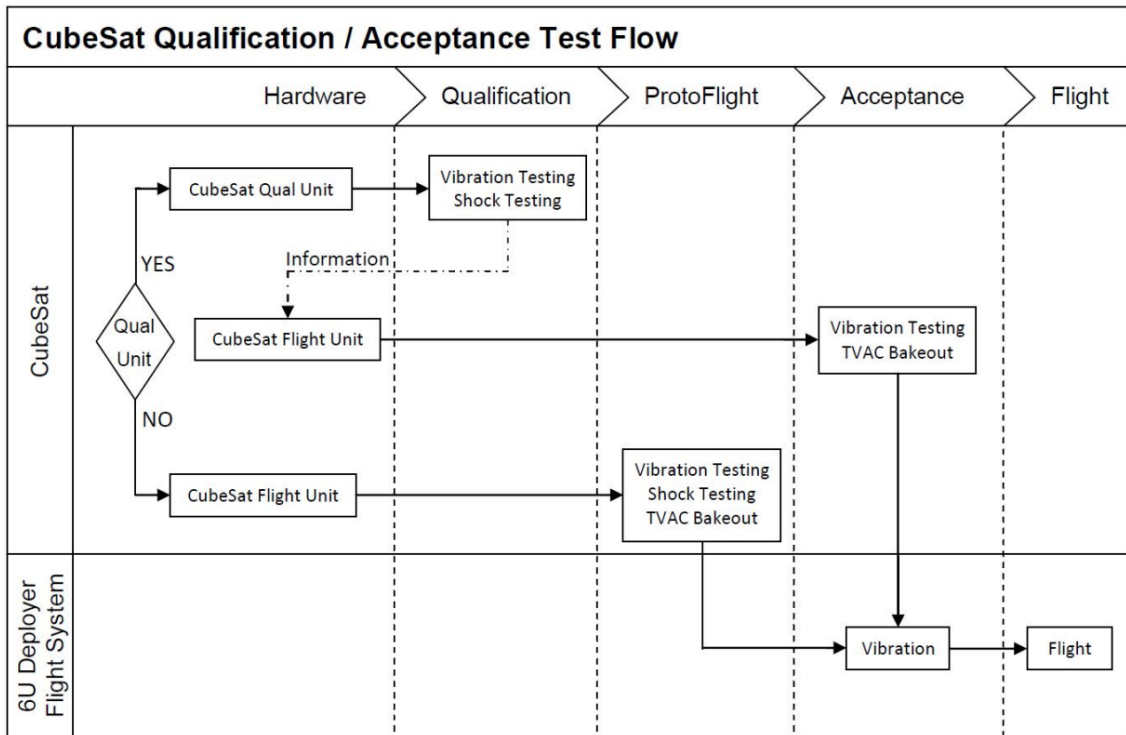


Figure 4: CubeSat General Testing Flow Diagram

Note: CubeSat test flows will vary from mission to mission; the Mission Integrator will provide the CubeSat Developer with the approved test flow for a specific mission.

Figure 2.16

2.4.5 Waivers

If any of the I-MISSED's specifications are outside of the realm of these regulations, such as the mass of the I-MISSED being slightly heavier than the limits for a 6U cubesat, it is possible to complete a Deviation Waiver that will allow the I-MISSED to be launched while outside of some regulations. [12]

2.4.6 Requirements for End of Life

Finally, there are also regulations on how to dispose of the I-Missed at its end of life. The cubesat will have to be able to end all of its radio frequency emissions [14]. Not only do radio frequency emissions have to cease, but also all stored energy within the spacecraft must be depleted at its end of life [14]. Lastly, the spacecraft must have a plan for disposal, which in the case of I-Missed will be transferring to a graveyard orbit.

Chapter 3

Guidance, Navigation, and Control

The Guidance, Navigation, and Control (GNC) sub-team of I-MISSED will ensure spacecraft guidance (ascent, on-orbit, etc.), navigation (position/orientation determination, etc.), and control (spacecraft and control system stability, etc.). Team members will choose avionics technology based on information provided to ensure this success.

3.1 Orbital Elements for I-MISSED

In order to provide clients with full 360 degree imagery of their satellite, it was decided to use a formation flying arrangement, such that in the frame of the parent satellite, the cubesat would effectively be in an orbit around it. Because the parent satellite will be in a circular orbit, the required cubesat orbit must have an identical period to the parent satellite and be slightly eccentric. As a result, the perigee radius would be just inside of the parent satellite orbit while the apogee radius would be just outside of it. Using this formation, an STK simulation was run to determine the radial distance from the parent satellite to the cubesat over time. Simulation results showed that with this type of formation, the effective orbit around the parent satellite was elliptical, with the parent at the center, with the ratio of the semi-major axis to semi-minor axis being approximately 2:1. Selection of the specific following distance of the cubesat was primarily constrained by the range from which the imager could provide quality images and by the ability for the cubesat to be at a close following range without causing risk to the parent satellite. The selected imager was decided to have produce quality images from a range of around 10 km. A following distance is as safe as the

precision with which the cubesat and parent satellites positions can be determined. With the need for the imager to be within around 10 km of the parent satellite, an extremely high level of precision was needed for position determination for the cubesat to avoid the risk of getting too close to the GOES-T satellite. Balancing the need to stay at a safe following distance while being close enough to produce quality images for the mission, a final orbit was determined for the cubesat. This orbit was selected to have a closest following distance of 7.16 km and a farthest following distance of 14.80 km. The orbital elements for the selected orbit are as follows:

1. Semi-major axis: 42164.172 km
2. Eccentricity: 0.00018
3. Inclination: 0 deg
4. Right Ascension of the Ascending Node: 107.5 deg
5. Argument of perigee: 191.8 deg

3.2 Perturbations and Disturbances

The gravitational forces generated by the Sun and Moon create a gyroscopic precession of the orbit that causes variations in the right ascension of the ascending node, argument of perigee, and the mean anomaly [15]. The eccentricity of the cubesats orbit is nearly circular such that e^2 is approximately zero. This results in the following perturbation rate changes [15]:

Right Ascension of the Ascending Node:

$$\frac{d\Omega}{dt} = -0.00338 \frac{\text{deg}}{\text{day}} \text{ (Moon contribution)} \quad (3.2.1)$$

$$\frac{d\Omega}{dt} = -0.00154 \frac{\text{deg}}{\text{day}} \text{ (Sun contribution)} \quad (3.2.2)$$

Argument of Perigee:

$$\frac{d\omega}{dt} = -0.01340 \frac{\text{deg}}{\text{day}} \text{ (Moon contribution)} \quad (3.2.3)$$

$$\frac{d\omega}{dt} = 0.02680 \frac{\text{deg}}{\text{day}} \text{ (Sun contribution)} \quad (3.2.4)$$

The Earth is not a perfect sphere and instead is slightly shaped like a pear [15]. The oblateness of the Earth can be taken into consideration with an infinite series, but the terms become relatively small after the J2 perturbation. The potential differentiation caused by the Earth causes periodic variations to the orbital elements and most profoundly affects the right ascension of the ascending node and the argument of perigee. By only taking J2 into consideration these changes are [15]:

Right Ascension of the Ascending Node:

$$\frac{d\Omega}{dt} = -0.01340 \frac{\text{deg}}{\text{day}} \quad (3.2.5)$$

Argument of Perigee:

$$\frac{d\omega}{dt} = 0.02680 \frac{\text{deg}}{\text{day}} \quad (3.2.6)$$

These perturbations cause continual changes to the orbit of the spacecraft and require adjustments.

The disturbance torques experienced by a spacecraft are gravity gradient, solar radiation pressure, magnetic field, and aerodynamic drag. The gravity gradient can be found using

$$T_g = \frac{3\mu}{2R^3} |I_{zz} - I_{xx}| * \sin 2\theta \quad (3.2.7)$$

where T_g is the max gravity gradient, μ is Earth's gravity constant, R is the orbit radius (which can be assumed to be roughly circular since the eccentricity is approximately zero), I_{zz} and I_{xx} are the moments of inertia, and θ is the maximum deviation of the Z-axis from local vertical in radians [15]. To prepare for the worst case scenario, θ was taken to be $\frac{\pi}{4}$ to make the sine function equal to one. The satellite was also considered in the deployed configuration where the moments of inertia would be at a maximum. This resulted in a maximum gravity gradient of approximately 1.57 nNm. This is an order of magnitude less than the torque generated by the magnetorquers and five orders of magnitude less than the torque generated by the reaction wheels. The torque generated by the solar radiation pressure can be determined from

$$T_{sp} = F\Delta c \quad (3.2.8)$$

where

$$F = \frac{F_s}{c} A_s (1 + q) \cos i \quad (3.2.9)$$

and F_s is the solar constant ($1,367 \text{ W/m}^2$), c is the speed of light, A_s is the surface area, q is the reflectance factor, i is the angle of incidence of the sun, and Δc is the distance between the center of solar pressure and the center of gravity. The surface area is estimated to be approximately 0.8197 m^2 when the spacecraft is in its deployed configuration with both the solar array and antenna fully deployed. The reflectance factor of the spacecraft is difficult to determine and since the effects of solar radiation pressures are so small on a cubesat it is assumed to be one. The angle of incidence is also chosen to be zero degrees to create a worst case scenario and maximize the torque value. The distance between the two center points was assumed to be approximately 7.5 cm towards the solar array side. The maximum value of the solar radiation torque in a worst case scenario came out to be 560 nNm.

Earth's magnetic field was simulated in STK which uses the International Geomagnetic Reference Field (IGRF). The model is only updated every five years to provide predictions for the next five years. The most recent update occurred in 2015 with the next happening in 2020. This meant the latest the simulation could accurately model was the year 2020 [16]. Using the British Geological Survey online 12th generation IGRF, the following (Figure 3.1) calculations revealed the field model at the end of 2020 [17]:

Field Model Results				
Location	Latitude	Longitude	Altitude	Date
'T-MISSED'	0 degs 0 mins	-137 degs 0 mins	35786.03 km	2020.90
Component			Secular Variation	
Declination			-3.2 arcmin/year	
Inclination			-0.4 arcmin/year	
Horizontal Intensity			-0.1 nT/year	
North Component			-0.1 nT/year	
East Component			-0.1 nT/year	
Vertical Intensity			0.0 nT/year	
Total Intensity			-0.1 nT/year	

Figure 3.1: IGRF Field Model in 2020

This provided a basis of what the magnetic field was like at a single point to ensure more accurate predictions with the data taken from STK. STK gave the data in Figure 3.2 data for a single orbit of the cubesat.

The total magnitude of the magnetic field is relatively the same between the STK

F (nT)	B Field - ECF x (nT)	B Field - ECF y (nT)	B Field - ECF z (nT)
1.041e+02	2.175e+01	-2.608e+00	1.018e+02
1.041e+02	2.183e+01	-2.525e+00	1.018e+02
1.041e+02	2.189e+01	-2.460e+00	1.018e+02
1.041e+02	2.194e+01	-2.417e+00	1.017e+02
1.041e+02	2.195e+01	-2.399e+00	1.017e+02
1.041e+02	2.194e+01	-2.407e+00	1.017e+02
1.041e+02	2.190e+01	-2.442e+00	1.017e+02
1.040e+02	2.183e+01	-2.499e+00	1.017e+02
1.040e+02	2.175e+01	-2.576e+00	1.017e+02
1.040e+02	2.165e+01	-2.667e+00	1.017e+02
1.040e+02	2.155e+01	-2.766e+00	1.017e+02
1.040e+02	2.145e+01	-2.866e+00	1.017e+02
1.040e+02	2.135e+01	-2.961e+00	1.017e+02
1.039e+02	2.127e+01	-3.043e+00	1.017e+02
1.039e+02	2.120e+01	-3.107e+00	1.017e+02
1.040e+02	2.116e+01	-3.149e+00	1.017e+02
1.040e+02	2.115e+01	-3.166e+00	1.017e+02
1.040e+02	2.116e+01	-3.157e+00	1.018e+02
1.040e+02	2.120e+01	-3.122e+00	1.018e+02
1.040e+02	2.127e+01	-3.064e+00	1.018e+02
1.040e+02	2.135e+01	-2.987e+00	1.018e+02
1.041e+02	2.145e+01	-2.895e+00	1.018e+02
1.041e+02	2.155e+01	-2.796e+00	1.018e+02
1.041e+02	2.166e+01	-2.696e+00	1.018e+02
1.041e+02	2.175e+01	-2.602e+00	1.018e+02

Figure 3.2: Simulation of Single Orbit in STK

and IGRF calculator and shows that it only changes -0.1 nT/year. Meanwhile, the STK graph shows that there is little to no variations in the magnetic field across the spacecrafts orbit. This allows us to take an average value of the magnetic field across a single period to make torque calculations. The average values are 104 nT, 21.56 nT, -2.775 nT, and 101.7 nT for magnitude, x-axis, y-axis, and z-axis, respectively. The torque caused by the magnetic field can be found with

$$T_m = DB \quad (3.2.10)$$

where D is the residual dipole for the vehicle and B is the Earths magnetic field [15]. According to the SMAD, a small-sized spacecraft has a dipole of approximately 1 Am². This results in a torque of 104 nNm. Since the satellite is orbiting in GEO, the aerodynamic drag of the satellite can be deemed negligible and requires no calculations.

3.3 Orbit Maintenance

The mission requirements set forth by I-MISSED require specific maneuvers to correct the orbital elements of the cubesat from perturbing forces. While in GEO, orbital maintenance must occur to correct for the perturbations caused by the Earth's oblateness and from the third-body gravitational effects of the Sun and Moon. The nonspherical Earth causes an acceleration in the plane of orbit known as East-West drift. The gravitational effects of the Sun and Moon cause out-of-plane accelerations known as North-South drift. North-South and East-West stationkeeping requires approximately 46 m/s/year and 2 m/s/year, respectively [15]. This would result in a total stationkeeping ΔV of about 480 m/s for the entire mission life.

At the end of the mission, the satellite must be disposed of appropriately to prevent additional space debris in GEO. The traditional course for most satellites is to deorbit them and return them to Earth. However, the ΔV to deorbit the cubesat would be approximately 2.258 km/s. The magnitude of this maneuver rules out deorbiting the cubesat. Instead, the cubesat will be placed in a graveyard orbit. The graveyard orbit is the typical resting place for GEO satellites because it pushes them 200 km or more above GEO which removes them as a potential space debris hazard. This maneuver would instead cost a ΔV of 7.4 m/s while raising the perigee to roughly 42,357 km [15].

3.4 Scheduling

The scheduling of the cubesat satellite will be autonomous with optional operator control from the ground when communications is established. The majority of the control will occur autonomously to both reduce operation costs and risks. Similarly, the low thrust of the electric propulsion system does not require supervisor oversight because even if a watchdog timer were to fail the low thrust would not endanger other space systems [15]. Manual control can occur any time connection is properly established with the spacecraft. When connection is established, ground control can transmit the appropriate data to adjust the spacecraft as they see fit including a different view angle for images. In the event of system failure posing risk to GOES-T, the cubesat will be able to immediately use the thruster to inject itself into the graveyard orbit before the schedule end of life. Even if the attitude control system has failed, the thruster would be able to perform both attitude control and the graveyard

orbit transfer itself. This capability provides a reliable failsafe for the mission in a necessitating circumstance.

The primary modes for the cubesat throughout mission life are imaging, station-keeping, and data transfer. Imaging is the default mode, and is in effect whenever any of the other modes are not. During this time, the attitude control system will ensure that the camera is pointed at the parent satellite. Because the imager will not be able to produce good images during the eclipse, the time spent in eclipse will be used for communications with the ground. The orbit will be set up such that during the eclipse, the cubesat will be between the Earth and GOES-T. By setting up the orbit this way, the antenna will already be pointing towards the Earth, so the satellite will have to do minimal additional pointing to point the antenna towards the ground station. The eclipse time will last approximately 52 minutes, during which the attitude control system will keep the antenna within the pointing requirement. Stationkeeping will occur during daylight so that the thruster can run solely off of power from the solar panels to reduce strain on the batteries. North-South station keeping will occur on a daily basis. At the beginning of life with about 12.5 kg of mass, the thrusters will be fired for 42 minutes. As the fuel gets consumed, this time will decrease slightly. Assuming the cubesat only uses the 540 m/s of ΔV , the thrusters would need to be fired for 39 minutes per day at end of life. East-West stationkeeping will be performed twice per month. The thrusters will need to be fired for 26 minutes per period at the beginning of life, and 24 minutes at the end of life.

3.5 Attitude Determination and Control System

The attitude determination and control system (ADCS) determines the orientation, positioning, and velocity of the spacecraft. The ADCS is composed of sensors, actuators, thrusters, and a computer.

The cubesat requires 3-axis control while both thrusting and non-thrusting. This control is achieved through a combination of attitude sensors and torquers. Both passive and full active control were explored to meet the 3-axis control requirement. The passive controls which include using gravity gradient and magnetorquers provide a coarse accuracy. Meanwhile, the active control methods using thrusters and reaction wheels provide high accuracy. The actuation systems taken into consideration were the following (Table 3.1):

ADCS Actuation	Information
Magnetorquer	Lightweight, reliable, simple, and energy-efficient
Reaction Wheel	Finer pointing accuracy and low fuel requirements
Thruster	Large torque and translational velocity as well as attitude

Table 3.1: Actuator Information

A magnetorquer provides the coarsest attitude control for a spacecraft. It creates a magnetic field that creates a torque when it interacts with Earth's magnetic field. In order to achieve 3-axis control, the spacecraft would require three orthogonal rods. This would generate a torque in any direction allowing for proper attitude control. The strength of these magnetorquers can be varied to adjust the strength and direction of the torque placed on the cubesat. However, magnetorquers are dependent entirely on the Earth's magnetic field. The integrated system elaborated upon later includes electromagnets capable of a magnetic dipole moment of 0.108 Am^2 [18]. With the strength of the magnetic field at GEO, the electromagnets are able to generate a torque of approximately 11.23 nNm . The three electromagnets alone are not capable of three axis stabilization. However, they can be used to counteract the torque generated by the gravity gradient.

Reaction wheels increase the attitude control capabilities significantly in comparison to magnetorquers. In order to obtain 3-axis stabilization, a system of reaction wheels must be used so that one is placed along each axis. However, reaction wheels can become saturated and require momentum dumping by another actuator. Reaction wheels vary in mass, power, momentum, and torque. The table in Figure 3.3 provides a list of various reactions wheels [19]:

The appropriate reaction must be able to counteract the worst disturbance torque with a margin factor taken into consideration. The disturbance torque experienced in every case is in nNm which is well below any of the reaction wheels under consideration. If slew rates are taken into consideration, then the max slew would be caused by a rotation along the z-axis to orient the spacecraft. The torque required to perform this slew in two minutes can be found with

$$T = \frac{4I\theta}{t^2} \quad (3.5.1)$$

Vendor	Type	Dimensions (mm)	Mass (g)	Peak Power (W)	Momentum (mNms)	Torque (mNm)
Sinclair	Wheel (Picosat)	50x50x30	120	0.7	10 (3410 RPM)	1
Maryland Aerospace	Wheel (MAI-300)	69x69x33	317	1.75	7.6 (10000 RPM)	0.625
Blue Canyon Tech.	Wheel (Microsat)	43x43x18	150	1	18 (6000 RPM)	0.6
Maryland Aerospace	Wheel (MAI-400)	33x33x39	90	2.05	11 (10000 RPM)	0.635

Figure 3.3: List of Reaction Wheels

where θ is the slew degree, I is the inertia, and t is the time to accomplish it. This results in a torque of 0.188 mNm which is still below the torques of all the reaction wheels. With torque not being a limiting deciding factor, the momentum storage capability for the reaction wheel was taken under consideration. The momentum storage requirement was calculated using

$$h = (T_D) \frac{OrbitalPeriod}{4} (0.707) \quad (3.5.2)$$

where T_D is the maximum torque disturbance, orbital period is the time for one period, one-fourth is when the maximum disturbance could accumulate, and 0.707 is the rms average of the sinusoidal function [15]. This results in a worst-case momentum build up of 8.5 mNms. The only reaction wheel eliminated by this requirement was the Maryland Aerospace MAI-300 wheel while all others were capable of sustaining it.

Taking into consideration the mission requirements need for both precision and redundancy, the Maryland Aerospace MAI-400 Integrated ADACS was chosen. The integrated system is the size of 1/2U and includes three reaction wheels, a 3-axis magnetometer, three electromagnets, an ADACS computer, and two sensors (including Star Trackers, IR Earth Horizon sensors, and Sun Sensors). The integrated system was originally chosen with a Star Tracker and an IR Earth Horizon Sensor. However, further investigation allowed the use of the payload imaging system to multitask as a star tracker. This significantly reduced the cost of the integrated system while al-

lowing it to be switched to a Sun Sensor. All three different sensors are still included into the system to add redundancy. A mission as high risk as I-MISSED requires redundancy to ensure the safety of not only itself, but the GOES-T satellite. In order to further the redundancy, an additional reaction wheel (same model as the ones used in the MAI-400) is added to the cubesat to bring the total reaction wheels to four. The final specs of the MAI-400 Integrated ADACS system are as follows [18].

- Dimensions: 10 x 10 x 5.16 cm
- Mass: 694 g
- Momentum Storage @10000 RPM: 11.076 mNms
- Max Torque: 0.635 mNm
- Magnetic Dipole Moment: 0.108 Am²
- Magnetometer: +/- 900 T
- Operating Voltage: 5V
- Minimum Power: 0.82 W
- Average Power: 1.13 W
- Peak Power: 2.05 W
- Operating Temp: -20 to 60 °C
- 4Hz sample rate
- B-dot algorithm
- Contains magnetic model of Earth
- Performs orbit propagation
- Provides telemetry

The integrated system allowed for adjustable configurations and minimal design adjustments since it came as a complete unit by itself.

3.6 Thruster Selection

To perform orbit maintenance, get in and out of the phase shift orbit, and to reach a graveyard orbit, a thruster had to be selected that would fit on the cubesat, and have enough ΔV capability to perform each of these maneuvers for the course of the 10 year mission life span. With the required stationkeeping ΔV of 480 m/s, 52 m/s of ΔV for the phase shift orbit transfers and insertion, and 7.4 m/s of ΔV needed for putting the satellite into a graveyard orbit, the total ΔV requirement for the mission is 540 m/s. In the event of unforeseen circumstances requiring additional maneuvers, or if during the mission life the thruster was required to perform attitude control due to other system failure, a factor of safety of 1.4 was decided on, raising the mission ΔV requirement to about 750 m/s. The secondary selection criteria for the thruster was the magnitude of thrust produced. Due to the persistent need for stationkeeping throughout mission life, a thruster with lower thrust capability would require a greater percentage of time thrusting for orbit maintenance, which would reduce the amount of time that could be spent imaging. In addition to these requirements it was determined that the thruster must not take up more than 2U of space on the 6U cubesat, to allow sufficient space for the imager, antenna, and batteries. Thruster selection was further constrained by the required power input. A thruster with too large of a power requirement would necessitate either larger batteries or solar panels that would be incompatible with the 6U design. The thruster also had to be able to be vectored so that it could perform momentum dumping for the reaction wheels and to perform attitude control to mitigate the risk of attitude control system failure.

With these requirements, a number of different kinds of thrusters were immediately determined to be unviable. Electrospray thrusters provided too little thrust, electrothermal thrusters required too much volume for fuel, and Hall thrusters required too much power. A trade study was performed on other thruster options that were considered more viable for both the types of propulsion, and specific models of each type, including RF Ion thrusters, Field Emission Electric Propulsion systems (FEEP) and hydrazine thrusters. The results of this study are shown in Figure 3.4.

This trade study revealed that despite the appeal of having very small thrusting times, the length of the mission required too much fuel volume for hydrazine thrusters to be used on a 6U cubesat. After ruling out hydrazine, the trade between an RF Ion

Criteria	Scale	Hydrazine Thruster	RF Ion Thruster	FEEP Thruster
Thruster Weight	1 = Best	1	3	2
Fuel Weight	3 = Worst	3	2	1
Thruster Volume		1	3	2
Fuel Volume		3	2	1
Percent of time station keeping		1	2	3
Power Requirements		1	3	2

Criteria	Hydrazine Thruster	BIT-3 RF Ion Thruster	IFM Nano Thruster
Weight (kg)	0.33	1.5	0.64
Fuel Weight (kg)	2.84	1.5	1.1
Thruster Volume (dm^3)	0.21	1.61	0.78
Fuel Volume (dm^3)	2.78 (SINGLE MODULE)	(SINGLE MODULE)	
Percent of time station keeping	0.00258	2.88	6.1
Power Requirement (W)	15	56	40

Figure 3.4: Thruster Trade Study

thruster and FEEP was that the ion thruster gave more thrust but took more power, mass, and space, and the FEEP system produced less thrust, but took less power, mass, and space. When considering specific models, it was found that the Busek BIT-3 RF Ion Thruster was set on a 2-axis gimbal to allow for thrust vectoring, whereas the IFM Nano Thruster required multiple thruster modules for the thrust to be vectored, removing the weight and space advantage it previously held. After considering the benefits of the gimbaled thruster and the lower required daily stationkeeping time, the Busek BIT-3 RF Ion Thruster [20] was selected as the thruster for this mission. Using the rocket equation, with an operating ISP of 1400 s, a required ΔV of 756 m/s, and an estimated dry mass of around 12 kg, the required fuel mass for the mission is about 0.7 kg.

3.7 GPS Orbit Determination

Since the follower cubesat will be flying in close proximity to the GOES-T, it is important to ensure that the follower cubesat has a very accurate estimation of its position and attitude. While traditionally, three attitude sensors can be used to triangulate position, this method does not give an accurate and precise enough estimate of position when traveling 7 km from another satellite. To give guarantees on a minimal risk of catastrophic collision, it is worth investing into a very precise method of orbital determination.

3.7.1 Using GPS in MEO for Orbit Determination in GEO

According to Stuart et al., it is possible to use GPS in GEO even though the GPS satellites are in MEO by using the GPS signals when the GPS satellites are on the opposite side of the Earth, as seen in Figure 3.5. In fact, this scheme is currently in practice for GOES-T [21]. The accuracy of GPS at GEO with certain receivers such as MosaicGNSS is up to $< 150m$ and $< 0.02m/s$ in position and velocity at a time under 750 ns; while less accurate than GPS in GEO ($< 10m$, $< 0.01m/s$, under 100 ns), this level of accuracy is enough for flying within 7km of GOES-T [22]. While MosaicGNSS has been studied to fly in GEO and have a receiver strong enough to receive signals from GPS satellites, the GNSS receiver chosen (NewSpace GNSS GPS receiver) has not been studied for this gain; with time for a further iteration of the design, this particular feature would be studied to confirm that the GPS receiver is powerful enough to receive the GPS signals.

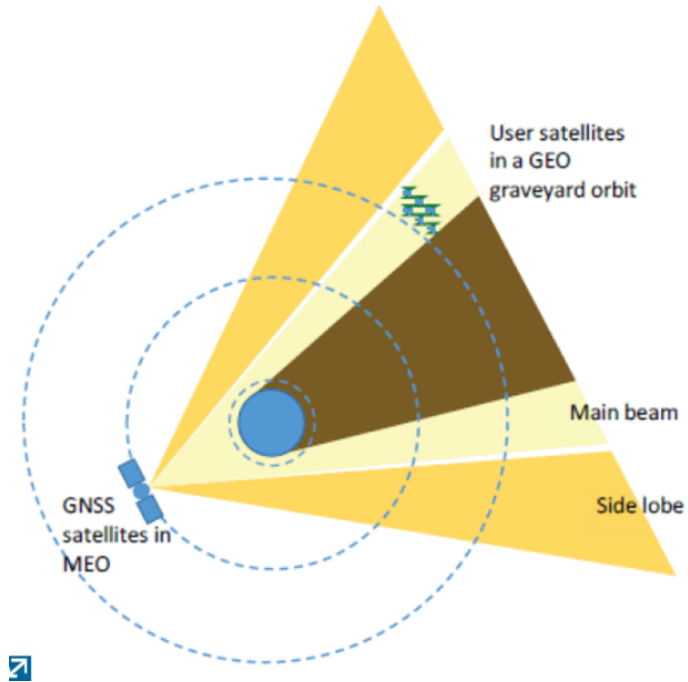


Figure 3.5: Method of Orbit Determination Using GPS for GEO

In order for this method to be used, we need to ensure that there is at all times at least 4 GPS satellites within view of the follower cubesat. This is shown to be indeed the case through an access STK simulation as shown in Figure 3.6, where it is seen that the cubesat has access to 4+ satellites at all points in its orbit and the orbits of the GPS satellites, ensuring this precise orbital determination will not be lost at any point during its orbit.

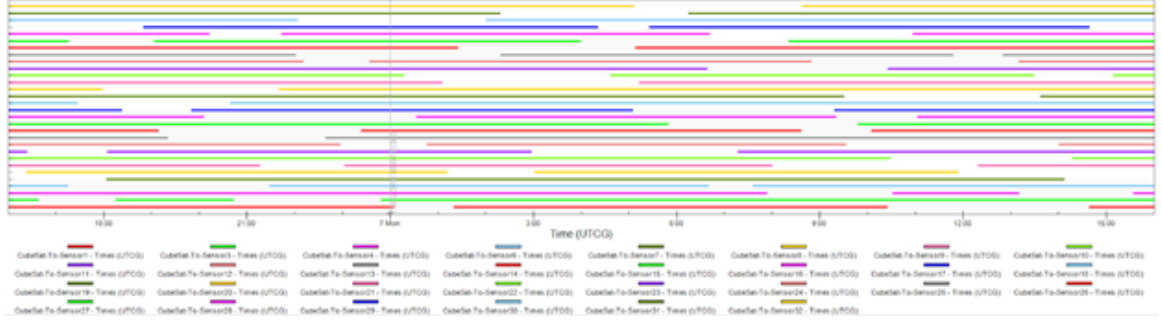


Figure 3.6: Access to GPS satellites in MEO in one orbit of I-MISSED in GEO

3.7.2 Using Payload Imager

Another method of orbit determination as a back-up method is to use the payload itself since the payload is an imager. If it is assumed GOES-T stays vertical, any change in the number of pixels GOES-T takes up in the payload's images would likely mean that the cubesat is closer/farther than its nominal position rather than a change in the attitude of GOES-T. Qualitatively, if GOES-T takes up more pixels in the cubesat's imager than in its nominal position, GOES-T is closer than expected. If GOES-T takes up less pixels in the cubesat's imager than in its nominal position, GOES-T is farther than expected. Quantitatively, however, this method does not provide better information than the GPS in GEO method discussed earlier. As explained in Chapter 4, at a distance of 10 km, the cubesat's imager provides a resolution of 21 pixels to cover the 6.1 meter GOES-T [23]. If the imager detects that GOES-T now covers 22 pixels for example, this would mean that the cubesat is 9.545 km away from GOES-T, rather than 10km as in its nominal orbit based upon Equation 3.7.1 and specifications provided in Chapter 4 for the imager where $\frac{Swath(km)}{2*\text{@altitude}} \frac{1000*Swath(km)}{GSD(m)} = 1.452 * 10^{-5}$, calculated from backing out 21 pixels at 10 km. Thus, this method would provide information if the cubesat drifted 0.455 km closer to GOES-T.

$$Distance\ from\ GOES(km) = \frac{SatelliteSize(km)}{Pixels * 2 * \frac{Swath(km)}{2*\text{@altitude}} \frac{1000*Swath(km)}{GSD(m)}} \quad (3.7.1)$$

Figure 3.7 shows the distance from GOES-T based upon the number of pixels it takes up in the imager's pictures, proving it can be used as a method of orbital determination. Since the GPS in GEO method provides accuracy $< 0.150km$, this method may be used as a back-up rather than the primary method of orbit determination, helping with assuring confidence that the cubesat will not hit GOES-T.

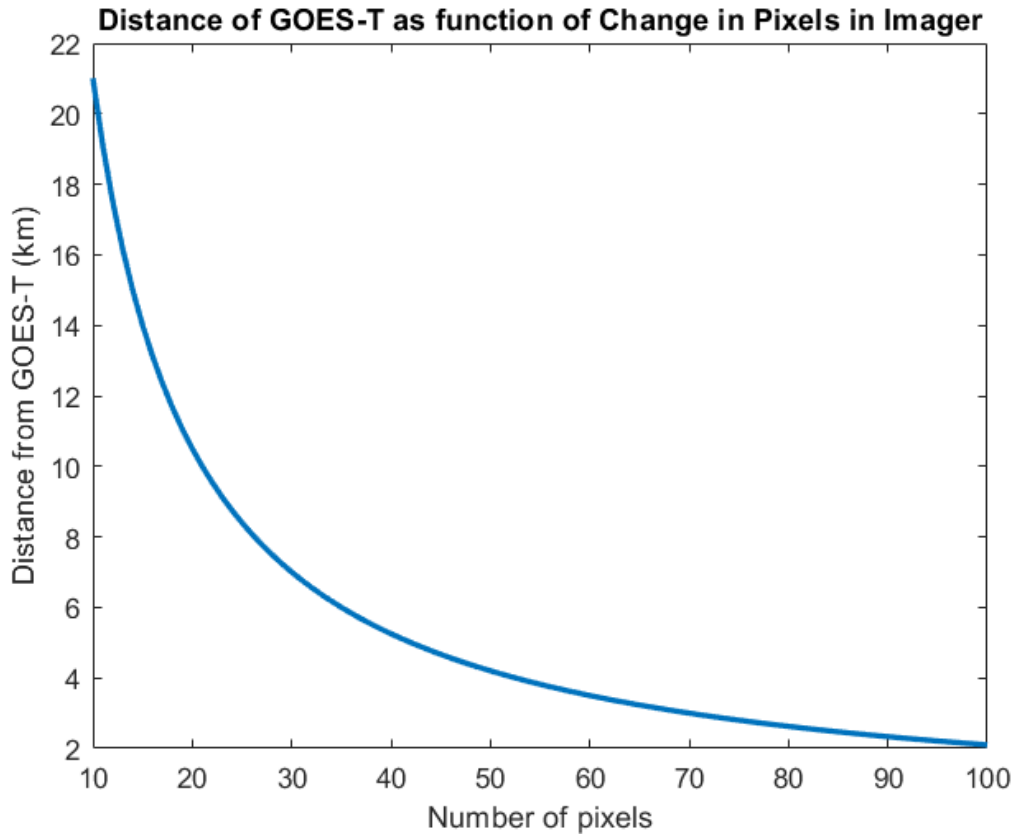


Figure 3.7: Orbit determination using imager

3.8 Detumbling

When the cubesat is ejected from the dispenser, it will have an initial rotation. Attitude control must be achieved before it can properly deploy its solar array and begin its mission. The exact determination of detumbling can not be perfectly calculated because the exact moment of ejection has numerous variables that can not be accounted for. The cubesats internal computer will gauge these conditions upon ejection from the dispenser and perform the necessary adjustments to stabilize the spacecraft. However, if the worst case scenario is taken into consideration, then the spacecraft will be able to detumble under most conditions. The despin maneuver will be achieved utilizing the reaction wheels. The initial tumbling rate can be determined with the following data (Figure 3.7) [24]:

This shows that the worst case of the tumbling rate would occur about the yaw (y-axis) with approximately 10 deg/sec. The time necessary to detumble can be taken

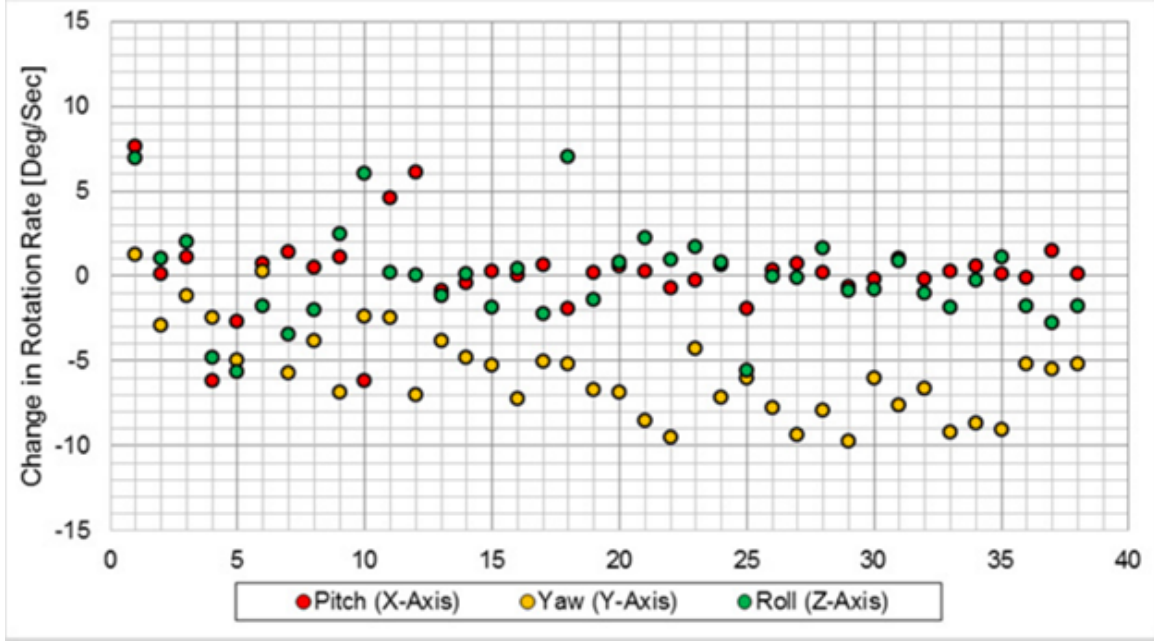


Figure 3.8: Change in Rotation Rate for the First 40 Seconds

assumed to be [25]:

$$Torque = I_{yy}\dot{\omega}_y = I_{yy} \frac{\Delta\omega}{\Delta t} \quad (3.8.1)$$

We assume $\dot{\omega}_y$ to be 10 deg/sec, I_{yy} to be $4.216 \times 10^6 gcm^2$, and the torque of a reaction wheel to be 0.635 mNm. This makes the time necessary to detumble to be roughly 32 secs.

3.9 Control Simulation

As a demonstration of the ADCS components selected being able to do the necessary maneuver, a control simulation was done that shows that the needed maneuvers are possible in a reasonable amount of time. The attitude control is modeled through the which can be simplified as a system of double integrators, given in the transfer function in Equation ???. This system can also be modeled as a state-space system as given in Equation 3.9.1 where $\dot{x} = Ax + Bu$,

$$A = \begin{bmatrix} 0 & 1 \\ 0 & 0 \end{bmatrix} B = \begin{bmatrix} 0 \\ \frac{1}{I_{xx}} \end{bmatrix} C = \begin{bmatrix} 1 & 0 \\ 0 & 1 \end{bmatrix} \quad (3.9.1)$$

where the moment of inertia matrix is modeled as a diagonal matrix and the simulations are done for one decoupled system; thus, only one angle at time and only I_{xx} used. Linear quadratic regulator (LQR) control is a form of optimal control in which the algorithm minimizes the cost function to give a control input u as given in Equation 3.9.2, allowing for the control engineer to adjust the weights placed on accuracy of the states and the penalty on control effort [26].

$$J_{LQR} = \int_0^{\infty} (\mathbf{x}^T Q \mathbf{x} + \mathbf{u}^T R \mathbf{u}) dt \quad (3.9.2)$$

The Q and R matrices used here in Equation 3.9.3

$$Q = \begin{bmatrix} 1 & 0 \\ 0 & 1 \end{bmatrix} \quad R = [0.1] \quad (3.9.3)$$

were chosen in order to ensure the control effort was not above the maximum torque of the reaction wheels (0.00635 Nm) and that the system responded to references or disturbances in an acceptable amount of time.

The initial condition response to an initial condition of the maximum perturbation the cubesat could experience in this environment (orbit plane rotation from third body effects of Sun and Moon equal to -0.00984 deg/day) is given in Figure 3.9 with the associated control effort given in Figure 3.10. The step response to a reference scaled to the maximum input of the reaction wheel is given in Figure 3.11. As shown by the rise time and settling time of the response being under 6 seconds, this system can be stabilized and track a reference in an acceptable amount of time.

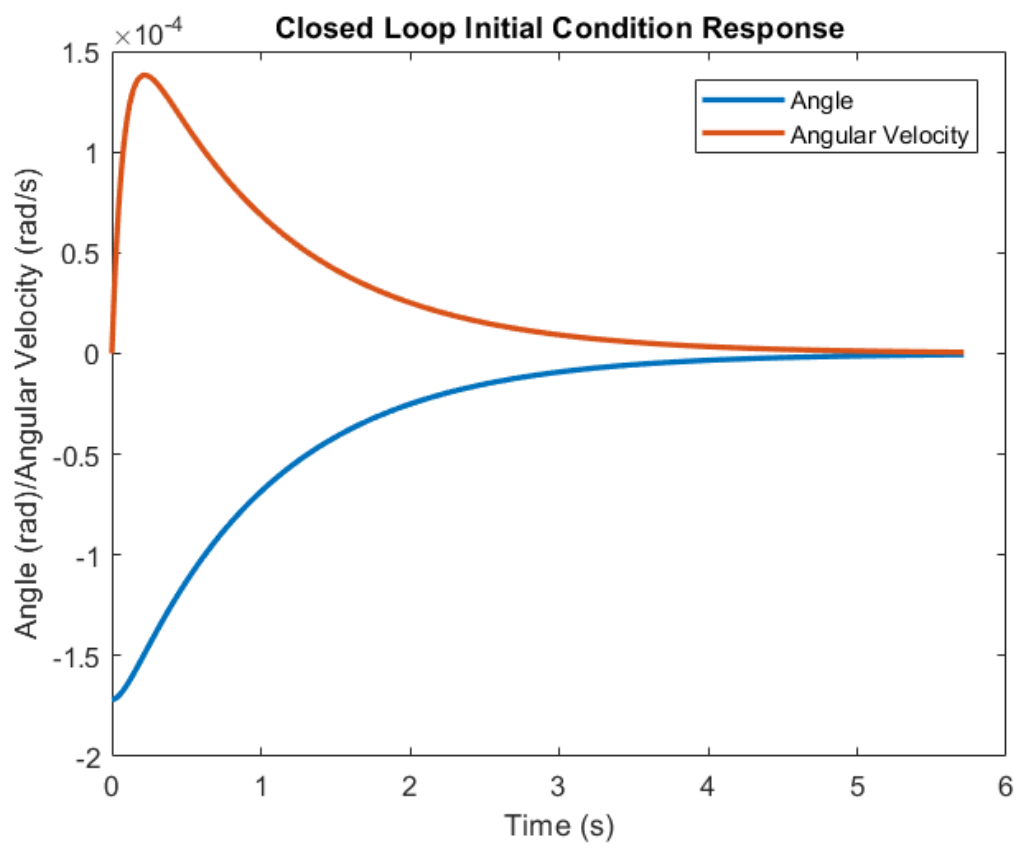


Figure 3.9: Initial Condition Response

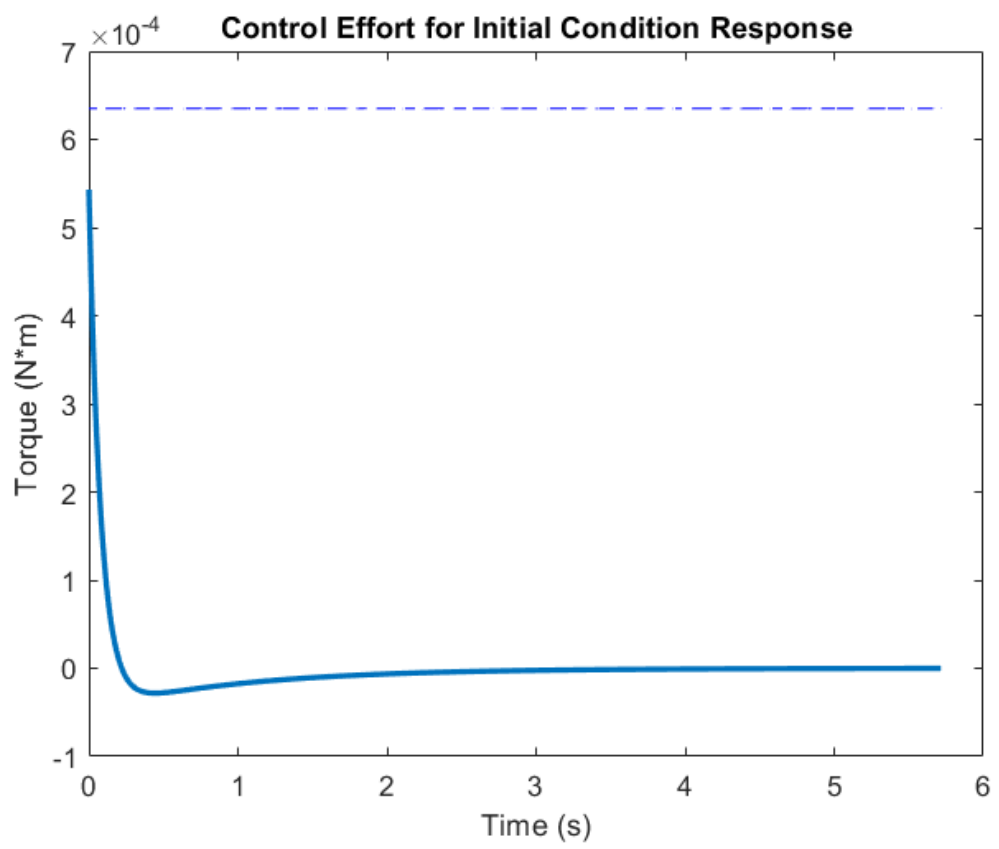


Figure 3.10: Control Effort for Initial Condition Response

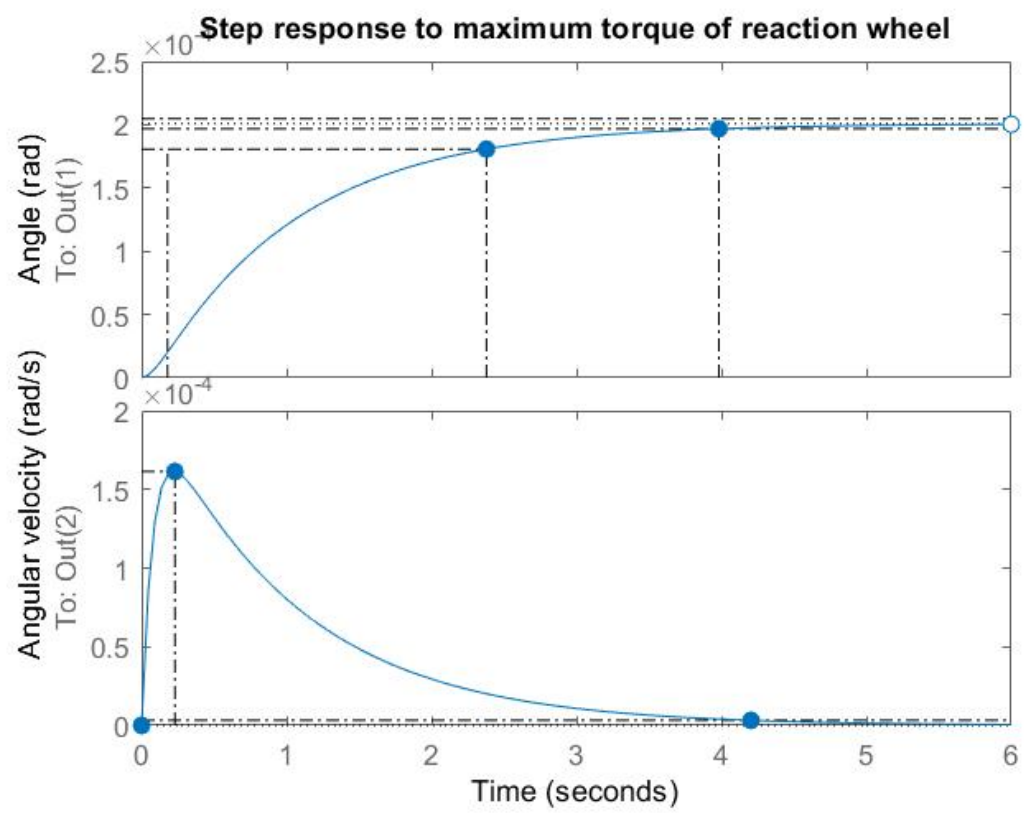


Figure 3.11: Response to Step Input

Chapter 4

Payload

The purpose of the Payload/Communications subteam is to both determine the hardware required to complete the mission of imaging the positions of objects of interest (other satellites and space debris) and to plan for the communication of the satellite with the ground. This team will determine the mass, thermal, and electrical requirements of each of the components and relay the data to the other teams for analysis.

4.1 Imager

The primary objective of the I-MISSED mission is to observe its subject satellite, GOES-T, and provide NOAA with physical information of GOES-T that could be integral to the success and longevity of the GOES mission. To that end, an appropriate imager is required to accumulate that information. I-MISSED requires an imager that has high angular resolution from the distance it's imaging from, yet is compact enough to fit within a 1U (10 cm^3) cube. To meet these requirements the Payload Team began by researching high resolution space-grade imagers. Initially, the Team aimed for a camera that could achieve an image resolution of 100 pixels along the axis of the GOES-T satellite from a distance of 10 km.

4.1.1 Imager Selection

As illustrated in the chart below, the Team performed a series of trade studies to narrow down the viable options and determine what features of the imager were most important for the success of the mission. There were certain rigid requirements that

the imager had to meet, including fitting within 1U and requiring a minimal power draw. Many of the preliminary imagers were either not designed for a cubesat, thus incompatible with a 1U allocation of space, or fell far short of the goal to achieve 100 pixels along the axis of GOES-T from 10 km away.

Mission/Imager	GSD (m)	@Altitude (km)	Swath (km)	@Altitude (km)	Aperture (mm)	Pixels along one axis	Size
Beijing-1	32	700	600	700		13.125	Satellite: 60 cm x 60 cm x 60 cm, plus antennas
DubaiSat-1 DMAC (PAN)	2.5	680	20	680	300	163.2	Satellite: 120cm diameter, 135cm height
DubaiSat-1 DMAC (Multi-spectral)	5	680	20	680	300	81.6	Satellite: 120cm diameter, 135cm height
DubaiSat-2 HiRAIS	1	600	12	600	400	360	Satellite: 150cm diameter, 195cm height
UrTheCast	4	590	12	600	420	90	Satellite: 150cm diameter, 195cm height
SkySat 1	1	450	8	450		270	Satellite: 60cm x 60cm x 80cm
Dove-2	4.4	575	24x16		400	90	3-5 m/pixel
Razak	2.5	685	20	685		164.4	
SCS Gecko	39	500	80	500		7.692307692	Imager: <1U (97 mm x 96 mm x 60 mm)
NigeriaSat-2	2.5	700	20	700		168	Satellite ~~~120 cm x 120 cm
HyperScout	40	300	164	300		4.5	
Hyperion	30	705	7.5	705	120	14.1	Satellite: 39cm x 75cm x 66cm
DoveSat-PS0/PS1	4	620					
NanoCam C1U	30	650					
Salantis	1.1						
LANDMAPPER-HD	2.5	650	25	650		156	16U
STARE						21	1U imaging system

Figure 4.1: Imager Trade Study

To determine the number of pixels along an axis of GOES-T, the Payload Team used the following equation:

$$Pixels = \frac{SatelliteSize(km)}{2 * (DistanceFromGOES(km)) * (\frac{Swath(km)}{2 * @altitude(km)}) * (\frac{1000 * Swath(km)}{GSD(m)})} \quad (4.1.1)$$

As the Team went through the available options and configurations for an imager, an emphasis was placed on finding a COTS package. This led the Team to consider the SCS Gecko and HyperScout, among others. Unfortunately, these two imagers would provide only 8 and 5 pixels along an axis of GOES-T, respectively. These numbers were deemed unacceptable for our mission concept, as such low resolution imagery would not yield much physical information about the GOES-T satellite beyond a basic confirmation that the satellite is indeed there. The primary difficulty of choosing an imager came down to an underlying problem of the lack of COTS cubesat imagers capable of meeting our mission objective. The Team weighed the pros and cons of the restriction placed on COTS hardware, and decided to expand the search to hardware that may not be COTS, but has been successfully tested in a similar cubesat configuration and is at a TRL of at least 7.

4.1.2 STARE Imager

With an expanded field of view, the Payload Team decided to model I-MISSED's imager on the imaging system employed by the Space-based Telescopes for the Actionable Refinement of Ephemeris (STARE) mission. The STARE mission objective is functionally similar to that of I-MISSED, as STARE aimed to "observe space debris that is predicted to pass close to a valuable space asset." [23] The STARE mission employs a modified Cassegrain telescope with a Cypress IBIS5-B-1300 CMOS imager, all packaged into a 1U unit. Most importantly, the mission was successfully launched in 2012, and so the integrated hardware package is at TRL 8. Features of the Cypress imager are summarized in Table 4.1 below.

Characteristic	Cypress IBIS5-B-1300 Imager
Active Pixels	1280 (H) x 1024 (V)
Frame Rate	27 fps
S/N Ratio	64 dB
Supply Voltage	Digital: 3.3 V
Power Consumption	175 mW
Operating Temperature	-30 degrees C to +65 degrees C
Color Filter Array	Mono RGB Bayer Pattern

Table 4.1: Cypress IBIS5-B-1300 Imager

The telescope, as seen below in Figure 4.2, has a focal length of 225 mm, an aperture of 85 mm, and a resolution of 29 μ rad/s. At a range of 10 km, the telescope will provide images with about 29 cm/pixel. The field of view of the telescope is 2.08 x 1.67 degrees. The STARE mission ran into a critical problem implementing this Cassegrain telescope in regards to the extreme temperature fluctuations in space and due to the lack of an onboard focusing mechanism. Without modification a Cassegrain telescope would be free to thermally expand and contract without any correction to its focus point, potentially rendering images useless. The STARE mission designed their Cassegrain telescope to have a depth of focus of 10 microns and employed an Invar support structure to protect against thermal expansion and contraction. I-MISSED's antenna will have the same constructive features. STARE's preliminary tests show that the focus will be maintained if the telescope is kept within a temperature range of -20 degrees C to +60 degrees C.

The full optical payload of I-MISSED has a mass of less than 1.83 kg.

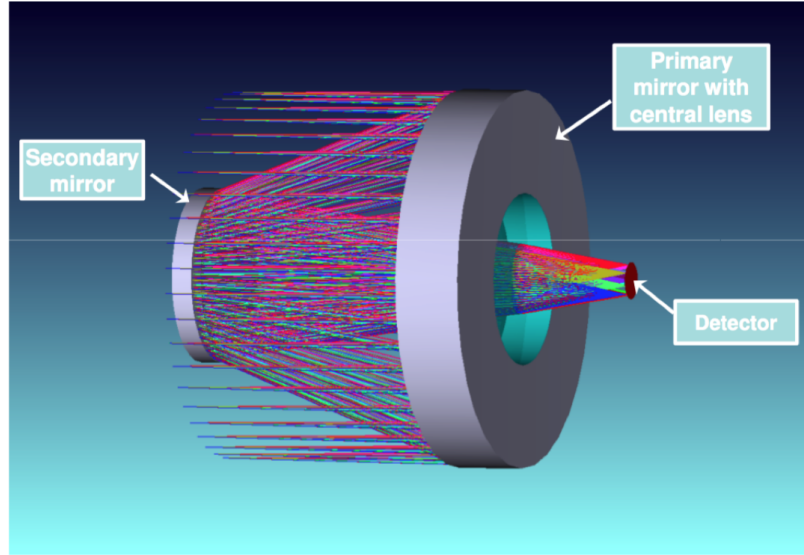


Figure 4.2: STARE’s Modified Cassegrain Telescope [23]

4.2 Telecommunications, including telemetry and Control

The most important aspect of the mission after recording images is getting those images back to the ground. In this regard, the Payload Team considered several methods of data transmission. The first method that was considered was to communicate directly to the ground with a high gain, high directivity antenna. This approach, although viable, seemed ambitious for a cubesat at GEO. So, the Team explored a second option of communicating directly to GOES-T and using GOES-T’s communication system to transmit I-MISSED images along with its data. This would require data transmission at a frequency that GOES-T receives at, which is in the L-band [27]. Third, the Payload Team also considered transmitting to the third party TDRSS data relay satellite system.

4.2.1 Antenna Selection

Initially, for a cubesat to ground network, the Payload Team looked into transmitting in the S-band to utilize high gain antennas that transmit S-band frequency and that have been developed for cubesat setups. In particular, a Boeing antenna from their Phantom Works program was particularly attractive. Their Miniature Deployable High Gain Antenna has been tested and is currently a working prototype, featuring

a gain of 18 dBi and weight less than 1 kg [28]. Although not immediately available, this led the Team to research other high frequency options for a direct ground link.

4.2.2 Ground Stations

At 137 degrees West, the location of GOES-T, the nearest ground stations were determined to be in Hawaii, where there are a variety of options. The transmitted frequency for a ground link system is constrained by the capabilities of the ground station. The options the Payload Team considered were ground stations at Honolulu Community College (L, X-band), Kauai Community College (VHF, UHF, L, S-band), and University of Hawaii at Manoa (UHF, S-band) [29].

As mentioned in Section 2.1, the environmental constraint on transmission imposed by the atmosphere requires a transmission frequency of at least 29 MHz. Data transmission at this low of a frequency was never considered, therefore environmental constraints did not play a meaningful role in our communication system design. The only other constraint comes from power, consumption of which was a high priority in the transceiver selection. Intuitively, transmitting data at higher frequencies requires more powerful transceivers, which place a greater power draw on our cubesat.

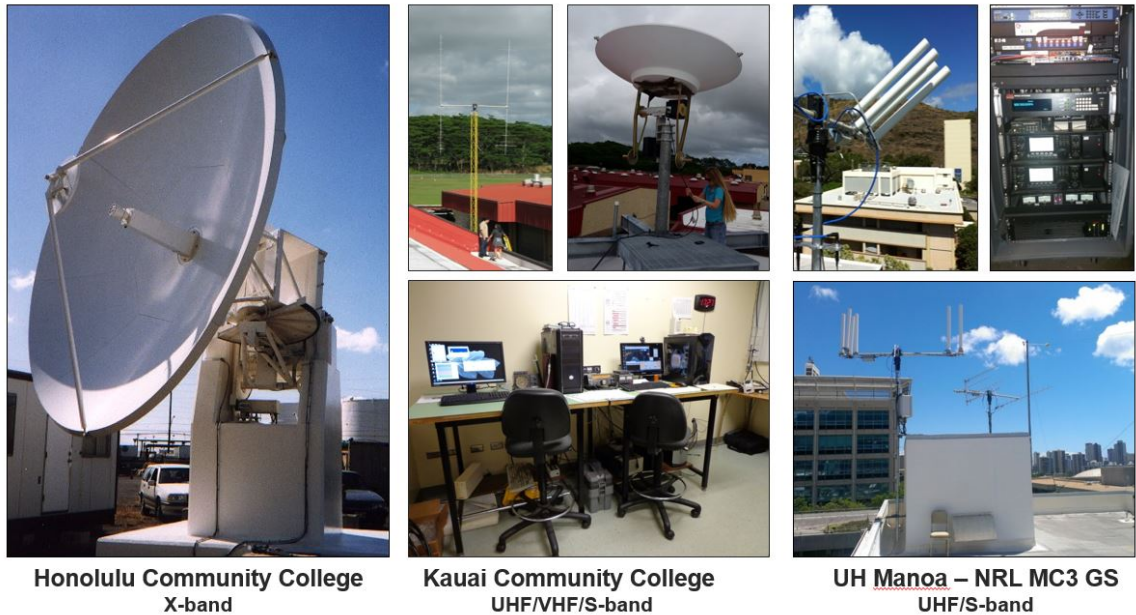


Figure 4.3: Possible Ground Stations In Hawaii [30]

4.2.3 Link Budgets

To keep the power draw to a minimum, the Payload Team first calculated a link budget to the Kauai Community College ground station using the lower UHF-band. The Payload Team calculated a link margin of 1.5 dB and a high SNR of 39.8 dB. These numbers indicate a realistic and sound connection. This system was found to be attractive for a couple of reasons. First, as mentioned, transmitting in the UHF band requires less power than transmitting at a higher frequency. Second, directly communicating to the ground bypasses the dependency on GOES-T's communication system. The mission objective of I-MISSED is to provide valuable physical information on GOES-T, and physical information may not be more valuable than when GOES-T is not properly working. That is, it is possible that GOES-T may not be transmitting its data correctly and reasonable to assume that mission command would want a look at GOES-T's antenna system. If I-MISSED was dependent on GOES-T to transmit its data, I-MISSED would fail on its mission objective in such a scenario. Furthermore, I-MISSED will be on-orbit for about a year before GOES-T is on-orbit, meaning mission command would be without communication for this time if I-MISSED was without the ability to transmit to the ground. This effectively eliminated the idea of transmitting directly to GOES-T from consideration by the Payload Team. Additionally, the Payload Team found communication with TDRSS impossible due to TDRSS's Earthwards field of view. With the decision made to transmit directly to the ground, the communication system design of I-MISSED then came down to frequency and ground station selection.

Item	Unit	Sat->Earth Value	Item	Unit	Sat->Earth Value
Frequency	Hz	4.37E+08	Atmospheric loss	dB	4
Transmit power	dBm	27	Received power	dBm	-102.5
	W	0.50		dBW	-132.4
	dBW	-3		W	5.69E-14
Transmitter antenna gain	dBi	11.5	System noise temperature	K	362
Antenna return loss	dB	10+	Data rate	bps	1200
Receiver antenna gain	dB	39.9	SNR	dB	39.8
Distance	m	3.59E+07		Scalar	9.49E+03
Wavelength	m	6.87E-01	EIRP	dB	8.00
Path loss	dBW	176.4	Receiver sensitivity	dBm	-104
	dBm	206.4	Link margin	dBm	1.5
Line loss	dB	0.5			

Figure 4.4: I-MISSED's UHF Downlink Link Budget

Item	Unit	Earth->Sat Value	Item	Unit	Earth->Sat Value
Frequency	Hz	1.46E+08	Atmospheric loss	dB	4
Transmit power	dBm	27	Received power	dBm	-98.4
	W	0.50		dBW	-128.4
	dBW	-3		W	1.43E-13
Transmitter antenna gain	dBi	34.4	System noise temperature	K	221
Antenna return loss	dB	10+	Data rate	bps	1200
Receiver antenna gain	dB	11.5	SNR	dB	45.9
Distance	m	3.59E+07		Scalar	3.92E+04
Wavelength	m	2.06E+00	EIRP	dB	30.9
Path loss	dBW	166.8	Receiver sensitivity	dBm	-104
	dBm	196.8	Link margin	dBm	5.6
Line loss	dB	0.5			

Figure 4.5: I-MISSED’s VHF Uplink Link Budget

To determine the received power, the Payload Team used the following equation in Figure 4.6:

$$P_r = P_t + G_t + G_r - 20 \log_{10} \left(\frac{4\pi d}{\lambda} \right)^2 - A_R - A_G$$

Figure 4.6: Friis Transmission Equation

To determine the signal to noise ratio, the Payload Team used the following equation in Figure 4.7:

$$\begin{aligned} \text{SNR}_{dB} &= 10 \log_{10} \left(\frac{E_b}{N_0} \right) \\ &= 10 \log_{10} \left(\frac{P_t G_t G_r}{k T_s R L_p} \right) \\ &= P_{t,dBm} - 30 + G_{t,dBi} + G_{r,dBi} - L_{p,dB} \\ &\quad - 10 \log_{10} k - 10 \log_{10} T_s - 10 \log_{10} R. \end{aligned}$$

Figure 4.7: Signal to Noise Ratio Equation

4.2.4 Transceiver Frequencies

To determine the optimal transmission frequency the Payload Team ran trade studies for transceivers in the VHF, UHF, X, L, and S-bands. The reasons for using higher

frequencies, other than for available bandwidth, is for faster data transmission and greater leniency provided in antenna size. That is, higher frequencies can be picked up by smaller-sized antennas. On the opposite side of those two perks is the increased power requirement of transmitting at higher frequencies. Weighing the pros and cons of higher frequency transmission and considering the link margins afforded by each option, the Payload Team determined transmitting to the Kauai Community College ground Station in the UHF frequency range to be the best. Transmitting in UHF requires less power than transmitting at the higher frequencies. Furthermore, from the link budgets shown in Figures 4.4 and 4.5, the Payload Team demonstrates the feasibility of using the UHF antenna at Kauai Community College, thus alleviating the need to transmit at a higher frequency. Additionally, transmitting at a lower frequency results in less path loss, enhancing our link margin. The reason the Payload Team opted for UHF over VHF, which requires less power and results in 10 dB less path loss than UHF, is due to the availability of a Northrup Grumman high-gain antenna developed and tested for cubesat use in the UHF frequency band. There is no similar antenna option that transmits in the VHF-band. As demonstrated in the below link budget, Figure 4.8, transmitting at VHF and using a COTS VHF antenna and transmitter available from CubeSatShop.com, the high gain UHF antenna outweighs the pros of transmitting at VHF. Clearly, the inadequate link margin of -4 dB is vastly inferior to the link margin of 1.5 dB achieved using the UHF frequency and Northrup Grumman's high gain, high directivity antenna.

Item	Sat->Earth Value		Item	Sat->Earth Value	
Frequency	Hz	1.46E+08	Received power	dBm	-108.4389406
Transmit power	dBm	23		dBW	-138.4389406
	W	0.1995262315		W	1.43E-14
	dBW	-7	Line loss	dB	0.5
Transmitter antenna gain	dBi	0	Atmospheric loss	dB	4
Antenna return loss	dB	10+	System noise temperature	K	362
Receiver antenna gain	dB	39.9	Data rate	bps	1200
			EIRP	dB	-7.5
Distance	m	3.59E+07	Receiver sensitivity	Scalar	-104
Wavelength	m	2.05E+00			
Path loss	dBW	166.8389406	Link margin	dB	-4.438940571
	dBm	196.8389406			

Figure 4.8: VHF Downlink Link Budget

The Northrop Grumman deployable antenna features a free deployment, deploying entirely with stored strain energy in about 2 seconds [31]. Furthermore, the antenna

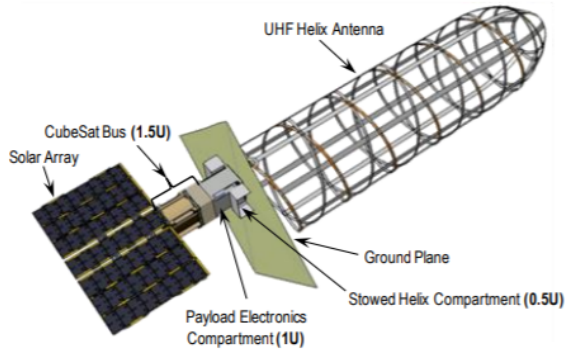


Figure 4.9: Northrop Grumman High Gain, Deployable, UHF, Helical Antenna

features an exceptionally high gain and directivity for a cubesat as can be seen in the below graphs.

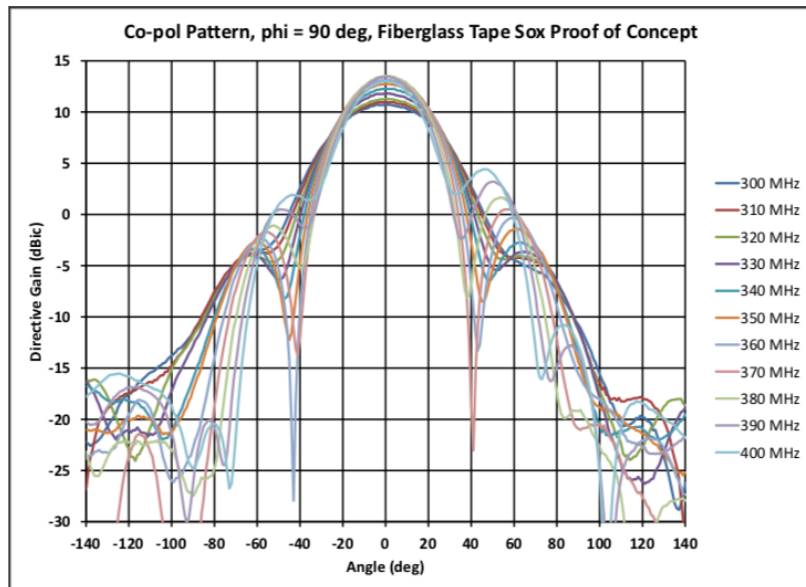


Figure 4.10: Directive Gain of I-MISSED's Antenna

I-MISSED will be on orbit for about a year before GOES-T arrives on orbit, and will need to adjust its location to hone in on GOES-T. During the transfer orbit where I-MISSED lowers and then raises its altitude, communication to ground stations other than Kauai become advantageous. Thus, during the transfer orbit I-MISSED will transmit to three different ground station - Kauai Community College in Hawaii, Goldstone Deep Space Communications Complex in California, and Wallops Island in Virginia. As I-MISSED moves throughout its transfer orbit I-MISSED will be able to transmit to one of the three ground stations about every two weeks.

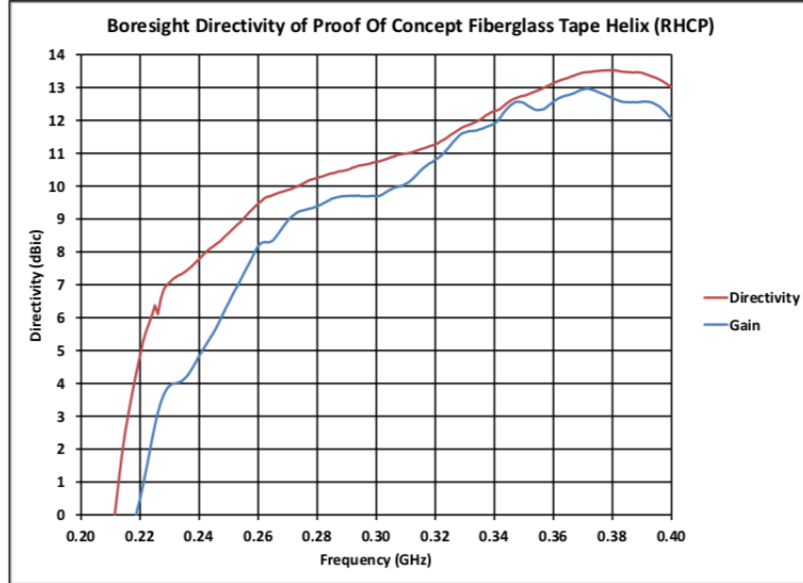


Figure 4.11: Directivity and Gain of I-MISSED’s Antenna



Figure 4.12: ISIS UHF Full Duplex Transceiver

4.3 Data

A requirement of I-MISSED’s mission objective is to have a meaningful number of pixels along an axis of the GOES-T. This would ensure that a informative image would be taken. An initial goal of 100x100 pixels was found to be unrealistic and COTS equipment put the number around 10x10 pixels. With the STARE optical system the Payload Team expects to see 21 pixels along an axis of GOES-T.

4.3.1 Data Handling

Based on the specifications of the transceiver, the lowest transmit rate, of 1200 Bd, was chosen to minimize power requirements. At this data transfer rate, transmitting

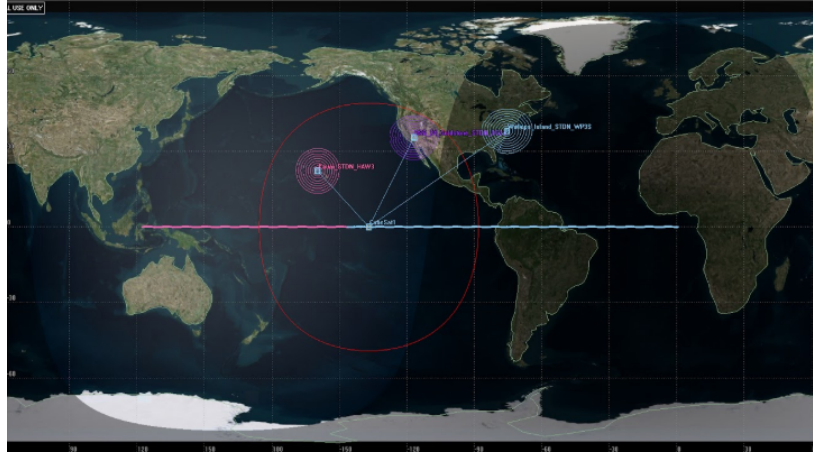


Figure 4.13: I-MISSED Ground Track and Kauai Community College Ground Station

a full 1.3 megapixel raw image from the CMOS chip would require over two hours. To minimize this time, a processor built into the STARE telescope will employ an algorithm to clean up the image and make it easier to handle. Since the vast majority of each image will be black space, algorithms can be used to reduce the size of an image by only keeping the important pixels. One of the easiest ways to do this would be to pick a threshold for the amount of black to accept, and remove all pixels below that threshold. However, doing so also has the challenge of keeping other non-useful information such as the pixels corresponding to the Sun or Earth. Other algorithms can be used to differentiate between these objects, by looking at size, brightness and other factors.

As set by the ground stations, modulation schemes used will be QPSK (Quadrature Phase-Shift Keying) for NASA Near Earth Network ground stations on the way to GEO and AFSK (Audio Frequency-Shift Keying) for the final ground station at Kauai Community College.

4.3.2 Size of Data

Transmitting only meaningful information could yield an image size as small at 50x50 pixels. To be sure, an image size of 60x60 pixels would be appropriate, where each pixel will have three 8-bit numbers corresponding to its RGB value. This would correlate to 10.5 kB per image and the transceiver would require under 9 seconds to transmit each image. This would correspond to 400 images to the ground per hour of transmission.

4.3.3 Scheduling for Data

The observation schedule will involve 22 hours of imaging per day. There will be 42 minutes of thrusting and an average of 52 minutes of eclipse time. During eclipse time, transmitting at 1.2 kBd over 52 minutes, 3744 kB will be transmitted. This consists of 5 minutes for downlinking spacecraft telemetry and other data (totalling 360 kB), 5 minutes for uplinking commands (totalling 360 kB), and 42 minutes for downlinking images (3024 kB), with 1 hour downtime. 3024 kB, with 10 kB per image, means 302.4 images, and 21 hours of imaging time for 302 images, results in an image being taken once every 250 seconds.

This value can also be reduced further by implementing various compression algorithms to reduce the size of an image further. This would mean that more pictures could be taken if an image is compressed enough. Since most of the images will be very similar, it also means the compression could be very efficient. However, assuming there is no compression factor gives a better lower bound on the number of images that can be taken to later be transmitted.

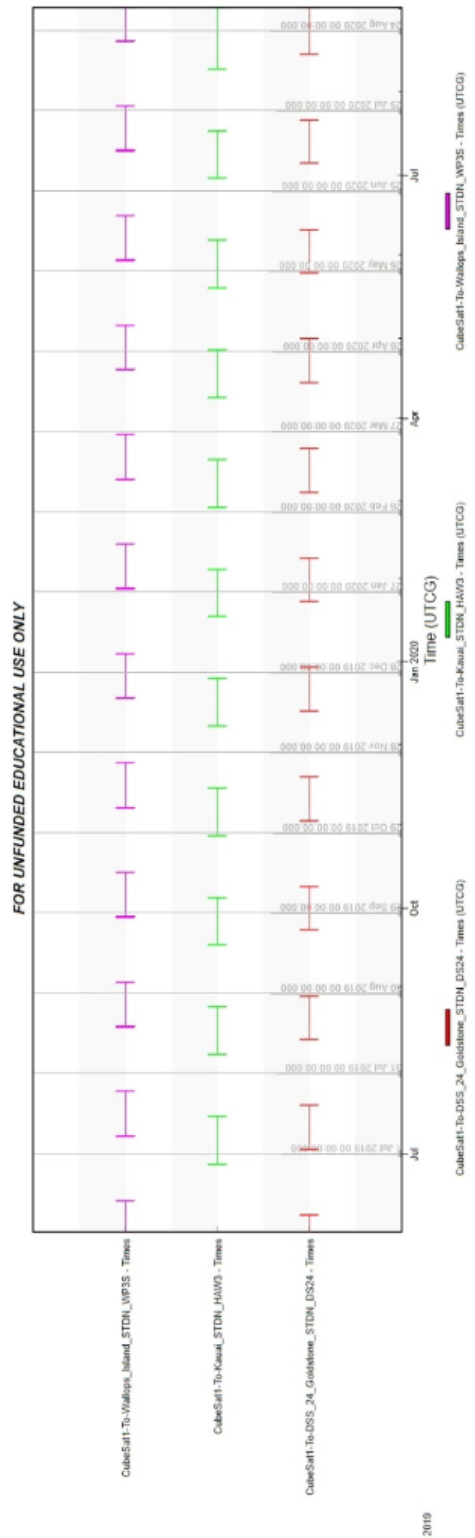


Figure 4.14: Ground Station Access during Longitude Shift

Chapter 5

Power and Thermal Control

The Power and Thermal Control (PTC) subteam designs and implements the mechanisms through which the spacecraft extracts and stores power. Additionally, this subsystem takes into account the design and implementation of the Thermal Control System (TCS), which ensures that all spacecraft components are within acceptable temperature ranges during all mission phases, through both passive and active means. PTC engineers were also responsible for estimating the power consumption of the spacecraft's electronic components.

As will be described in the sections that comprise this chapter, after identifying the power requirements of the spacecraft, an off-the-shelf lithium ion secondary battery and an off-the-shelf solar array was chosen to provide power for the entirety of the mission. Additionally, after quantifying the effect of various heat fluxes on the spacecraft, in order to maintain all electrical components of the spacecraft at operating temperatures, the following thermal system was implemented: a black paint coating and louver system on the surface area of the chassis surrounding the thruster, an iron oxide coating on the rest of the chassis, and a teflon gold backing on the back of the solar array.

5.1 Power Loadings

Four power modes required to complete the mission were identified: Standby, Imaging, Data Link, and Thrust.

Standby Mode consists of the electrical components assumed to run continuously throughout the duration of the mission—the flight computer and most of the attitude

determination and control system (ADCS) suite. As seen in Table 5.1, Standby Mode requires the least power of all power modes. This is the average power mode, due to it being the mode the spacecraft is in most of the time, in usage even during eclipse.

Imaging Mode considers the power load of the imager and is used for 6 minutes per day (the amount of time it takes to take 360 images). Data Link Mode considers the transceiver and is used for an hour (the amount of time it takes to send the 360 images taken). Thrust Mode considers the thruster and is used for 42 minutes per day for station-keeping, also accounting for any scenario in which the spacecraft may have to communicate and thrust at the same time; this is the peak power load. Note that these three aforementioned power loads are utilized while in daylight, for reasons expounded upon in the following section.

Table 5.1: Power Budget

Subsystem	Component	Power Mode Demand (W)			
		Standby	Imaging	Data Link	Thrust
Payload	On Board Computer	0.550	0.550	0.550	0.550
Payload	Image Sensor	—	0.175	—	—
Payload	Duplex Transceiver	—	—	4.000	4.000
GNC	ADACS	7.230	7.230	7.230	7.230
GNC	Reaction Wheel	0.088	0.088	0.088	0.088
GNC	Sun Sensor	0.050	0.050	0.050	0.050
GNC	GPS Receiver	1.000	1.000	1.000	1.000
GNC	Ion Thruster	—	—	—	56.000
Total Power (W)		8.918	9.093	12.918	68.918
Average Daily Usage (hr)		22.2	0.1	1.0	0.7
Energy Demand (W hr)		197.980	0.909	12.918	48.243

Considering the above power budget, power sources were selected and sized appropriately to meet the average and peak power load requirements, as detailed in subsequent sections.

5.2 Power Storage

5.2.1 Secondary Battery

Secondary batteries are rechargeable batteries used to repeatedly charge and discharge power throughout the duration of the mission. When choosing a secondary battery material, lithium ion batteries were prioritized, primarily for their higher energy densities relative to other commonly used materials, their higher cycle durability, and their high charge and discharge efficiency ranges, as seen in Table 5.2 [32] [33].

Table 5.2: Secondary Battery Trade Study

Options	Specific Energy Density (W h kg ⁻¹)	Cycle Durability	Charge/Discharge Efficiency (%)
Lithium Ion	100 - 250	500 - 1,200	80 - 90
Nickel-Metal Hydride	60 - 200	300 - 500	66 - 92
Nickel Cadmium	45 - 80	1,000	70 - 90
Lead Acid	33 - 42	200 - 300	50 - 95

When sizing the battery, the decision was made to size the battery to provide sufficient power such that the spacecraft is able to run on Standby Mode whenever it is in eclipse for the duration of the mission; the battery would not be expected to provide power to the spacecraft whenever it is not eclipse. This decision was made primarily due to the limited number of cycles a cubesat lithium ion battery possesses. Thus, given that 6U of internal volume does not allow the PTC engineers to simply stack batteries until a certain cycle life is reached, to even attempt to match the 10-year mission duration of I-MISSED, the battery should only be expected to provide power during eclipse. The spacecraft bus, imager, transceiver, and thruster would thereby be powered directly from the solar array, meaning that the Imaging, Data Link, and Thrust Modes may only be utilized in daylight when the solar array is collecting power. This decision is made feasible by the fact that, as seen in Table 5.3, the spacecraft spends most of its time in sunlight, experiencing an average of 0.240 eclipses (or umbrae) per day, with each eclipse lasting an average of 0.877 hours long.

Table 5.3: Sunlight, Penumbra, and Umbra Times

Type	Time (s)	Time (hr)	Energy Demand (W hr)
Sunlight	Total	312,415,978.291	86,782.216

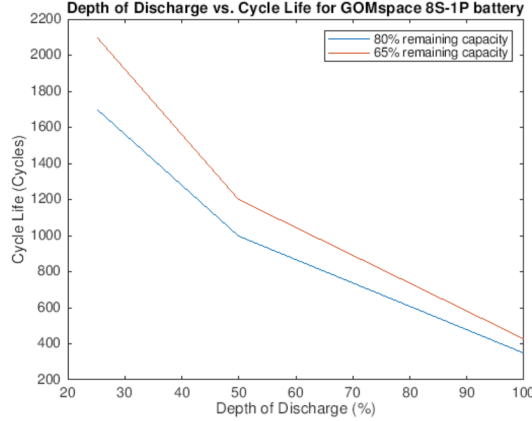


Figure 5.1: Cycle Life of GOMspace BPX

Type		Time (s)	Time (hr)	Energy Demand (W hr)
Sunlight	Max	12,095,510.200	3,359.864	6.836
Sunlight	Min	2,759.635	0.767	29,963.267
Sunlight	Average	323,411.986	89.837	801.163
Penumbra	Total	431,495.626	119.860	1,068.911
Penumbra	Max	4,715.336	1.310	0.176
Penumbra	Min	70.906	0.020	11.681
Penumbra	Average	234.127	0.065	0.580
Umbra	Total	2,771,726.083	769.924	6,866.181
Umbra	Max	4,048.864	1.125	0.413
Umbra	Min	166.730	0.046	10.030
Umbra	Average	3,156.863	0.877	7.820

Note that in the above table, energy demand was calculated using the average power load—in other words, Standby Mode. Given that the total amount of time spent in eclipse is 769.92 hours and that the average is 0.877 hours, the spacecraft is known to undergo 878 eclipses over the course of the mission. Thus, at least 878 battery cycles would be needed to sustain the spacecraft throughout the periods of shadow in which it does not collect power.

Keeping in mind the energy demand in eclipse, as shown in Table 5.3, the GOMspace BPX 8S-1P battery was chosen as the secondary battery due to the fact that it meets the required capacity. GOMspace states that a BPX 8S-1P has a capacity of 2.6 A hr and requires a bus voltage of 24 V [34], equivalent to a capacity of 62.4 W hr. Thus, a depth-of-discharge of about 12.53% to provide the required 7.820 W hr of energy

in eclipse. Additionally, referring to Figure 5.1, created using information provided by GOMspace [35], a depth-of-discharge of less than 20% would allow for at least 1,800 cycles, which meets the cycle life demand. Note that the GOMspace 8S-1P was also chosen due to its small dimensions at 9.17 by 8.59 by 4.00 cm [34], enabling it to consume as little precious internal volume as possible. The required capacity of a battery is quantified as:

$$C_r = \frac{P_e T_e}{(DOD) N n} \text{ W hr} \quad (5.2.1)$$

To calculate the number of batteries needed, Equation 5.2.1 is re-arranged as written:

$$n = \frac{P_e T_e}{(DOD) N C_r} \text{ batteries} \approx 0.502 \text{ batteries} \quad (5.2.2)$$

The variables are defined as follows: P_e is the power required in eclipse at 8.918 W, T_e is the average eclipse time at 0.877 hours, DOD is the upper limit depth-of-discharge, C_r is the battery capacity at 62.4 W hr, and n is the transmission efficiency at 90%. The result shows that 0.520 batteries would be needed, meaning that one GOMspace BPX 8S-1P battery pack would need to be installed in the spacecraft.

5.2.2 Primary Battery

The other type of battery that must be selected is the primary battery. Primary batteries are non-rechargeable; they contain all their usable energy when assembled and can only discharge power. So as not to use up more internal volume for batteries, especially since primary batteries essentially become useless mass once all their energy is discharged, it was decided that no separate primary battery would be used. Instead, the secondary batteries would simply be pre-charged prior to launch to provide enough energy to power the spacecraft through Standby Mode for the first 30 minutes of the mission. This would mean charging the battery to a minimum of 4.954 W hr (given, again, a 90% transmission efficiency), which would amount to about 7.94% of one battery pack's capacity.

The aforementioned 30-minute duration includes a de-tumbling time of about 32 seconds, as well as the fact that, according to Requirement 3.4.4 in cubesat Design Specification, “All deployables such as ... solar panels shall wait to deploy a minimum of 30 minutes after the cubesat’s deployment switch(es) are activated from P-POD ejection” [36].

5.3 Power Generation

5.3.1 Sizing the Solar Array

As mentioned in the previous section, since the batteries are expected to only provide power in eclipse, the solar array must be sized so that they can provide for the peak power demand. The minimum size the solar arrays must be to meet average power is:

$$P_{sa} = \frac{\left(\frac{P_e T_e}{X_e} + \frac{P_d T_d}{X_d} \right)}{T_d} \quad (5.3.1)$$

P_e and P_d were the power loads in eclipse and daylight, respectively, both at 8.918 W in Standby Mode; T_e was the average eclipse time at 0.877 hours; T_d was the average time spent in daylight minus the amount of time spent thrusting; and X_e and X_d were the efficiencies of the paths from the solar arrays through the batteries and the path directly from the loads at 0.60 and 0.80, respectively, assuming peak-power tracking. Note that the power bus will implement peak-power tracking, as will be described in the "Power Distribution" section. To meet average power demand, approximately 11.704 W would need to be provided by the solar array.

To size the solar arrays for meeting peak power, the process was similar, except that the eclipse term in Equation 5.3.1 is completely disregarded, and the P_d term is changed to the amount of time spent thrusting at 0.700 hours. To meet peak power demand, approximately 86.148 W would need to be provided.

When considering what solar cell material the team should implement, among the two most common options of Silicon (Si) or Gallium Arsenide (GaAs), GaAs was chosen due to its lower temperature coefficient (a measure of performance loss versus temperature changes), a higher conversion efficiency, and a record for being used with thinner layers which would reduce mass on the spacecraft [37].

The next step is to calculate the beginning-of-life (BOL) power production capability per unit area of the array, quantified by:

$$P_{BOL} = P_O I_d \cos \theta \approx 178.652 \text{ W m}^{-2} \quad (5.3.2)$$

The variables are defined as follows: P_O is the estimated power output with the Sun normal to the surface of a GaAs cell at 253 W m^{-2} ; I_d is the inherent degradation due to design efficiencies that result from the assembly of a solar array at the nominal value of 0.77; and $\cos \theta$ is the cosine loss, where θ is the worst-case Sun angle at 23.5

deg between equatorial and ecliptic planes [15]. Given these variable definitions, as shown in Equation 5.3.2, it was found that 178.652 W m^{-2} would be provided at BOL.

Using the result for P_{BOL} , the end-of-life (EOL) power production for the solar array can be quantified as:

$$P_{EOL} = P_{BOL}L_d \approx 135.178 \text{ W m}^{-2} \quad (5.3.3)$$

Note that L_d is the lifetime degradation of the solar array, which can be estimated using:

$$L_d = (1 - \text{degradation/yr})^{\text{satellite life}} \approx 0.757 \quad (5.3.4)$$

Assuming that a GaAs cell in GEO experiences 2.75% of degradation per year [15], as shown in Equation 5.3.3, the solar array produces 135.178 W m^{-2} at EOL.

At this point, the solar array must be sized using EOL parameters. Given the EOL power production capability, the minimum area required to meet both average and peak power demands can be quantified as follows:

$$A_{sa} = \frac{P_{sa}}{P_{EOL}} \quad (5.3.5)$$

To reiterate, given that 11.704 W would need to be provided by the solar array, in order to meet average power demand, the minimum area of the solar panel would need to be at least 866 cm^2 . Calculated in the same manner, given that 86.148 W would need to be provided by the solar array, in order to meet peak power demand, the minimum area would have to be $6,373 \text{ cm}^2$.

5.3.2 Off-the-Shelf Solar Array

The challenge thereafter was to find an off-the-shelf product that met these area specifications. After some research, the Enhanced High Watts per Kilogram (eHaWK) Solar Array from MMA Design was found. Optimized for a 6U cubesat, it is TRL 7 as of writing, built using 30.7% efficiency GaAs XTJ Prime solar cells. While the default configuration, the top right image in Figure 5.2 [38], is a $3,600 \text{ cm}^2$ array that weighs 0.85 kg [39]—this weight includes the accompanying Solar Array Drive Assembly (SADA)—the solar array provides other configurations that increase the surface area of the array, such that its expanded area meets the $6,373 \text{ cm}^2$ requirement at peak

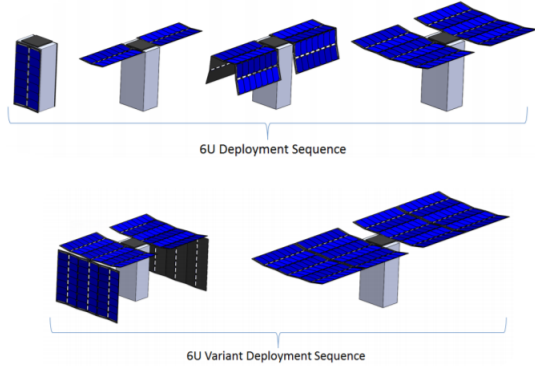


Figure 5.2: eHaWK Deployment Sequence

power. Again referring to Figure 5.2, the bottom right configuration shows the 6U Variant Deployment Sequence [38], which increases the surface area to $7,200 \text{ cm}^2$, thereby meeting the minimum area requirement for peak power.

It is imperative to note, though, that since the area of the eHaWK solar array is larger than the minimum area requirements, it will be collecting a lot of excess power if the entire surface area is always normal to the sun. This will be especially egregious when the solar array only needs to provide for average power or slightly above average power whenever the spacecraft is in any power mode other than Thrust Mode (this will be the case for almost entire length of each day, except for the 42 minutes devoted to station-keeping). So as not to collect too much excess power that would eventually lead to overheating, the solution would be to rotate the solar panels such that they are more edge-on to the Sun, exposing less surface area of the solar array to sunlight.

5.4 Power Regulation and Distribution

Beyond power generation and power storage, a system must be developed in which this power is regulated and distributed to the various electrical components of the spacecraft. The other major components that comprise the power system include chargers, regulators, and distributors. To ensure compatibility between all components of the power system, all components of the power system except the solar array were specifically chosen from the same manufacturer that produced the NanoPower BPX 8S-1P batteries. The modular NanoPower P60 System, as described in the following subsections, offers a way to take care of charging, regulation, and distribution with a single small-scale, lightweight system optimized for nanosatellites.

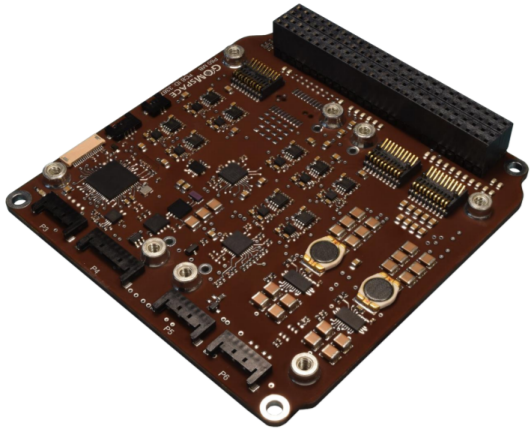


Figure 5.3: NanoPower P60 Dock

5.4.1 Charging

The GOMspace NanoPower P60 Dock, pictured in Figure 5.3, is a module that can fit a total of four Array Conditioning Unit (ACU) and Power Distribution Unit (PDU) modules, of which will be described in subsequent subsections. Its dimensions are 9.0 by 9.6 cm, and it weighs 80 g. It provides the charge inputs capable of charging the battery [40].

The GOMspace NanoPower P60 ACU-200, as previously mentioned, is a module that is able to fit onto the previously described NanoPower P60 Dock. It is pictured in Figure 5.4. Its dimensions are 6.53 by 4.00 by 1.23 cm, and it weighs 54 g. One ACU module contains six photovoltaic inputs, of which only two are expected to be utilized by the eHaWK Solar Array—one input for each wing. Thus, only one ACU module will be included in the power system. Each input utilizes maximum power point tracking (MPPT) boost converters [41], which is why, in Equation 5.3.1, when defining X_e and X_d , values for peak power tracking were assumed. Note that peak power tracking is essentially the same mechanism as MPPT, meant to extract the maximum power from a photovoltaic input by checking the output of the photovoltaic module, comparing it to the battery voltage, then converting to the most efficient voltage that would enable maximum current to travel to the battery [42].

5.4.2 Regulation and Distribution

Akin to the aforementioned NanoPower P60 ACU-200, the GOMspace P60 PDU-200 module, pictured in Figure 5.5, fits onto the NanoPower P60 Dock. Its dimensions



Figure 5.4: NanoPower P60 ACU-200



Figure 5.5: NanoPower P60 PDU-200

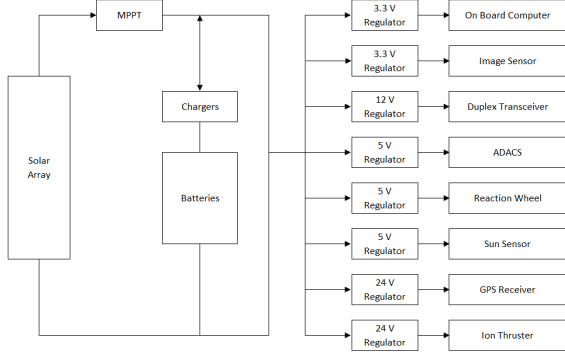


Figure 5.6: Power Bus Schematic

are 6.56 by 4.01 by 0.47 cm, and it weighs 57 g. It acts as a regulator and distributor, with each module possessing nine inputs that can be routed to the power system's various electrical components. Configurable output voltages are 3.3, 5, 8, 12, 18, or 24 V, with the latter three being possible when using two channels [40].

Table 5.4: Electrical Component Voltages

Subsystem	Component	Voltage (V)	Number of Outputs
Payload	On Board Computer	3.3	1
Payload	Image Sensor	3.3	1
Payload	Duplex Transceiver	6.5 - 12.5	2
GNC	ADACS	5	1
GNC	Reaction Wheel	5	1
GNC	Sun Sensor	5	1
GNC	GPS Receiver	24	2
GNC	Ion Thruster	12 or 28	2

In order to decide how best to construct the power system architecture, the operating voltage of each electrical component was compiled, as shown in Table 5.4. Note that also included within Table 5.4 is a count of how many PDU outputs each electrical component will need; as eleven outputs are needed in total, two PDU modules will be included in the power system.

Given that there are several different operating voltages, a regulated distributed system was chosen to be the best way to distribute power, in which there would be one regulator dedicated to each electrical component, each configured for a different voltage appropriate for the specifications of each component. A schematic displaying how the power bus will be organized is shown in Figure 5.6.

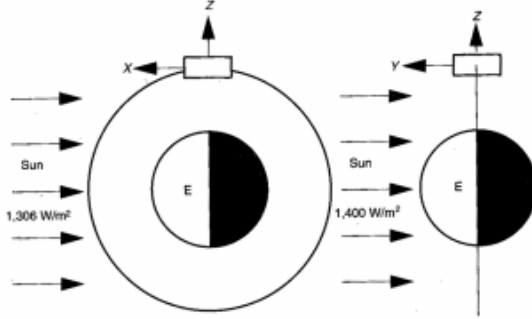


Figure 5.7: Orbital cases for Minimum (left) and Maximum (right) sun cases

5.5 Thermal Loadings

5.5.1 Steady State Thermal Analysis

The cubesat was subdivided into three nodes (Spacecraft, Thruster, and Solar Array), and steady state thermal analysis was performed on each, assuming negligible heat conduction between nodes. The major heat fluxes affecting each node were considered: solar flux Q_{su} , Earth thermal flux Q_{et} , Earth albedo flux Q_{er} , and internal heat flux Q_{int} . For each of these thermal fluxes, minimum and maximum cases were considered. The minimum case for our cubesat was defined as the orbit in which the velocity vector was in the same orbital plane as the sun vector (\mathbf{s}), and the maximum case corresponded to when the velocity vector was perpendicular to the sun vector, as shown in Figure 5.7.

Solar Flux

The solar flux acting upon each node was calculated as follows:

$$Q_{su} = PAS_{av} H_{su} \quad (5.5.1)$$

H_{su} was the solar constant at 1 AU and varied from 1306 to 1400 W m^{-2} for the minimum and maximum sun cases [15]. PAS_{av} was the average area projected in the direction of the sun vector over an orbit, considering both minimum and maximum sun cases, using:

$$PAS_{av} = \frac{1}{2\pi} \int_0^{2\pi} \mathbf{A} \cdot \mathbf{s} d\beta \quad (5.5.2)$$

Utilizing the geometry of each of the node components and the orbital trajectory,

solar heat fluxes for each node were calculated and depicted below. More details of these solar fluxes are shown in Appendix A.

	Spacecraft	Thruster	Solar Array
Minimum Q_{su} (W)	17.8	17.2	895
Maximum Q_{su} (W)	28.0	28.0	1,008

Earth Thermal Flux

The effect of the thermal flux radiating from Earth was described by:

$$Q_{et} = F_{et} A_{sc} H_{et} \quad (5.5.3)$$

F_{et} was the Earth thermal view factor at 0.0068, calculated based on the orbital altitude for GEO; A_{sc} was the surface area of the node exposed to the surface of the Earth; and H_{et} was the constant for Earth-emitted IR energy flux and ranged from 208 to 224 W/m^2 [15]. Calculated Earth thermal fluxes for each node component are shown below:

	Spacecraft	Thruster	Solar Array
Minimum Q_{et} (W)	0.14	0.08	0.65
Maximum Q_{et} (W)	0.15	0.09	0.70

Earth Albedo Flux

The heat flux induced by the reflection of light from the Earth's surface was found for each node using:

$$Q_{er} = a F_{et} A_{sc} H_{su} \quad (5.5.4)$$

where a was the albedo factor for Earth at 0.36 [15], F_{et} and A_{sc} variables were the same for those in Equation 5.5.3, and H_{su} values were the same for those in Equation 5.5.1. Calculated Earth albedo fluxes for each node component are shown below:

	Spacecraft	Thruster	Solar Array
Minimum Q_{er} (W)	0.102	0.061	0.466
Maximum Q_{er} (W)	0.109	0.065	0.500

Internal Flux

The minimum and maximum internal fluxes for the spacecraft node were found by taking the power usage of the electronic components during the standby phase (darkness) and fully operational phase (daytime) respectively. For the thruster, the power usages for OFF and ON cases were considered. For the solar panels, the minimum, average, and maximum power were taken into account. For each node, it was assumed that 50% of the power used/generated was dissipated as heat. Calculated internal fluxes for each node are presented below:

	Spacecraft	Thruster	Solar Array
Minimum Q_{int} (W)	6.4	0.0	0.0
Maximum Q_{int} (W)	10.4	28.0	48.7

5.5.2 Transient Thermal Analysis

A transient thermal analysis during eclipse was also conducted to gain better insight into the change in spacecraft temperature over the dark period. The transient temperature equation is expressed by Equation 5.5.5,

$$\frac{dT}{dt} = \frac{-\sigma\epsilon_{IR}A_{sc}T_{sc}^4}{mc_p} + \frac{Q_{et} + Q_{int}}{mc_p} \quad (5.5.5)$$

where m is the mass of the spacecraft at 8.47 kg, c_p is the specific heat of the spacecraft material at $900 \text{ J kg}^{-1} \text{ K}^{-1}$ for the aluminum chassis, and only the Earth thermal flux and internal flux are considered to be the primary factors acting on the body over an eclipse. At an initial temperature of 14.5°C , which is the expected temperature of the cubesat upon entering the darkness phase, Equation 5.5.5 can be solved to yield Figure 5.8, which depicts the change in spacecraft temperature over time.

From Figure 5.8, it can be seen that the temperature drop over the 52.2 min period in darkness only corresponds to a drop of 8.45°C . This suggests that active thermal controls to maintain spacecraft temperatures during this period are unnecessary.

5.6 Thermal Control

Passive thermal control was initially performed on the three primary nodes of our cubesat: Spacecraft, Thruster, and Solar Array. More specifically, thermal coating

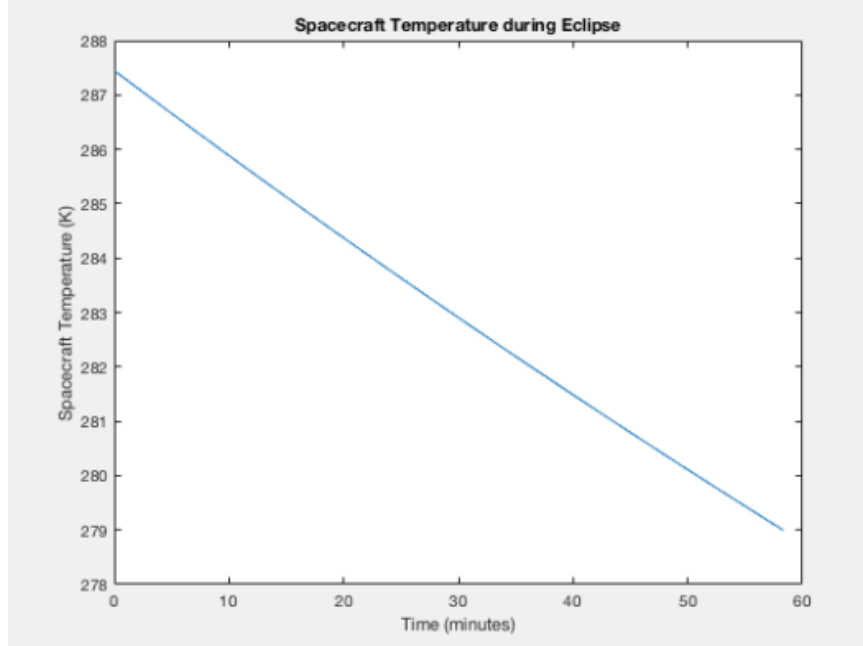


Figure 5.8: Spacecraft temperature drop during eclipse period

was first explored for each of these nodes, as this thermal control method was the simplest in design and control. Coatings with varying optical parameters, namely solar absorptivity α_{su} and infrared emissivity ϵ_{IR} , were plugged into an equation that would then output the temperature of the node being evaluated. Said equation is written as:

$$T_{sc} = \left(\frac{Q_{int} + \alpha_{su}Q_{su} + \alpha_{su}Q_{er} + \epsilon_{IR}Q_{et}}{\sigma\epsilon_{IR}A_{sc}} \right)^{1/4} \quad (5.6.1)$$

Based on the temperature output by Equation 5.6.1, different calculations were iterated through until the optimal thermal coating was found. In the case of the thruster, as will be explained in the “Thruster Thermal Control” subsection, a thermal coating was found to not be sufficient to passively control the thruster’s temperature, as the temperatures when the thruster was turned on and off were so drastic that one method of passive control could not keep the two temperatures within an operable temperature range.

5.6.1 Temperature Range

Table 5.5: Operating Temperatures of Electrical Components

Purpose	Component	Min Temp (°C)	Max Temp (°C)
Power Supply	Solar Array	15	35
Power Supply	Secondary Battery (Charge)	0	45
Power Supply	Secondary Battery (Discharge)	-20	60
Power Supply	NanoPower P60 Dock	-35	85
Power Supply	NanoPower P60 ACU-200	-35	85
Power Supply	NanoPower P60 PDU-200	-35	85
Command	On Board Computer	-25	65
ADCS	ADACS	-20	60
ADCS	Reaction Wheel	-40	85
ADCS	GPS Receiver	-10	50
Thrust	Ion Thruster	-20	50
Imaging	Image Sensor	-20	60
Communication	Transmitter	-40	60
Communication	Duplex Transceiver	-20	60
Communication	Antenna	—	140
Operational Temperature Range		0	35

Before embarking on the previously described iterative calculations, it was necessary to first identify an ideal operational temperature range. The operating temperature ranges for each of the electrical components was compiled, as shown in Table 5.5. Note that, with the exception of the solar array and secondary battery, all temperatures listed are minimum and maximum survival temperatures. For the solar array, minimum and maximum temperatures at which the solar array may still operate at highest efficiency were listed. For the battery, the minimum and maximum temperatures at which the battery is able charge or discharge. From the compiled list of temperatures, it was found that the spacecraft should stay within the range of 0°C to 35°C.

5.6.2 Spacecraft Thermal Control

To clarify, this node refers to the surface area of the spacecraft structure that does not surround the thruster; this would be the 4U section that houses most of the spacecraft bus: the batteries, ADCS suite, and any other component that requires power except

the thruster.

The target operating temperature range for the main spacecraft was set to 0 to 35°C. An iron oxide coating was chosen with an α_{su} of 0.85 and an ϵ_{IR} of 0.56 [43]. Using Equation 5.6.1, at minimum cold, the spacecraft's temperature was found to be 2.64°C, and at maximum hot, it was 14.44°C; for reference, the minimum and maximum cases are shown in Figure 5.7. This range of operating temperatures was within the prescribed target operating temperature range. Therefore, a passive thermal control of iron oxide coating was assumed to be sufficient in providing a sensible environment for onboard electronics.

A study was also done to see whether the iron oxide coating would experience any corrosion on top of the tantalum radiation shielding layer on the spacecraft. However, it was found that tantalum is one of the most corrosion resistant metals due to its naturally occurring thin oxide film, and studies have shown that tantalum/iron alloys have extremely high corrosion resistance in laboratory environments [44].

5.6.3 Thruster Thermal Control

The thruster, given that it is the source of the highest amount of internal heat flux, is planned to be thermally insulated well enough such that it can be assumed to be thermally isolated from the rest of the spacecraft. A coating for the surface area of the chassis surrounding the thruster was chosen based on what coating would keep the thruster at operating temperature whenever it was turned off and not dissipating heat. This coating was chosen to be black paint, with an α_{su} of 0.975 and an ϵ_{IR} of 0.874 [15]. When these values are plugged into Equation 5.6.1, the calculations show that the thruster is able to stay above the minimum survival temperature at about -17.76°C even when the thruster is turned off in the minimum case shown in Figure 5.7; referencing back to Table 5.5, the minimum survival temperature is -20°C. However, whenever the thruster is turned on in the maximum case, the temperature is above the maximum survival temperature at about 70.74°C; the maximum survival temperature is 50°C. Thus, it is clear that another method of thermal control must be added.

As such, after some research, it was decided that the surface area of the chassis surrounding the thruster should be outfitted with louvers, to lower the temperature of the thruster whenever it is active. An off-the-shelf TRL 8 louver system developed by the NASA Goddard Space Flight Center, optimized for a 6U system, is pictured in Figure 5.9; note that the illustration is provided by NASA for reference, and it



Figure 5.9: Louver mechanism for radiating heat

is not meant to be a representation of how the louver would be configured on the I-MISSED spacecraft. The louver system requires no power to operate, which reduces stress on the power budget. The way it works is that “Bimetallic springs serve as a passive control mechanism for opening and closing flaps.” The springs expand and contract with changes in surrounding temperature “due to the difference in thermal expansion rates of their two fused metals (hence bimetallic)” [45], which alters the thermal radiation properties of this section of the spacecraft as appropriate.

Generally, a louver in its fully open state can raise heat rejected by as much as a factor of 6 [46]. When factoring this into Equation 5.6.1, it was found that the temperature of the thruster was brought down to an adequate operating temperature of 18.07°C. However, even a significantly more conservative estimate in which the heat rejected is increased by only a factor of 2, the temperature is decreased to a still more than satisfactory 23.40°C.

Thus, it was found that a combination of black paint coating and a louver system would be the best method to thermally moderate the thruster. Note that the louver system is expected to operate such that it is only in its fully open state whenever the thruster is in operation and is closed whenever the thruster is inactive. Also note that, assuming that the 6U louver system operates similarly to other commonly used louver systems used today such as the Starsys, the point at which the louvers open and close can be set at any point between -20°C and 50°C [46], which corresponds to the minimum and maximum survival temperatures of the thruster, respectively.

Before moving on, the method through which the thruster will be thermally in-

sulated should be touched upon. The thruster will be insulated using a lightweight high-density polyimide foam, which is expected to insulate the thruster effectively while adding minimal weight to the spacecraft. The required thickness is calculated using Fourier's law of heat conduction:

$$Q = -\kappa A \frac{dT}{dx} \quad (5.6.2)$$

After re-arranging Equation 5.6.2 such that the dx is isolated, the variables of the law were defined as follows: the thermal conductivity κ of the foam was $0.09 \text{ W m}^{-1} \text{ K}^{-1}$ [47]; the area of the insulating wall A was 20 by 10 cm; Q was the difference in radiated heat between the main spacecraft bus and the thruster; and dT was the difference in temperature (assuming the aforementioned means of passive control have already been applied) between the main spacecraft bus and the thruster. Substituting in the appropriate values for the variables, it was found that an insulating wall of around 4.1 mm is needed, which amounts to 2.87 g in mass. Given the extremely low thermal conductivity of the foam and given that a minimum thickness was calculated, as previously stated, it was assumed that the thruster is thermally insulated enough such that it could be treated as a separate node during steady-state calculations.

5.6.4 Solar Array Thermal Control

Table 5.5 suggests a temperature range of 15 to 35°C in order to maintain optimal solar array performance. However, heat flux analysis revealed that the direct solar flux factor would be the most significant challenge, with values from 900 to 1000 W. If left unchecked, this heat flux initially drove the solar array temperatures to over 300°C. It would also not be economical to carry any onboard, active thermal controls to lower this temperature, so a passive coating that possessed a fairly high emissivity and low absorptivity was desired. A 0.5 mil teflon gold backing coating with an α_{su} of 0.24 and an ϵ_{IR} of 0.43 was chosen [43]. The total mass of the coating, when covering the entire backside of the solar array, came out to merely 100.6 g, an incredibly small value. During the standby phase in darkness where all the heat fluxes were minimum, the temperature of the solar was found to be 6.65°C. During the minimum and maximum when the solar array was angled such that only enough power to meet average demand was collected, temperatures of 9.38°C to 17.58°C were recorded. For the case corresponding to an unfolded solar array experiencing all the maximum heat fluxes, only a value of 28.58°C was reached. Thus, teflon gold backing coating yielded an overall range of operating temperatures within the target range

for optimal solar array performance.

Chapter 6

Structure

The Structures subsystem of I-MISSED holds the various components of the satellite together and ensures that the satellite can handle the loads imposed on it by the space and launch vehicle environment. Subteam members outlined the final mass budget of the satellite and worked to integrate each of the subsystems into the main satellite bus.

The main structure will consist of an off the shelf, standard, GOMspace 6U cubesat chassis that each subsystem of I-MISSED must fit inside.

6.1 Mass Breakdown

Component	Mass [g]	CAD Volume [cm^3]	Density [g/cm^3]
6U Frame	1,060	329	3.22
Antenna (stowed)	304	474	0.64
Transceiver	75	55.2	1.36
Thruster	2,250	1,600	1.41
GOMspace 8S-1P	500	174	2.87
NanoPower P60	191	48.3	3.95
Solar Panels	1,200	1,120	1.07
MAI-400 ADCS	694	493	1.41
MAI-400 RW	90	18.6	4.84
Imager	1,830	354	5.17
Flight Computer	94	34.8	2.71
SADA	180	62.0	2.90
Radiation Shielding	4,600	370	12.4
Teflon Gold Sheet	101	—	—
Louvers	132	—	—
Total	13,300		
7.5% Mass Margin	14,300		

Table 6.1: Total mass breakdown of all satellite components and their average densities

6.2 Deployment Interface and Constraints

The orbital deployment mechanism selected for I-MISSED was the Canisterized Satellite Dispenser (CSD) developed by Planetary Systems Corporation. The CSD, available in 6U, 12U, and 27U versions, is a container for housing cubesats during launch that attaches to the ESPA ring of the launch vehicle as shown in Figure 6.1 from [48]. This attachment orientation fixes the directions of the launch loads experienced by the cubesat. Once the launch vehicle has reached orbit, the CSD ejects the cubesat by opening its door and guiding it out along a rail system. These rails are the locations at which the cubesat is connected to the CSD, and are therefore the locations that were held fixed for the finite element analysis discussed later in this Chapter. There are several other brands of cubesat dispensers on the market, but the CSD was chosen for this mission primarily for its relatively long list of successful missions and also for the availability of its specifications, constraints, and CAD files.

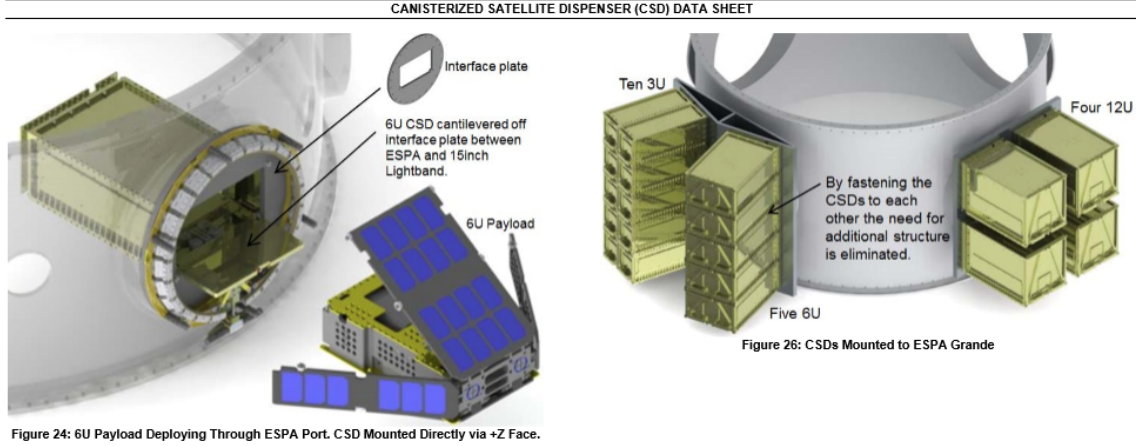


Figure 24: 6U Payload Deploying Through ESPA Port. CSD Mounted Directly via +Z Face.

Figure 6.1: Attachment between the ESPA ring and the orbital deployment mechanism

Any cubesat using the 6U CSD must comply with the mass and dimensional requirements outlined in the CSD user's guide [49], a subset of which are listed in Figure 6.2. As shown in Table 6.1, The total mass of the components needed for I-MISSED (13.3 kg) exceeds the 12 kg allowable mass of a cubesat for the 6U CSD. Given that the components of the cubesat are all off-the-shelf, yet the mass of many small components such as wiring remain unaccounted for, a reasonable growth factor is 1.075, which bring the total mass up to 14.3 kg. While there is room to reduce chassis mass by relying more on the heavy radiation shielding for structural support, this concern, along with geometric difficulties associated with the deployed antenna, are the two primary reasons why future developers of I-MISSED should consider shifting from a densely packed 6U cubesat structure to a sparsely filled 12U cubesat.

The coordinate system used for the requirements of the CSD is located and oriented as shown in Figure 6.3. The dimensions of the I-MISSED cubesat in its stowed configuration are shown below in Figure 6.4. The maximum width of the cubesat from its center in the X direction is 11.848 cm, and the maximum height of the cubesat in the Y direction is 10 cm. Both of these dimensions are compliant with the standards set by the CSD user's guide.

6.3 Configurations and Analysis

The final set of constraints associated with the CSD have to do with the center of mass (COM) of the cubesat. To properly address these constraints, the components

 PAYLOAD SPECIFICATION FOR 3U, 6U, 12U AND 27U

3. PARAMETERS

Symbol	Parameter	Conditions	Unit	3U		6U		12U		27U	
				Min	Max	Min	Max	Min	Max	Min	Max
M	Mass	At launch	kg [lb]	-	6.0 [13.2]	-	12.0 [26.4]	-	24.0 [52.9]	-	54.0 [119.0]
CMx	Center of mass, X	Stowed in CSD	mm [in]	-20 [-.79]	20 [.79]	-40 [-1.57]	40 [1.57]	-40 [-1.57]	40 [1.57]	-60 [-2.36]	60 [2.36]
CMy	Center of mass, Y	Stowed in CSD	mm [in]	10 [.39]	70 [2.76]	10 [.39]	70 [2.76]	55 [2.17]	125 [4.92]	100 [3.94]	180 [7.09]
CMz	Center of mass, Z	Stowed in CSD	mm [in]	133 [5.24]	233 [9.17]	133 [5.24]	233 [9.17]	133 [5.24]	233 [9.17]	133 [5.24]	233 [9.17]
Height	Maximum payload depth, +Y dimension		mm [in]	-	109.7 [4.319]	-	109.7 [4.319]	-	222.8 [8.771]	-	332.8 [13.102]
Width	Maximum payload width from origin, \pm X dimension		mm [in]	-	56.55 [2.226]	-	119.7 [4.713]	-	119.7 [4.713]	-	176.25 [6.939]

Figure 6.2: Payload mass and dimensional requirements of the orbital deployment mechanism

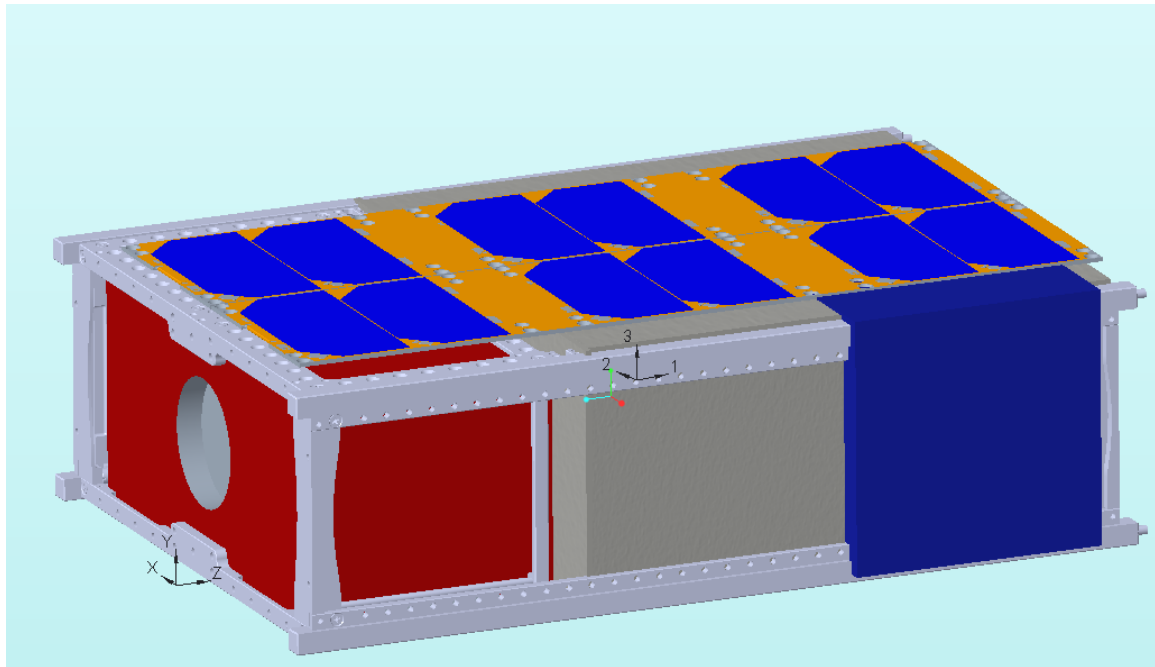


Figure 6.3: The XYZ coordinate system used to verify the COM of the stowed configuration. The 123 coordinate system is centered at the COM with axes in the directions of the moments of inertia.

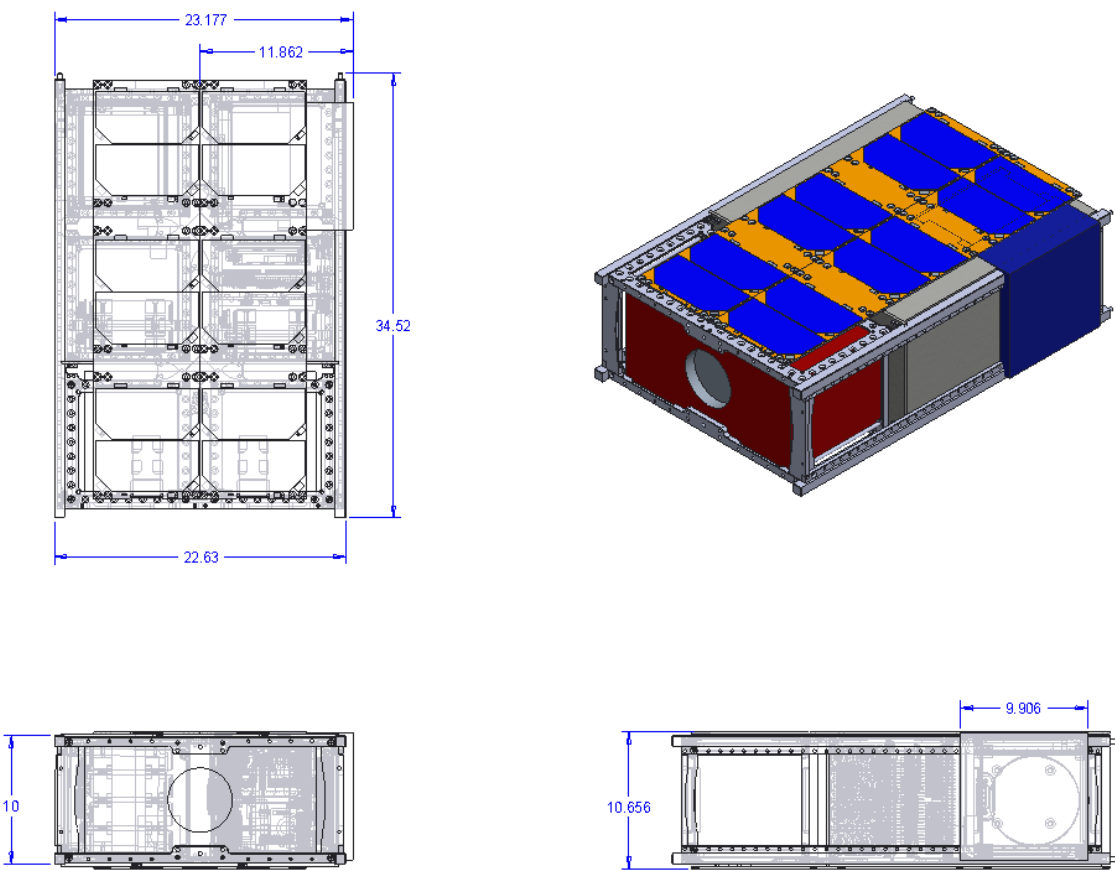


Figure 6.4: Dimensions of I-MISSED in its stowed configuration, given in cm.

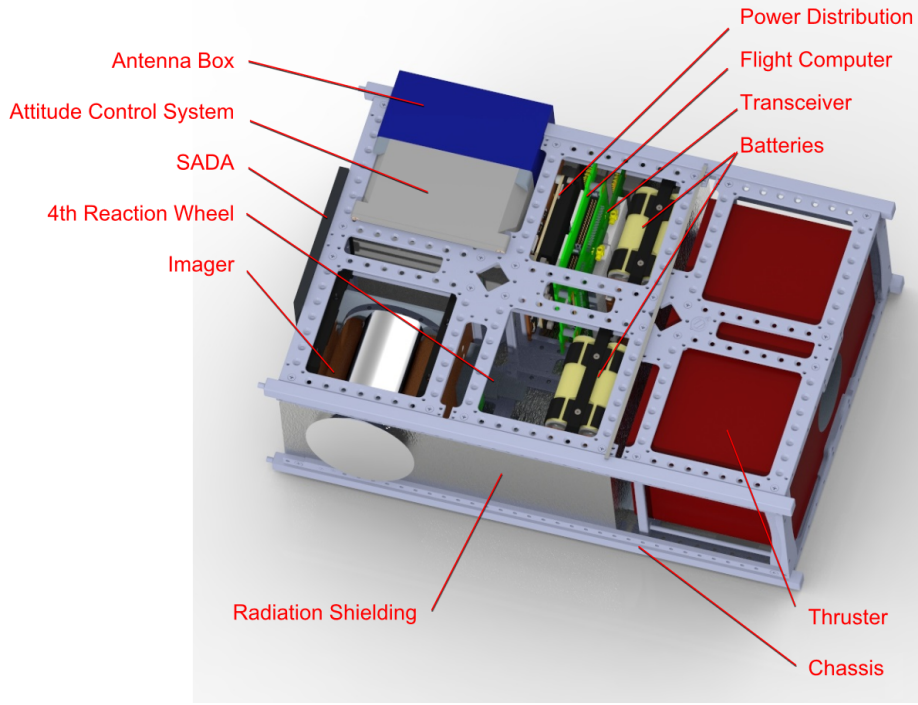


Figure 6.5: Layout of the components in I-MISSED. Note that the battery pack next to the electronics is no longer present.

of the various subsystems of I-MISSED must be integrated into the 6U chassis. The first step in this process was to gather as many CAD files as possible from component vendors. Any parts whose CAD files that could not be found, such as the thruster, imager, antenna box, and fourth reaction wheel, were approximated as simplified geometric shapes. The configuration of these components is shown in Figure 6.5. The components list for I-MISSED changed constantly, so the configuration pictured above is not entirely to date. Notable recent changes include the removal of the redundant battery pack placed next to the electronics, the addition of a thermally-isolating layer of foam between the remaining battery pack and the thruster, and the addition of louvers around the thruster to provide additional heat dissipation.

To approximate the mass distribution of the CAD assembly, the total mass of each individual component was taken from vendor data and divided by the Creo-obtained volume of the CAD component to find the average density of the component. The components in the CAD file were approximated as having a constant density equal to their average density. From there, the COM and moments of inertia were calculated using a built-in tool provided by Creo. There were three configurations of interest for analysis, pictured in Figure 6.6. The first configuration was of the cubesat in its

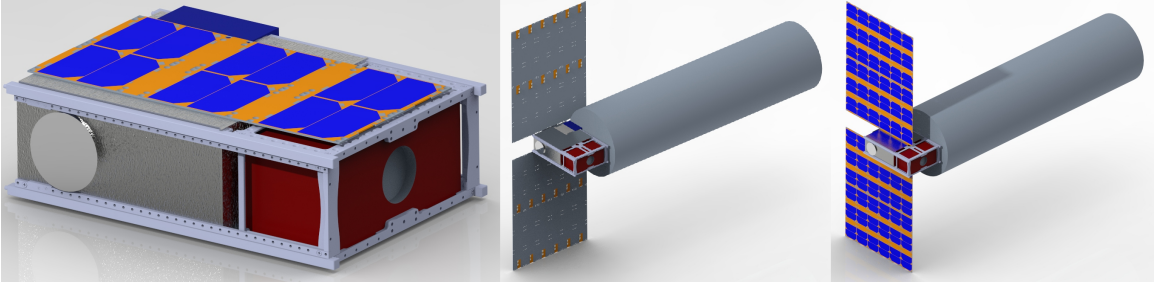


Figure 6.6: I-MISSED in the three configurations of interest: stowed (left), deployed (center), and deployed with rotated solar panels (right).

stowed state, as it would be stored inside the CSD. The COM of this configuration was required to verify that it was within the bounds of the CSD requirements. For the two deployed configurations, one with the solar panels in their starting position and the other with the solar panels rotated 90°, the location of the COM was needed to confirm an acceptable proximity to the thrust vector of the cubesat. For all three configurations the moments of inertia were required by the GNC subteam to determine the approximate power needs of the attitude control system.

The COM and moment of inertia values for each of the three configurations are listed in Figures 6.7, 6.8, and 6.9. The coordinate systems used to obtain these results are shown in Figures ?? and 6.10. The stowed coordinate system is defined exactly as is defined in the CSD requirements document, placed at the center of the cubesat chassis in the X direction and at the edges of the cubesat in the Y and Z directions. For the other two configurations, this coordinate system was switched to the center of the cubesat chassis in all three directions. This was done both to place the coordinate system near the COM of the cubesat, and to facilitate thrust vector calculations: the thrust vector of these coordinate systems is simply the Z axis, so the discrepancy between the COM and thrust vector can be calculated by simply combining the X and Y discrepancies.

The COM of the stowed configuration was located at (.635, 5.56, 18.9) cm in the XYZ coordinate system, well within the limits imposed by the CSD. The moments of inertia were used by the GNC subteam to validate the attitude control system of I-MISSED. While the deployed antenna is quite large relative to the size of the cubesat, it only weighs 300 g, so the distance of the COM from the thrust vector for the two deployed configurations was still relatively small, 1.4 cm in the X direction and negligible in the Y direction, close enough to the thrust vector such that the

VOLUME = 1.5178332e+05 CM³
SURFACE AREA = 4.4079723e+04 CM²
AVERAGE DENSITY = 8.1831449e-02 GRAM / CM³
MASS = 1.2420649e+04 GRAM

CENTER OF GRAVITY with respect to ACS5 coordinate frame:
X Y Z -1.1322504e+00 5.9924203e-03 -2.4182877e+00 CM

INERTIA with respect to ACS5 coordinate frame: (GRAM * CM²)

INERTIA TENSOR:

I_{xx} I_{xy} I_{xz} 2.4168268e+06 -2.3556468e+03 1.9729517e+05
I_{yx} I_{yy} I_{yz} -2.3556468e+03 4.3051313e+06 -6.4870326e+02
I_{zx} I_{zy} I_{zz} 1.9729517e+05 -6.4870326e+02 4.3252792e+06

INERTIA at CENTER OF GRAVITY (GRAM * CM²)

INERTIA TENSOR:

I_{xx} I_{xy} I_{xz} 2.3441889e+06 -2.4399199e+03 2.3130424e+05
I_{yx} I_{yy} I_{yz} -2.4399199e+03 4.2165707e+06 -8.2869580e+02
I_{zx} I_{zy} I_{zz} 2.3130424e+05 -8.2869580e+02 4.3093556e+06

PRINCIPAL MOMENTS OF INERTIA: (GRAM * CM²)

I₁ I₂ I₃ 2.3173281e+06 4.2165634e+06 4.3362238e+06

ROTATION ANGLES from ACS5 orientation to PRINCIPAL AXES:
angles about x y z 0.532 6.624 0.000 (degrees)

RADIi OF GYRATION with respect to PRINCIPAL AXES:

R₁ R₂ R₃ 1.3659086e+01 1.8424986e+01 1.8684595e+01 CM

Figure 6.7: COM and moments of Inertia of I-MISSED in its stowed configuration.

VOLUME = 4.3212913e+03 CM³
SURFACE AREA = 1.4920411e+04 CM²
AVERAGE DENSITY = 2.8748290e+00 GRAM / CM³
MASS = 1.2422973e+04 GRAM

CENTER OF GRAVITY with respect to ACS11 coordinate frame:
X Y Z 6.3583088e-01 5.3630892e+00 1.8970500e+01 CM

INERTIA with respect to ACS11 coordinate frame: (GRAM * CM²)

INERTIA TENSOR:

Ixx Ixy Ixz 6.0237737e+06 -3.9429088e+04 -2.4612791e+05
Iyx Iyy Iyz -3.9429088e+04 6.0683420e+06 -1.2645715e+06
Izx Izy Izz -2.4612791e+05 -1.2645715e+06 1.0680917e+06

INERTIA at CENTER OF GRAVITY: (GRAM * CM²)

INERTIA TENSOR:

Ixx Ixy Ixz 1.1956770e+06 2.9334721e+03 -9.6281632e+04
Iyx Iyy Iyz 2.9334721e+03 1.5925415e+06 -6.5212311e+02
Izx Izy Izz -9.6281632e+04 -6.5212311e+02 7.0575071e+05

PRINCIPAL MOMENTS OF INERTIA: (GRAM * CM²)

I1 I2 I3 6.8750842e+05 1.2138955e+06 1.5925654e+06

ROTATION ANGLES from ACS11 orientation to PRINCIPAL AXES :
angles about x y z -90.090 0.445 -79.271 (degrees)

RADIi OF GYRATION with respect to PRINCIPAL AXES:

R1 R2 R3 7.4391999e+00 9.8850271e+00 1.1322331e+01 CM

Figure 6.8: COM and moments of Inertia of I-MISSED in its deployed configuration.

VOLUME = 1.5178332e+05 CM³
SURFACE AREA = 4.4079723e+04 CM²
AVERAGE DENSITY = 8.1831449e-02 GRAM / CM³
MASS = 1.2420649e+04 GRAM

CENTER OF GRAVITY with respect to ACS8 coordinate frame:
X Y Z -1.1280871e+00 5.9924203e-03 -2.4222415e+00 CM

INERTIA with respect to ACS8 coordinate frame: (GRAM * CM²)

INERTIA TENSOR:

I_{xx} I_{xy} I_{xz} 2.5412774e+06 -2.1833500e+03 1.9817142e+05
I_{yx} I_{yy} I_{yz} -2.1833500e+03 4.3067960e+06 -8.2179507e+02
I_{zx} I_{zy} I_{zz} 1.9817142e+05 -8.2179507e+02 4.2024934e+06

INERTIA at CENTER OF GRAVITY: (GRAM * CM²)

INERTIA TENSOR:

I_{xx} I_{xy} I_{xz} 2.4684018e+06 -2.2673132e+03 2.3211083e+05
I_{yx} I_{yy} I_{yz} -2.2673132e+03 4.2181146e+06 -1.0020819e+03
I_{zx} I_{zy} I_{zz} 2.3211083e+05 -1.0020819e+03 4.1866867e+06

PRINCIPAL MOMENTS OF INERTIA: (GRAM * CM²)

I₁ I₂ I₃ 2.4375973e+06 4.2164736e+06 4.2191322e+06

ROTATION ANGLES from ACS8 orientation to PRINCIPAL AXES:
angles about x y z 52.085 4.716 -5.915 (degrees)

RADIi OF GYRATION with respect to PRINCIPAL AXES:

R₁ R₂ R₃ 1.4009055e+01 1.8424790e+01 1.8430598e+01 CM

Figure 6.9: COM and moments of Inertia of I-MISSED in its deployed and rotated configuration.

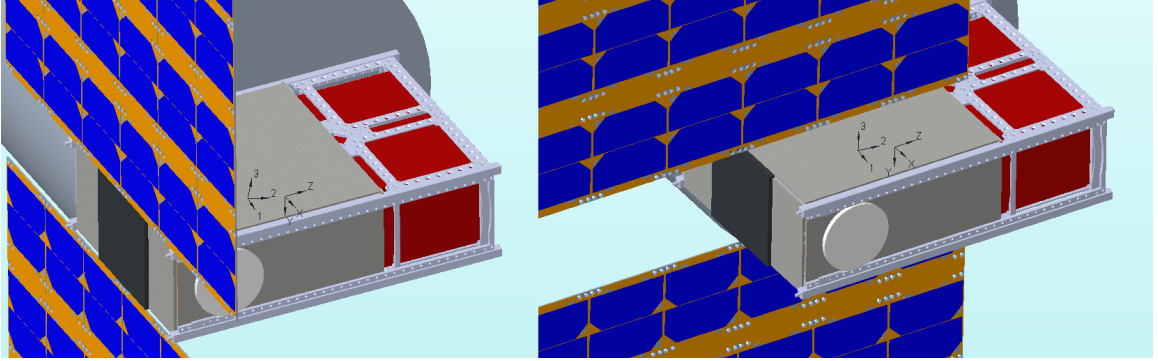


Figure 6.10: The XYZ coordinate systems used to verify the COM of the deployed configurations, located at exactly the same spot with respect to the chassis. The 123 coordinate system is centered at the COM with axes in the directions of the moments of inertia.

gimbals of the thruster can still point it through the COM. However, the size of the antenna does restrict the rotation of the solar panels from a full 360° to 125° . This difficulty might be circumvented by switching the cubesat body from 6U to 12U.

6.4 Structural Validation

A modal frequency and static stress analyses were performed on a simplified model of the integrated cubesat. The modal analysis allows the engineers to identify the natural frequency of the structure and compare it to that of the forced frequencies during ascension.

Modal Frequency Analysis

Assuring that the natural and forced frequencies of the chassis and internal components are different is crucial to mission success. High vibrational loads can cause dislocation or destruction of sensitive equipment leading to a multitude of issues including a transient COM or payload failure. The acoustic frequencies and vibration levels of the launch vehicle are shown in Figure 6.11 and 6.12, respectively.

Figure 6.13 summarizes the results of these analyses. There are two frequencies, 281 and 295 Hz, that have significant forcing effects on the structure. Thankfully, these modes are outside the vibrational range of the launch vehicle by 180 Hz. However, this range experiences 120-130 dB of acoustic pressure. To ensure that the satellite is fit for launch, physical testing under these conditions is required. The entire simulation report is available in Appendix B.

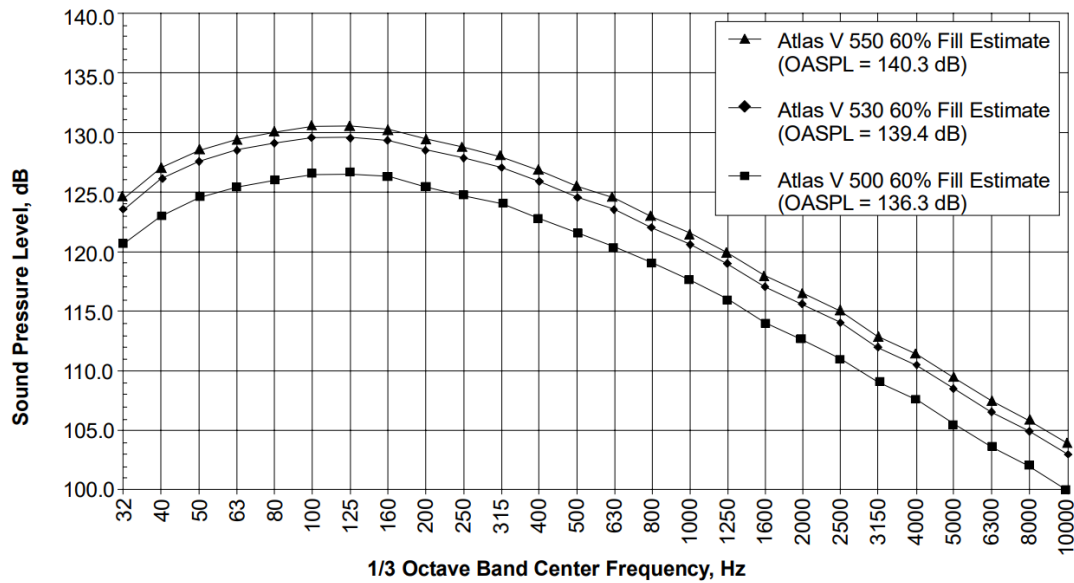


Figure 6.11: Estimated Acoustic Levels for Atlas V 5-m Short PLF

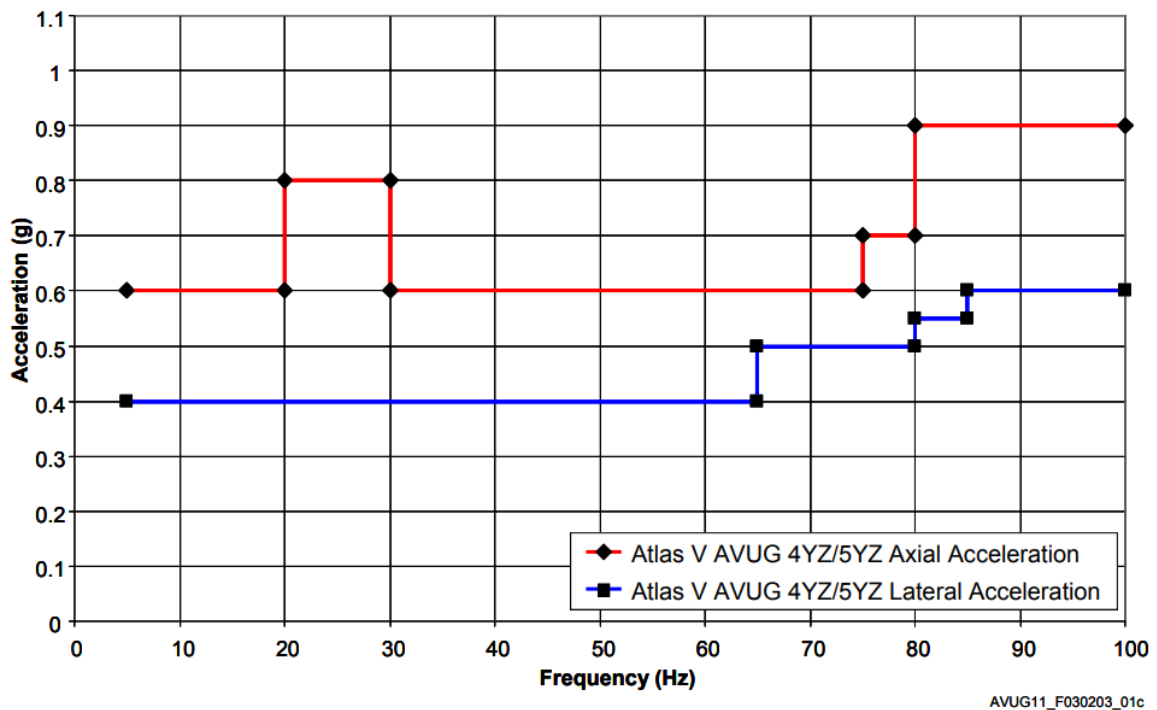


Figure 6.12: Quasi-Sinusoidal Vibration Levels for Atlas V 400 Series and Atlas V 500 Series Based on SRS

Frequency	Participation X	Participation Y	Participation Z
Mode 1: 281.1 Hz	0	5.05850017	0.0003
Mode 2: 295.3 Hz	0	4.77240011	0.0003
Mode 3: 392.5 Hz	0.180099998	0	0
Mode 4: 393.9 Hz	0.173500006	0	0
Mode 5: 572.9 Hz	0	0.0008	0.0008
Mode 6: 584.9 Hz	0	0.0014	0.0025
Mode 7: 592.4 Hz	0.0008	0	0.0001
Mode 8: 627.3 Hz	0.043099999	0	0

Figure 6.13: Modal Frequency Analysis Results

Static Stress Analysis

Linear global loads were applied to the simplified model to simulate forces experienced during launch. According to the Atlas V specifications, illustrated in Figure 6.14, the max acceleration loads of 5.5G axially and 2G laterally occur during Booster Engine Cutoff (BECO) . To include a safety factor of 1.5, 10G axial and 3G lateral loads were chosen. The results from the axial analysis under 10G can be seen in Figure 6.15. There was a maximum displacement of 0.05 mm in the tantalum shielding section. This remains in the elastic region, well below any distances needed for buckling or yielding for the material. Graphic results of the three axes analysis are shown in Figures 6.17 - 6.18. Lateral displacements were found to be negligible, being less than or equal to 0.01 mm. The full static analysis reports and their summaries are available in Appendix B.

Load Condition	Direction	Atlas V 500 Steady State, g	Atlas V 500 Dynamic, g
Launch	Axial Lateral	1.6 —	± 2.0 ± 2.0
Flight Winds	Axial Lateral	2.4 ± 0.4	± 0.5 ± 1.6
Strap-On SRM Separation	Axial Lateral	3.0 —	± 0.5 ± 0.5
BECO	Axial Lateral	5.5 —	± 0.5 ± 1.0
MECO (Max Axial)	Axial Lateral	4.8-0.0*	± 0.5 ± 0.2
(Max Lateral)	Axial Lateral	0.0 —	± 2.0 ± 0.6
<ul style="list-style-type: none"> • Sign Convention: • Longitudinal Axis: + (Positive) = Compression - (Negative) = Tension • Pitch Axis: \pm May Act in Either Direction • Yaw Axis: \pm May Act in Either Direction • Lateral & Longitudinal Loading May Act Simultaneously During Any Flight Event • Loading Is Induced Through the cg of the Spacecraft 			
Note: * Decaying to Zero			

Figure 6.14: Atlas V Limit Load Factors

6.5 Failure Tree Analysis

To analyze the reliability of I-MISSED over a 10 year period, a static failure tree analysis was performed. Table 6.2 contains the probabilities used in the analysis and their sources.

The SpaceWorks Enterprises Inc. reliability database is an internal company database that we requested access to. They perform a market yearly assessment of over 30,000 cubesats and their components [51]. The imager probability was estimated via a mean-time-to-failure analysis from an estimated lifetime of CMOS imagers [50]. The thruster probability was calculated from the use over the expected lifetime assuming that thrusting would occur for an hour a over 10 years: $\frac{3650}{20,000} = 0.1825$. This analysis assumes an equal probability that the thruster will fail at any point in its lifetime. The Atlas V probability was derived from 0 launch failures. For this reason it seems quite unlikely that it would be a reliability issue. Failure was estimated to be 1% for this reason. Deployment and batteries have a long track record of success. Therefore the probability estimated was less than 1%. Due to high speeds and wear,

Name	Minimum	Maximum
Safety Factor		
Safety Factor (Per Body)	12.17	15
Stress		
Von Mises	4.28E-05 MPa	45.86 MPa
1st Principal	-9.476 MPa	54.14 MPa
3rd Principal	-47.28 MPa	6.362 MPa
Normal XX	-17.78 MPa	20.47 MPa
Normal YY	-13.88 MPa	16.73 MPa
Normal ZZ	-40.15 MPa	46.88 MPa
Shear XY	-5.804 MPa	5.876 MPa
Shear YZ	-5.397 MPa	25.96 MPa
Shear ZX	-3.658 MPa	4.746 MPa
Displacement		
Total	0 mm	0.05327 mm
X	-0.001023 mm	0.001023 mm
Y	-0.05327 mm	1.079E-04 mm
Z	-0.001306 mm	0.001083 mm

Figure 6.15: Axial Static Stress Analysis Results

the reaction wheel probabilities were derived by a worse case scenario where each wheel is only reliable 20% of the time.

With these numbers the following Failure Tree Analysis model in Figure 6.19 was designed. All gates except the ADACS are OR gates. This means that the failure of any single component represents mission failure. To model the ADACS redundancy a Voting OR gate with $k = 2$ was utilized. This method conveys that at least two of the reaction wheels must fail before the entire ADACS system is considered compromised. The 10 year probability of mission failure due to each component is displayed in Figure 6.20. Results from the analysis can be seen in Figure 6.21. The probability of mission success was found to be approximately 92% — suitable for the 90% industry standard.

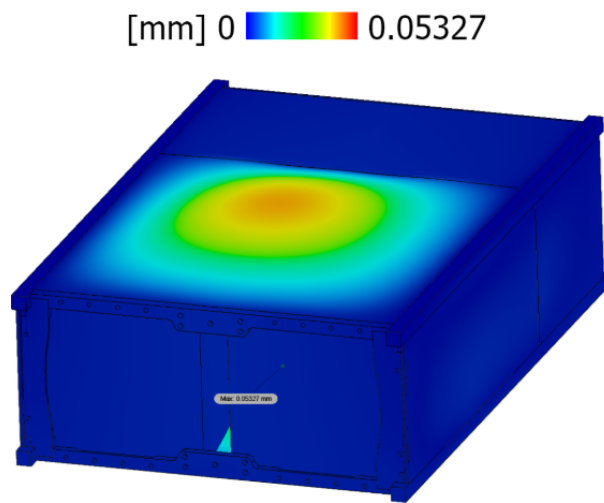


Figure 6.16: Axial Displacement Graphic Results

Component	Type	Probability of Failure	Source
Imager	MTTF	8.79E-07	NASA [50]
Hardware	Constant	8.51E-07	SEI Database
Solar Arrays	Constant	2.7E-04	SEI Database
Chassis	Constant	4.7E-05	SEI Database
Thermal Control	Constant	5.7E-04	SEI Database
Feed Lines	Constant	1E-06	SEI Database
Thruster	Constant	0.1825	Estimated
Atlas V	Constant	0.01	Estimated
Deployment	Constant	0.001	Estimated
Batteries	Constant	0	Estimated
Reaction Wheel	Constant	.20	Estimated

Table 6.2: Probability of Failure of Components

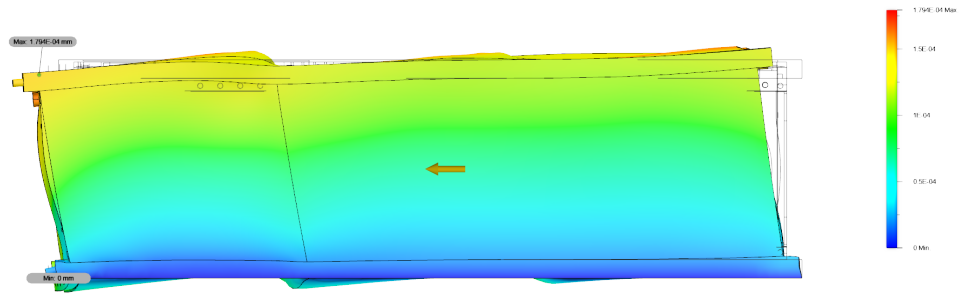


Figure 6.17: Major Axis Lateral Displacement Graphic Results

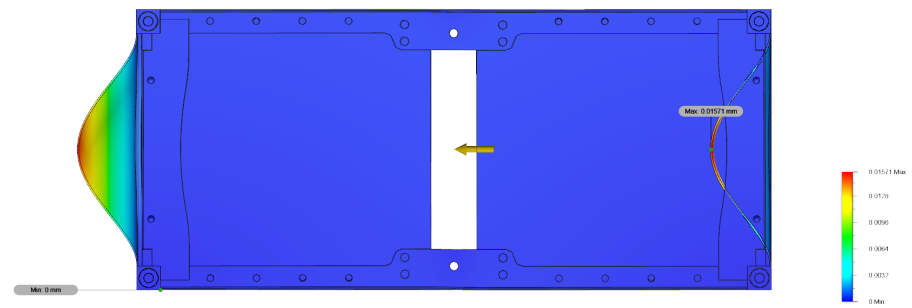


Figure 6.18: Minor Axis Lateral Displacement Graphic Results

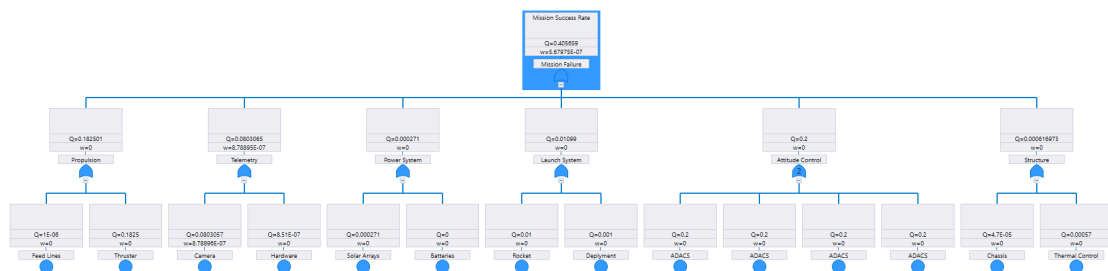


Figure 6.19: Failure Tree Analysis Model

Minimal Cut Set	Order	Unavailability	Contribution ?
ADACS	1	0.2	0.421323
Thruster	1	0.1825	0.384457
Camera	1	0.0803057	0.169173
Rocket	1	0.01	0.0210661
Deployment	1	0.001	0.00210661
Thermal Control	1	0.00057	0.00120077
Solar Arrays	1	0.000271	0.000570892
Chassis	1	4.7E-05	9.90108E-05
Feed Lines	1	1E-06	2.10661E-06
Hardware	1	8.51E-07	1.79273E-06
Batteries	1	0	0

Figure 6.20: Failure Tree Analysis Component Contributions. The reaction wheels were found to be the component most likely to be the cause of failure with a 42% certainty.

Variable	Value
Unavailability ?	0.405659
Availability ?	0.594341
Average Unavailability ?	0.380074
Unreliability ?	0.0803056
Reliability ?	0.919694
Unconditional Failure Intensity. Units [1/hour] ?	5.67975E-07
Average Unconditional Failure Intensity. Units [1/hour] ?	5.92425E-07
Conditional Failure Intensity. Units [1/hour] ?	9.55639E-07
Average Conditional Failure Intensity. Units [1/hour] ?	9.55639E-07
Expected Number of Failures ?	0.0518965
Total Down Time [hours] ?	33294.5
Probability of Failure on Demand (PFD) ?	0.405659
Average Probability of Failure on Demand (PFD Avg) ?	0.380074
Probability of Failure per Hour (PFH) ?	5.67975E-07
Average Probability of Failure per Hour (PFH Avg) ?	5.92425E-07

Figure 6.21: Failure Tree Analysis Results. The probability of mission success was found to be 92%.

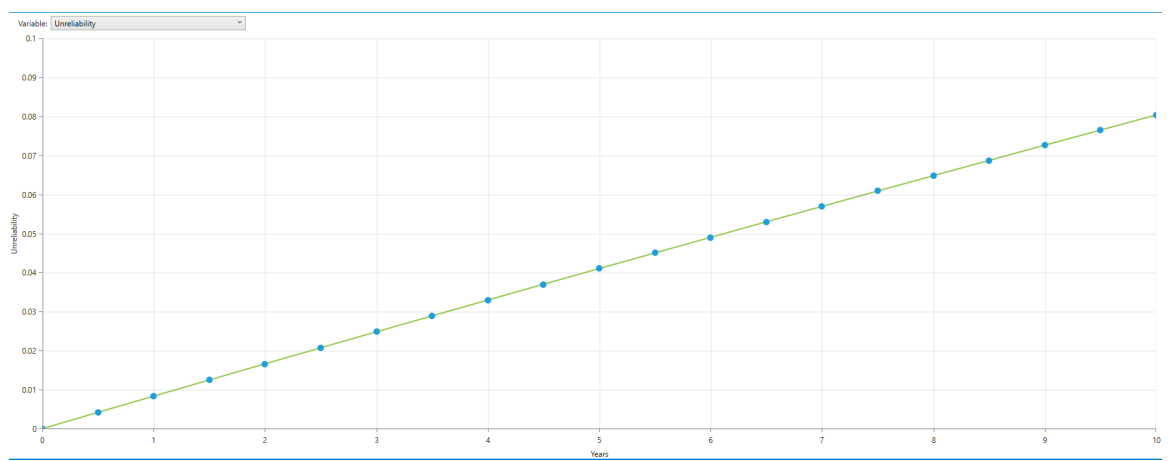


Figure 6.22: A plot of probability of Unreliability over a 10 year period. Notice that it begins near 0 at the beginning of the mission, and increases linearly to the predicted 8% for an overall reliability of 92%.

Chapter 7

Conclusions

Our design process has left a few open questions and several improvements to be made to the cubesat design. One issue with our design is the mass exceeding the dispenser mass capacity, even without added mass margins. Our total calculated mass is 13.3kg, 1.3 kg over the maximum 12 kg imposed by the 6U CSD dispenser. In the event that this cubesat were to actually be built, we would modify the commercially purchased chassis to eliminate external structural elements, instead using our radiation shielding to provide structure. A second geometric constraint imposed by the antenna restricts the rotation of our solar panel array from 360 degrees to 125 degrees. This restriction eliminates certain thrust vectors from being attainable at any given moment, but throughout the period of the orbit, these vectors will become attainable. Nevertheless, the restriction is less than ideal.

7.1 Potential Improvements

Both mass and volume constraints put on this project would be alleviated by upgrading from a densely packed 6U bus to a sparsely-packed 12U bus. The extra space would allow a reconfiguration of the spacecraft components such that the solar panels might attain a full 360 degree rotation. The pivot to a 12U bus would further allow upgrades to the imaging payload and allow for increased redundancy of spacecraft components, extending the expected lifespan of the cubesat. The primary issue with this upgrade would be the lack of 12U missions launched by the ESPA ring on the Atlas V launch platform, although the system has the capability.

The ability of our system to accomplish its primary mission to a commercially

viable spec is not assured. With the planned orbit and imager, the average image sent from the I-MISSED satellite to ground would provide an image of GOES-T represented by only 21 pixels across. This is astoundingly low resolution, ameliorated only by high contrast expected in space. There are a number of potential solutions to this problem. As it stands, the current imaging payload includes a 2/3" x 2/3" CMOS optical sensor and processor, which provides a low resolution image. This image sensor could be improved with something such as the 4/3", 8 megapixel ams AG CMV8000, which could be integrated into the system with no lens focal point adjustment [52]. However, if a telescoping mechanism is included, 1" - 22/16" sensors with 70 megapixel capabilities could theoretically be included. An upgrade from a 1.3 megapixel sensor would greatly improve imaging capability and increase the commercial viability of the system.

A second modification to the payload which would potentially improve our mission success and viability would be to remove the helical antenna and instead use the solar array as a reflect-array. A reflectarray, validated as a concept by the Integrated Solar Array and Reflectarray Antenna NASA cubesat mission, consists of a large solar array acting as a parabolic dish, and a small transmitter mounted near the middle of the chassis. On the back side of the solar array, a pattern of printed circuit boards was arranged and placed such that they collimated and reflected waves similar to how a parabolic dish would. Using this design, the ISARA mission achieved data transmission rates of up to 100 MBd from LEO [53]. Although a detailed quantitative analysis was not conducted to apply the reflectarray to I-MISSED cubesat, as STK analysis was inconclusive as to whether it would improve on the helical antenna, the reflectarray presents a unique potential solution to our communications problem which future designers of the I-MISSED mission should investigate, especially if success of a similar concept on the Mars Cube One mission moves the technology firmly to TRL 9.

A question which has not yet been addressed is the viability of the I-MISSED cubesat to be assembled and tested by the STP-3 launch date in June 2019. Typically, cubesat lifecycles include 1-2 years for building and testing, 1 year for deployment (including finding and integrating with a launch vehicle, establishing a ground system), and the remaining lifecycle is dedicated to operation and retirement. Because this mission expects a launch with the Air Force STP-3 mission aboard ULA's Atlas-V rocket, we can eliminate the time allotted to finding a launch vehicle. We can eliminate the remainder of the 1 year deployment cost because I-MISSED will communicate with pre-established ground stations, each part of the NASA Near Earth

Network. Since our system is compromised entirely of commercial off-the-shelf items, our assembly time should be relatively short compared to other custom-built cubesats. Given that we have just over 1 year to build, test, and integrate the cubesat, it would likely be a rush job, but feasible nonetheless.

7.2 Evaluating Success

In the opening chapter to this report, the following four criteria were presented for success of the mission:

- Design a cubesat that can operate in GEO through end-of-life
- Design a cubesat can inform mission operations for a larger subject satellite
- Design a cubesat can help with debris tracking in GEO
- Design a cubesat for GEO with a life-cycle on par with a larger subject satellite

The entirety of this white paper has shown that these specific goals were met, albeit with some caveats, and so we are satisfied.

This project has been a valuable exercise in systems engineering, and has been the first project of this scope that many of our team members have been a part of. We learned valuable knowledge through research of regulations and industry best-practices; we gained experience with industry-standard software tools such as STK, Spenvis, and Creo to aid design; we worked deeply on team dynamics and organization to expediently meet our goals; and gained a better appreciation of the interrelated and complicated nature of designing a vehicle for space.

Bibliography

- [1] Dan Leone, “Launch of GOES-R Satellite Delayed Six Months,” *SpaceNews*, 2015.
<http://spacenews.com/launch-of-goes-r-satellite-delayed-six-months/>.
- [2] B. R. Bhat, “Total Radiation Dose at Geostationary Orbit,” 2005.
- [3] M. Vuolo, “Shielding strategies for JUICE: material options,” 2016.
- [4] T. Wilcutt, “Process for Limiting Orbital Debris,” 2011.
- [5] NOAA & NASA, “Geostationary Operational Environmental Satellite - R Series A collaborative NOAA & NASA program,” <https://www.goes-r.gov/>.
- [6] “Atlas V Launch Services User’s Guide,” March 2010.
- [7] C. Bergin, “Free CubeSat rideshares offered by ULA for Atlas V launches,” <https://www.nasaspaceflight.com/2015/11/free-cubesat-rideshares-offered-ula-atlas-v-launches/>.
- [8] M. Di Carlo, M. Vasile, and S. Kemble, “Optimised GTO-GEO transfer using low-thrust propulsion,” *Optimised GTO-GEO Transfer Using Low-Thrust Propulsion*, Apr 2017.
https://strathprints.strath.ac.uk/62878/1/Di_Carlo_etalISTS_2017_Optimised_GTO_GEO_transfer_using_low_thrust_propulsion.pdf.
- [9] Bob Caffrey, “2nd Planetary CubeSat Science Symposium: Using Rideshare to Launch CubeSats ESPA S/C,” September 2017.
- [10] J. Ray, “Air Force selects Atlas 5 to launch multipurpose satellite to high orbit,” *Spaceflight Now — Falcon Launch Report — Successful launch for Falcon 1 rocket*, Jun 2017.

<https://spaceflightnow.com/2017/06/30/air-force-selects-atlas-5-to-launch-multipurpose-satellite-to-high-orbit/>.

- [11] P. Blau, “ULA Atlas V wins over SpaceX for Air Force STP-03 Launch Contract,” *LISA Pathfinder Spaceflight101*. <http://spaceflight101.com/ula-atlas-v-wins-over-spacex-for-air-force-stp-03-launch-contract/>.
- [12] C. P. S. The CubeSat Program, “6U CubeSat Design Specification Rev. PROVISIONAL,”
https://static1.squarespace.com/static/5418c831e4b0fa4ecac1bacd/t/573fa2fee321400346075f01/1463788288448/6U_CDS_2016-05-19_Provisional.pdf?fp=DevEx.LB.1,5494.1.
- [13] “Manual of Regulations and Procedures for Federal Radio Frequency Management (Redbook),” *A Nation Online: Entering the Broadband Age — National Telecommunications and Information Administration*.
<https://www.ntia.doc.gov/page/2011/manual-regulations-and-procedures-federal-radio-frequency-management-redbook>.
- [14] “47 cfr part 25 - satellite communications,” *LII / Legal Information Institute*.
<https://www.law.cornell.edu/cfr/text/47/part-25>.
- [15] W. J. Larson and J. R. Wertz, *Space Mission Analysis and Design*. El Segundo, California: Microcosm Press and Kluwer Academic Publishers, 1999.
- [16] I. A. of Geomagnetism and Aeronomy, “International Geomagnetic Reference Field,”
- [17] N. E. R. Council, “IGRF (12th Generation) Synthesis Form,”
- [18] A. M. Aerospace, “Self Contained ADACS Units for CubeSats and SmallSats,” 2018.
- [19] A. Marinan and K. Cahoy, “From CubeSats to Constellations: Systems Design and Performance Analysis,” Master’s thesis, Boston MA, 2013/09.
- [20] B. S. Propulsion and Systems, “BIT-3 RF Ion Thruster), publisher = Busek Co. Inc., year = 2018,” tech. rep.
- [21] J. Stuart, A. Dorsey, F. Alibay, and N. Filipe, “Formation flying and position determination for a space-based interferometer in GEO graveyard orbit,” in *Aerospace Conference, 2017 IEEE*, pp. 1–19, IEEE, 2017.

- [22] M. Mittnacht, E. Gottzein, M. Hartrampf, A. Konrad, P. Krauss, C. Kühl, D. Marareskoul, A. Grechkoseev, and E. Islentjev, “Commercial Use of GNSS Signals in GEO,” *IFAC Proceedings Volumes*, vol. 37, no. 6, pp. 1097–1102, 2004.
- [23] “Stare: Space-based telescopes for the actionable refinement of ephemeris,” <https://directory.eoportal.org/web/eoportal/satellite-missions/s/stare>.
- [24] P. S. Corporation, “Canisterized Satellite Dispenser (CSD) Data Sheet,” tech. rep., 2016.
- [25] D. May, “AMSAT Phase IV Propulsion and Attitude Control Systems Conceptual Design,” *The American Institute of Aeronautics and Astronautics*, 1989.
- [26] C. W. Rowley, *Introduction to Feedback Control*. Clarence W Rowley, 2016.
- [27] NOAA, “Frequently asked questions about noaa satellites and noaa satellite pictures and data,” <http://noaasis.noaa.gov/NOAASIS/ml/faqs.htmlfaq8>.
- [28] C. S. S. MacGillivray, “Miniature deployable high gain antenna for cubesats,” http://mstl.atl.calpoly.edu/bklofas/Presentations/DevelopersWorkshop2011/47_MacGillivray_Miniature_Antennas.pdf.
- [29] “Ground stations,” <https://www.hsl.hawaii.edu/facilities/ground-stations/UHM>.
- [30] H. S. F. Laboratory, “Ground stations,” <https://www.hsl.hawaii.edu/facilities/ground-stations/>.
- [31] M. C. Daniel Ochoa, Kenny Hummer, “Deployable helical antenna for nano-satellites,” http://www.northropgrumman.com/BusinessVentures/AstroAerospace/Documents/pageDocs/tech_papers/SmallSatDeployableHelical_ochoa_SSC14-IX-4.pdf.
- [32] B. University, “Bu-702: How to store batteries,” http://batteryuniversity.com/learn/article/how_to_store_batteries.
- [33] B. University, “Bu-107: Comparison table of secondary batteries,” http://batteryuniversity.com/learn/article/secondary_batteries.
- [34] GOMspace, “Nanopower bpx datasheet,” <https://gomspace.com/Shop/subsystems/batteries/nanopower-bpx.aspx>.

- [35] GOMspace, “Nanopower battery datasheet,”
<https://gomspace.com/Shop/subsystems/batteries/nanopower-bpx.aspx>.
- [36] “Cubesat design specification,” *California Polytechnic State University*.
https://static1.squarespace.com/static/5418c831e4b0fa4ecac1bacd/t/56e9b62337013b6c063a655a/1458157095454/cds_rev13_final2.pdf.
- [37] A. Devices, “Why use gallium arsenide solar cells?,”
<https://www.altadevices.com/use-gallium-arsenide-solar-cells/>.
- [38] E. McNaul, “Hawk solar array technology advanced deployable satellite power solution,”
<http://mstl.atl.calpoly.edu/~workshop/archive/2015/Spring/Day203/1200-McNaule-HaWK-High20Watts20per20Kilogram-Series20of20Solar20Arrays.pdf>.
- [39] M. Design, “ehawk solar array,”
<http://mmadesignllc.com/products/ehawk-solar-array/>.
- [40] GOMspace, “Nanopower p60 dock datasheet,”
<https://gomspace.com/Shop/subsystems/power-supplies/nanopower-p60.aspx>.
- [41] GOMspace, “Nanopower p60 acu-200 datasheet,”
<https://gomspace.com/Shop/subsystems/power-supplies/nanopower-p60.aspx>.
- [42] Leonics, “Basics of mppt solar charge controller,”
http://www.leonics.com/support/article2_14j/articles2_14j_en.php.
- [43] NASA, “Solar absorptance and thermal emittance of some common spacecraft thermal-control coatings,”
<https://ntrs.nasa.gov/archive/nasa/casi.ntrs.nasa.gov/19840015630.pdf>.
- [44] L. A. Gypen, M. Brabers, and A. Deruyttere, “Corrosion resistance of tantalum base alloys. elimination of hydrogen embrittlement in tantalum by substitutional alloying,”
- [45] NASA, “Cubesat form factor thermal control louvers,”
<https://technology.nasa.gov//t2media/tops/pdf/GSC-TOPS-40.pdf>.
- [46] R. K. B.E. Hardt and R. Eby, “Louvers,”
http://matthewturner.com/uah/IPT2008_summer/baselines/LOW

- [47] C. Resewski and W. Buchgraber, “Properties of new polyimide foams and polyimide foam filled honeycomb composites,”
<https://onlinelibrary.wiley.com/doi/pdf/10.1002/mawe.200390076>.
- [48] Andrew Kalman, “CANISTERIZED SATELLITE DISPENSER (CSD) DATA SHEET,”
- [49] Andrew Kalman, “PAYLOAD SPECIFICATION FOR 3U, 6U, 12U AND 27U,” 2016.
- [50] M. White, “Scaled CMOS Technology Reliability Users Guide - NASA,” *NASA Electronic Parts and Packaging*. https://nepp.nasa.gov/files/20273_09_102_5_JPL_White_Scaled_CMOS_Technology_Reliability_Users_Guide_1_10.pdf
- [51] “Forecast archive.”
- [52] Mouser Electronics, Inc, “CMV8000 Datasheet,”
<https://www.mouser.com/pdfdocs/cmv8000.pdf>.
- [53] “Integrated Solar Array and Reflectarray Antenna for High Bandwidth CubeSats,”
https://www.nasa.gov/sites/default/files/atoms/files/isara_fact_sheet-25apr2017-508-cumulos.pdf.
- [54] GOMspace, “Nanopower p60 pdu-200 datasheet,”
<https://gomspace.com/Shop/subsystems/power-supplies/nanopower-p60.aspx>.

Appendix A

Code

```
# Imports
import numpy as np

# SPACECRAFT
print '----- SPACECRAFT -----',
print

A_a = 10. * 20. * 1.e-4 # m^2 (Solar panel face)
A_b = 10. * 20. * 1.e-4 # m^2 (Adjacent face)
A_c = 20. * 20. * 1.e-4 # m^2 (North/south face)
A_sc = 2. * (A_b + A_c) + A_a # m^2 (Total spacecraft area)
A_sc_ex = A_sc - A_c # m^2 (Faces exposed to Earth/Sun)
Z = 35900.e3 # m (Altitude)
R_E = 6378.125e3 # m (Earth radius)

# Q_SUN -----
H_su_min = 1306. # W / m^2
H_su_max = 1400. # W / m^2
```

```

# Calculate average exposed area

beta = np.arccos(R_E / (R_E + Z)) # rad
PAS_avg = (1. / (2. * np.pi)) * ((A_b - A_a * np.sin(-np.pi / 2.)) + \
                                    (A_a * np.sin(beta) + A_b * np.cos(beta) - A_b))

Q_su_min = 2. * PAS_avg * H_su_min # W
Q_su_max = max(A_a, A_b) * H_su_max # W

print '----- Solar flux -----'
print 'Q_su_min =', Q_su_min, 'W'
print 'Q_su_max =', Q_su_max, 'W'
print

# Q_ET -----
H_et_min = 208. # W / m^2
H_et_max = 224. # W / m^2

Z_over_R_E = Z / R_E # Helps with looking up F
F_et = (4. * (10.**(-3.)) + 0.03) / 5. # From Fig. 5 in Thermal Notes
Q_et_min = F_et * A_sc_ex * H_et_min # W
Q_et_max = F_et * A_sc_ex * H_et_max # W

print '----- Earth Thermal Flux -----'
print 'Q_et_min =', Q_et_min, 'W'
print 'Q_et_max =', Q_et_max, 'W'
print

# Q_ER -----

```

```

eta_start = np.pi / 2. # rad
cos_eta_avg = 1. / np.pi * np.sin(eta_start)

a = 0.36 # Earth's albedo
F_er = F_et * cos_eta_avg
Q_er_min = a * F_er * A_sc_ex * H_su_min # W
Q_er_max = a * F_er * A_sc_ex * H_su_max # W

print '----- Earth Albedo Flux -----'
print 'Q_er_min =', Q_er_min, 'W'
print 'Q_er_max =', Q_er_max, 'W'
print

# Q_INT -----
P_acds = 7.23 + 0.088 + 0.05 # W
P_imager = 0.175 # W
P_comm = 4. # W
P_thermal = 1.5 # W
P_battery = 12. # W

P_frac_dis = 0.5 # Fraction of power dissipated

Q_sc_min = (P_acds + P_battery + P_thermal) * P_frac_dis # W (Standby in darkness)
Q_sc_av = (P_acds + P_comm + P_thermal) * P_frac_dis # W (Bus in daylight)

print '----- Internal Heat (Bus) -----'
print 'Q_int (Darkness) =', Q_sc_min, 'W'
print 'Q_int (Sunlight) =', Q_sc_av, 'W'

```

```

print

# T_SC ----

def get_T_sc(Q_int, Q_su, Q_er, Q_et):
    return ((Q_int + alpha_su * Q_su + alpha_su * Q_er + epsilon_ir * Q_et) / \
            (A_sc * sigma * epsilon_ir))**0.25 # K

sigma = 5.67e-8 # W / m^2 K^4 Stefan Boltzmann's constant
alpha_su = 0.766 # Titanium (6AL-4V) (Thermal Notes)
epsilon_ir = 0.472

alpha_su = 0.85
epsilon_ir = 0.56 # Iron Oxide (NASA PDF)

T_sc_min = get_T_sc(Q_sc_min, Q_su_min, Q_er_min, Q_et_min) # K
T_sc_av_cold = get_T_sc(Q_sc_av, Q_su_min, Q_er_min, Q_et_min) # K
T_sc_av_hot = get_T_sc(Q_sc_av, Q_su_max, Q_er_max, Q_et_max) # K

print '----- Temperatures (Passive Thermal Control) -----'
print 'Standby Temperature, Dark =', T_sc_min - 273.15, 'C'
print 'Average Temperature, Cold =', T_sc_av_cold - 273.15, 'C'
print 'Average Temperature, Hot =', T_sc_av_hot - 273.15, 'C'
print

# SPACECRAFT
print '----- THRUSTER -----',
print

A_a = 10. * 20. * 1.e-4 # m^2 (Solar panel face)

```

```

A_b = 10. * 10. * 1.e-4 # m^2 (Adjacent face)
A_c = 20. * 10. * 1.e-4 # m^2 (North/south face)
A_sc = 2. * (A_b + A_c) + A_a # m^2 (Total spacecraft area)
A_sc_ex = A_sc - A_c # m^2 (Faces exposed to Earth/Sun)

# Q_SUN -----
# Calculate average exposed area
beta = np.arccos(R_E / (R_E + Z)) # rad
PAS_avg = (1. / (2. * np.pi)) * ((A_b - A_a * np.sin(-np.pi / 2.)) + \
                                     (A_a * np.sin(beta) + A_b * np.cos(beta) - A_b))

Q_su_min = 2. * PAS_avg * H_su_min # W
Q_su_max = max(A_a, A_b) * H_su_max # W

print '----- Solar flux -----'
print 'Q_su_min =', Q_su_min, 'W'
print 'Q_su_max =', Q_su_max, 'W'
print

# Q_ET -----
Q_et_min = F_et * A_sc_ex * H_et_min # W
Q_et_max = F_et * A_sc_ex * H_et_max # W

print '----- Earth Thermal Flux -----'
print 'Q_et_min =', Q_et_min, 'W'
print 'Q_et_max =', Q_et_max, 'W'
print

```

```

# Q_ER -----
Q_er_min = a * F_er * A_sc_ex * H_su_min # W
Q_er_max = a * F_er * A_sc_ex * H_su_max # W

print '----- Earth Albedo Flux -----'
print 'Q_er_min =', Q_er_min, 'W'
print 'Q_er_max =', Q_er_max, 'W'
print

# Q_INT -----
P_thermal = 0. # W
P_thrust = 56. # W

Q_th_min = (P_thermal) * P_frac_dis # W
Q_th_max = (P_thermal + P_thrust) * P_frac_dis # W (Thrust)

print '----- Internal Heat (Bus) -----'
print 'Q_int (Thrust Off) = ', Q_th_min, 'W'
print 'Q_int (Thrust On) = ', Q_th_max, 'W'
print

# T_SC -----
def get_T_sc(Q_int, Q_su, Q_er, Q_et):
    return ((Q_int + alpha_su * Q_su + alpha_su * Q_er + epsilon_ir * Q_et) / \
            (A_sc * sigma * epsilon_ir))**0.25 # K

alpha_su = 0.975 # Black paint (Thermal Notes)

```

```

epsilon_ir = 0.874

T_th_min = get_T_sc(Q_th_min, Q_su_min, Q_er_min, Q_et_min) # K
T_th_max = get_T_sc(Q_th_max, Q_su_max, Q_er_max, Q_et_max) # K

print '----- Temperatures (Passive Thermal Control) -----'
print 'Thrust Temperature, Off =', T_th_min - 273.15, 'C'
print 'Thrust Temperature, Hot =', T_th_max - 273.15, 'C'
print

# Calculate temperature at high heat considering louver implementation
louver = 2. # Factor by which louver dissipates heat (Works up to factor of 2)
Q_sc_av = Q_sc_av / louver # W
T_th_dis = get_T_sc(Q_sc_av, Q_su_max, Q_er_max, Q_et_max) # K

print '----- Temperatures (Active Thermal Control) -----'
print 'Thrust Temperature, Hot =', T_th_dis - 273.15, 'C' # Louver
print

# Calculate thickness of insulator needed

def get_Q(Q_int, Q_su, Q_er, Q_et):
    return Q_int + alpha_su * Q_su + alpha_su * Q_er + epsilon_ir * Q_et

kappa_foam = 0.09 # W / m K (HD Polyimide foam)
A_wall = 20. * 10. * 1.e-4 # m^2
delta_x = -kappa_foam * A_wall * (T_th_max - T_sc_av_hot) / \
          (get_Q(Q_th_max, Q_su_max, Q_er_max, Q_et_max) -
           get_Q(Q_sc_av, Q_su_max, Q_er_max, Q_et_max)) #
delta_x = abs(delta_x) # m

```

```

delta_x = 4.1e-3 # m

rho_foam = 35. # kg / m^3
V_wall = A_wall * delta_x # m^3
m_wall = rho_foam * V_wall # kg

print '----- Insulation (HD Polyimide Foam) -----'
print 'Thickness of Wall =', delta_x * 1000., 'mm'
print 'Insulator Mass = ', m_wall, 'kg'
print

# SOLAR PANELS

print '----- SOLAR PANEL -----',
print

A_panel = 60. * 60. * 1.e-4 # m^2 (Fully deployed wing)
A_array = 2. * A_panel # m^2 (Both fully deployed wings)
A_sc = 2. * A_array # m^2 (Total Solar Array area)
A_sc_ex = A_array / (np.pi/2) # m^2 (Solar Array Faces exposed to Earth/Sun)

# Q_SUN -----

# Calculate average exposed area
beta = np.arccos(R_E / (R_E + Z)) # rad
PAS_avg = (1. / (2. * np.pi)) * (A_array * ((np.pi/2) + beta))

Q_su_min = 2. * PAS_avg * H_su_min # W
Q_su_max = A_array * H_su_max # W

print '----- Solar flux -----',

```

```

print 'Q_su_min =', Q_su_min, 'W'
print 'Q_su_max =', Q_su_max, 'W'
print

# Q_ET -----
H_et_min = 208. # W / m^2
H_et_max = 224. # W / m^2

Z_over_R_E = Z / R_E # Helps with looking up F
F_et = (4. * (10.**(-3.)) + 0.03) / 5. # From Fig. 5 in Thermal Notes

Q_et_min = F_et * A_sc_ex * H_et_min # W
Q_et_max = F_et * A_sc_ex * H_et_max # W

print '----- Earth Thermal Flux -----'
print 'Q_et_min =', Q_et_min, 'W'
print 'Q_et_max =', Q_et_max, 'W'
print

# Q_ER -----
eta_start = np.pi / 2. # rad
cos_eta_avg = 1. / np.pi * np.sin(eta_start)

a = 0.36 # Earth's albedo
F_er = F_et * cos_eta_avg
Q_er_min = a * F_er * A_sc_ex * H_su_min # W
Q_er_max = a * F_er * A_sc_ex * H_su_max # W

```

```

print '----- Earth Albedo Flux -----'
print 'Q_er_min =', Q_er_min, 'W'
print 'Q_er_max =', Q_er_max, 'W'
print

# Q_INT -----
P_min = 0. # Not generating any power
P_av = 17.038 # Minimum Power Generated by Solar Arrays
P_max = 97.3 # Maximum Power Generated by Solar Arrays

P_frac_dis = 0.5 # Fraction of power dissipated

Q_int_min = (P_min) * P_frac_dis # W (Darkness)
Q_int_av_cold = (P_av) * P_frac_dis # W (Bent solar array)
Q_int_max = (P_max) * P_frac_dis # W (Unfolded)

print '----- Internal Heat (Bus) -----'
print 'Q_int (Darkness) =', Q_int_min, 'W'
print 'Q_int (Sunlight) =', Q_int_max, 'W'
print

# T_SC -----
def get_T_sc(Q_int, Q_su, Q_er, Q_et):
    return ((Q_int + alpha_su * Q_su + alpha_su * Q_er + epsilon_ir * Q_et) / \
            (A_sc * sigma * epsilon_ir))**0.25 # K

sigma = 5.67e-8 # W / m^2 K^4 Stefan Boltzmann's constant
alpha_su = 0.4 # Indium Oxide/Kapton/Aluminum (Thermal Notes)
epsilon_ir = 0.71

```

```

alpha_su = .24
epsilon_ir = .43 # Teflon Gold Backing 0.5 mil (NASA PDF)

T_sa_min = get_T_sc(Q_int_min, Q_su_min, Q_er_min, Q_et_min) # K
T_sa_av_cold = get_T_sc(Q_int_av_cold, Q_su_min, Q_er_min, Q_et_min) # K
T_sa_av_hot = get_T_sc(Q_int_av_cold, Q_su_max, Q_er_max, Q_et_max) # K
T_sa_max = get_T_sc(Q_int_max, Q_su_max, Q_er_max, Q_et_max) # K

print '----- Temperatures (Passive Thermal Control) -----'
print 'Standby Temperature, Dark =', T_sa_min - 273.15, 'C'
print 'Average Temperature, Cold (Folded) =', T_sa_av_cold - 273.15, 'C'
print 'Average Temperature, Hot (Folded) =', T_sa_av_hot - 273.15, 'C'
print 'Peak Temperature, Hot (Unfolded) =', T_sa_max - 273.15, 'C'
print

thickness = 0.5 * 0.000127 # m
V_gold = thickness * A_array # m^3
rho_gold = 2200. # kg / m^3
m_gold = rho_gold * V_gold # kg

print '----- TEFLON GOLD -----'
print 'Mass =', m_gold, 'kg'

# OUTPUT -----
----- SPACECRAFT -----

----- Solar flux -----

```

Q_su_min = 17.7876491955 W

Q_su_max = 28.0 W

----- Earth Thermal Flux -----

Q_et_min = 0.14144 W

Q_et_max = 0.15232 W

----- Earth Albedo Flux -----

Q_er_min = 0.10176647174 W

Q_er_max = 0.109091164193 W

----- Internal Heat (Bus) -----

Q_int (Darkness) = 10.434 W

Q_int (Sunlight) = 6.434 W

----- Temperatures (Passive Thermal Control) -----

Standby Temperature, Dark = 2.64705508564 C

Average Temperature, Cold = -8.7653575386 C

Average Temperature, Hot = 14.4484627402 C

----- THRUSTER -----

----- Solar flux -----

Q_su_min = 17.1605003715 W

Q_su_max = 28.0 W

----- Earth Thermal Flux -----

Q_et_min = 0.084864 W

Q_et_max = 0.091392 W

----- Earth Albedo Flux -----

Q_er_min = 0.061059883044 W

Q_er_max = 0.0654546985157 W

----- Internal Heat (Bus) -----

Q_int (Thrust Off) = 0.0 W

Q_int (Thrust On) = 28.0 W

----- Temperatures (Passive Thermal Control) -----

Thrust Temperature, Off = -17.7612836287 C

Thrust Temperature, Hot = 70.7379210931 C

----- Temperatures (Active Thermal Control) -----

Thrust Temperature, Hot = 23.4009904697 C

----- Insulation (HD Polyimide Foam) -----

Thickness of Wall = 4.1 mm

Insulator Mass = 0.00287 kg

----- SOLAR PANEL -----

----- Solar flux -----

Q_su_min = 894.992226433 W

Q_su_max = 1008.0 W

----- Earth Thermal Flux -----

Q_et_min = 0.648313204346 W

Q_et_max = 0.698183450835 W

----- Earth Albedo Flux -----

```
Q_er_min = 0.466463146131 W
```

```
Q_er_max = 0.500037063234 W
```

```
----- Internal Heat (Bus) -----
```

```
Q_int (Darkness) = 0.0 W
```

```
Q_int (Sunlight) = 48.65 W
```

```
----- Temperatures (Passive Thermal Control) -----
```

```
Standby Temperature, Dark = 6.65240600803 C
```

```
Average Temperature, Cold (Folded) = 9.3814571083 C
```

```
Average Temperature, Hot (Folded) = 17.5894862065 C
```

```
Peak Temperature, Hot (Unfolded) = 28.5783372475 C
```

```
----- TEFLON GOLD -----
```

```
Mass = 0.100584 kg
```

Code for Orbit Determination (GNC)

```
X = 0.00001452;
```

```
Sat_size = 0.0061;
```

```
Pixels = [10:100];
```

```
D = Sat_size./(Pixels*2*X);
```

```
figure
```

```
plot(Pixels,D,'LineWidth', 2)
```

```
set(gcf,'color','white')
```

```
title('Distance of GOES-T as function of Change in Pixels in Imager')
```

```
xlabel('Number of pixels')
```

```
ylabel('Distance from GOES-T (km)')
```

Code for Control Simulation (GNC)

```
% %%%%%%%% MAE 342 %%%%%%%%
% Purpose: Simulate attitude control controller for cubesat
% %%%%%%%%
%
% % reaction wheel model
%
% R = 22; % ohms
%
% s = tf('s');
%
% K = 10;
%
% G_rw = 1/(1+s*(R/K));
%
% %stepplot(G_rw)
%
%
% % cubesat model
%
Ixx = 2.54*10^6;
Iyy = 4.30*10^6;
Izz = 4.202*10^6;
gcm2kgm2 = 10^(-7);
Ixx = gcm2kgm2*Ixx;
Iyy = gcm2kgm2*Iyy;
Izz = gcm2kgm2*Izz;
%
%
% % TF from torque to theta
%
G_CS_x = 1/(Ixx*s^2);
```

```

% G_cs_y = 1/(Iyy*s^2);
% G_cs_z = 1/(Izz*s^2);
% figure(1)
% impulse(G_cs_x)
% kp = 1;
% ki = 10;
% kd = 10;
% P = G_rw*G_cs_x;
% C = kp + ki/s +kd*s;
% G_er = 1/(1+P*C);
% figure(2)
% impulse(G_er)

```

```

%%
A = [0 1; 0 0];
B = [0; 1/Ixx];
C = eye(2);
D = [0; 0];
Q = [1 0; 0 1];
R = 0.1;

K = lqr(A, B, Q, R);
sys_sol = ss(A, B, C, D);

```

```

sys_cl = ss(A-B*K,B,C,D);
x0 = [deg2rad(-0.00984);0];
[y,t,x] = initial(sys_cl,x0);
[yol,tol,xol] = initial(sys_ol,x0);
figure(3)
plot(t,y,'LineWidth', 2);
title('Closed Loop Initial Condition Response')
xlabel('Time (s)')
ylabel('Angle (rad)/Angular Velocity (rad/s)')
set(gcf,'color','white')
legend('Angle','Angular Velocity')

figure(4)
plot(tol,yol,'LineWidth', 2);
title('Open Loop Initial Condition Response')
xlabel('Time (s)')
set(gcf,'color','white')
ylabel('Angle (rad)/Angular Velocity (rad/s)')

figure(5)
plot(t,-K*x,'LineWidth', 2);
title('Control Effort for Initial Condition Response')
xlabel('Time (s)')
ylabel('Torque (N*m)')

```

```

hold on

torque_lim_min = 0.000635;

plot(t,torque_lim_min*ones(size(t)), 'b--', 'HandleVisibility', 'off')
set(gcf, 'color', 'white')

hold off


figure(6)

step(0.000635*sys_cl)

ylabel('Angular velocity (rad/s)           Angle (rad)')
title('Step response to maximum torque of reaction wheel')
set(gcf, 'color', 'white')


% %% reaction wheel and cubesat together

% Krw = 2.5;

% full_loop_tf = (Krw/R*Ixx)/(s^2*(s+Krw/R));
% [num,den] = tfdata(full_loop_tf);
% [Afull,Bfull,Cfull,Dfull]=tf2ss([0 0 0 2.5],[1 2.5 0 0]);
%

```

Appendix B

Simulation Results

B.1 Frequency Analysis

Summary

Frequency	Participation X	Participation Y	Participation Z
Mode 1: 281.1 Hz	0	5.05850017	0.0003
Mode 2: 295.3 Hz	0	4.77240011	0.0003
Mode 3: 392.5 Hz	0.180099998	0	0
Mode 4: 393.9 Hz	0.173500006	0	0
Mode 5: 572.9 Hz	0	0.0008	0.0008
Mode 6: 584.9 Hz	0	0.0014	0.0025
Mode 7: 592.4 Hz	0.0008	0	0.0001
Mode 8: 627.3 Hz	0.043099999	0	0

Figure B.1: Modal Frequency Analysis Results

Study Report

Simulation Model 2:1

Study 1 - Modal Frequencies

Study Properties

Study Type	Modal Frequencies
Last Modification Date	2018-05-07, 03:20:02

Load Case1

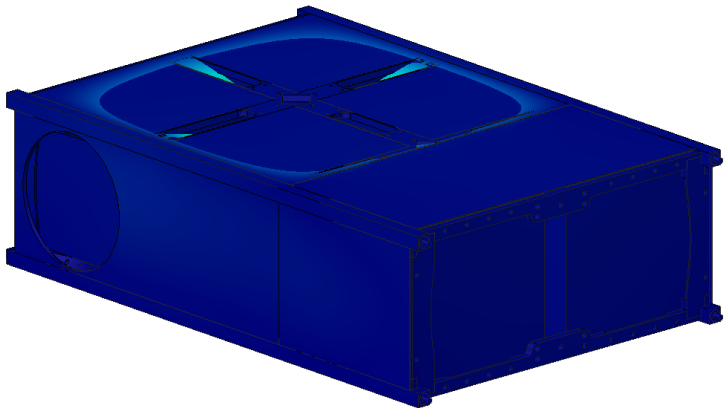
Results

Result Summary

Frequency	Participation X	Participation Y	Participation Z
Mode 1: 281.1 Hz	0	5.05850017	0.0003
Mode 2: 295.3 Hz	0	4.77240011	0.0003
Mode 3: 392.5 Hz	0.180099998	0	0
Mode 4: 393.9 Hz	0.173500006	0	0
Mode 5: 572.9 Hz	0	0.0008	0.0008
Mode 6: 584.9 Hz	0	0.0014	0.0025
Mode 7: 592.4 Hz	0.0008	0	0.0001
Mode 8: 627.3 Hz	0.043099999	0	0

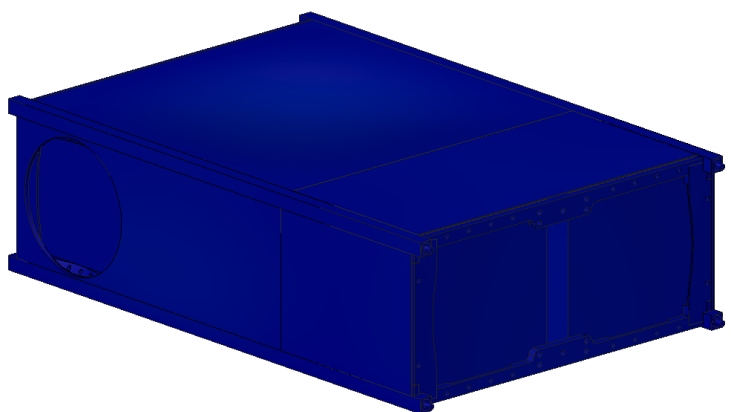
Total Modal Displacement

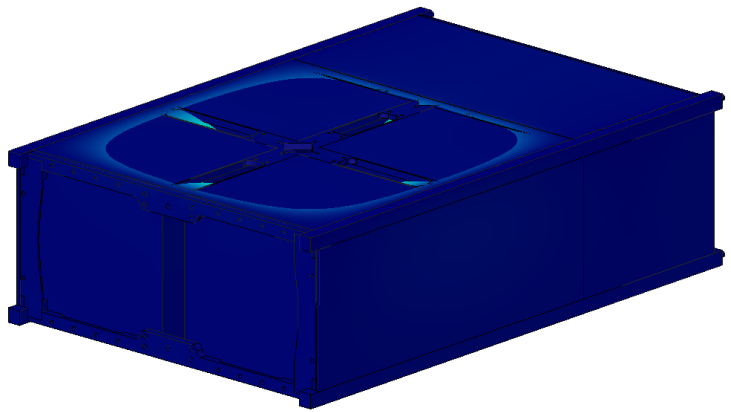
Mode 1: 281.1 Hz Total Modal Displacement
0  1



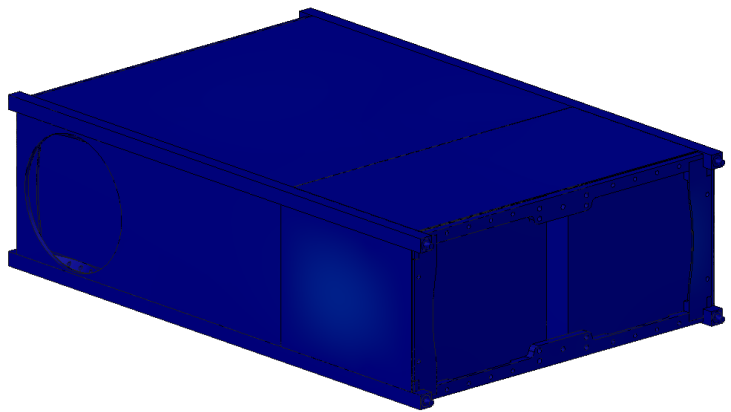


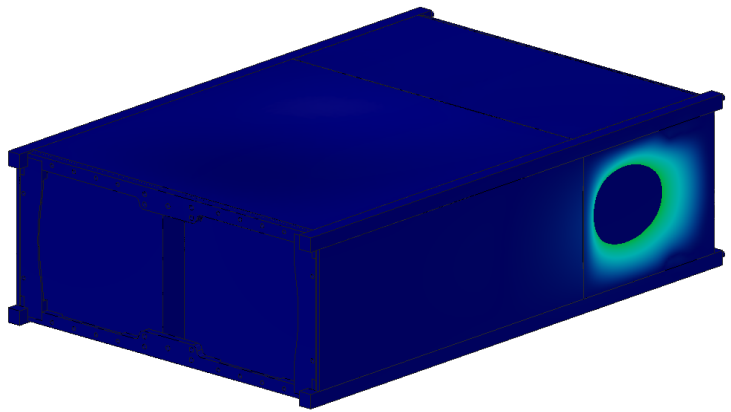
Mode 2: 295.3 Hz Total Modal Displacement
0 1



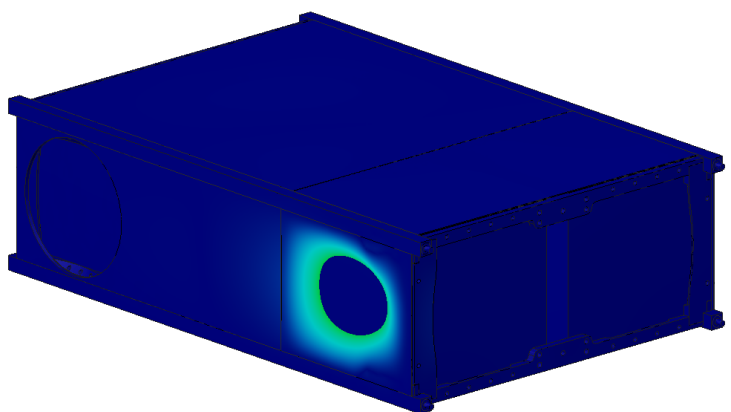


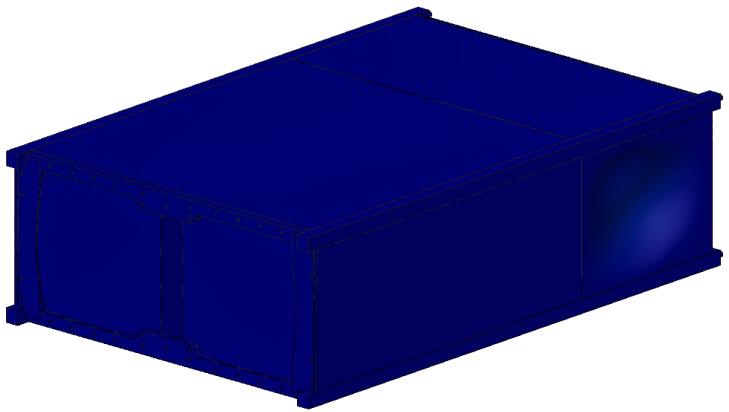
Mode 3: 392.5 Hz Total Modal Displacement
0 1



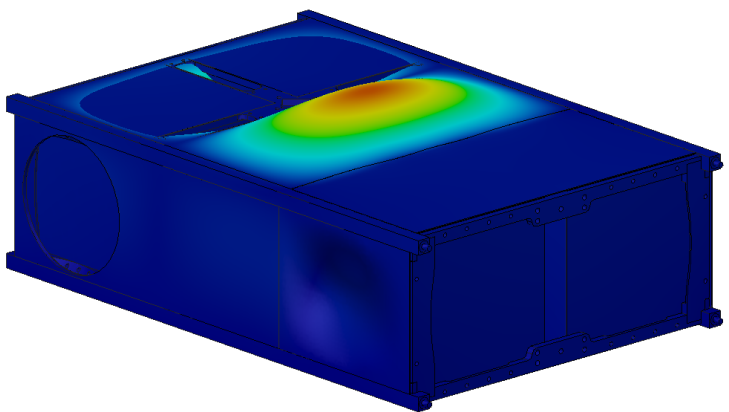


Mode 4: 393.9 Hz Total Modal Displacement
0 1



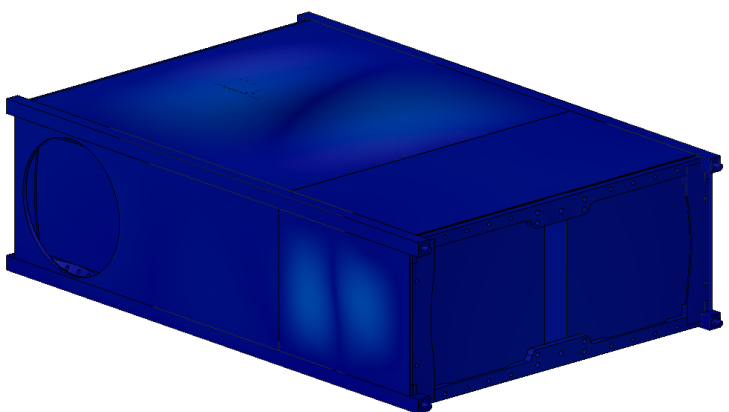


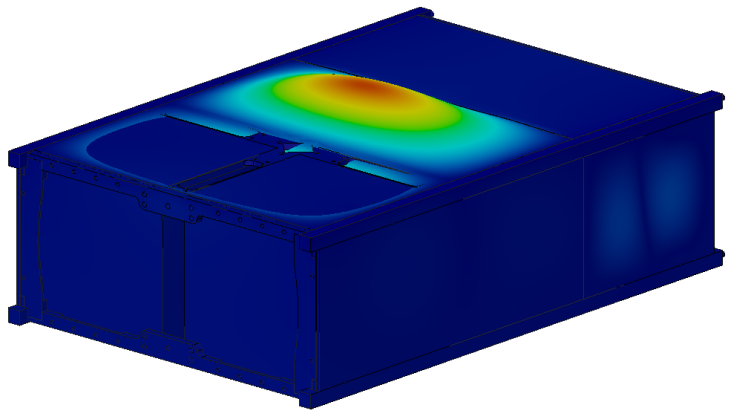
Mode 5: 572.9 Hz Total Modal Displacement
0 1



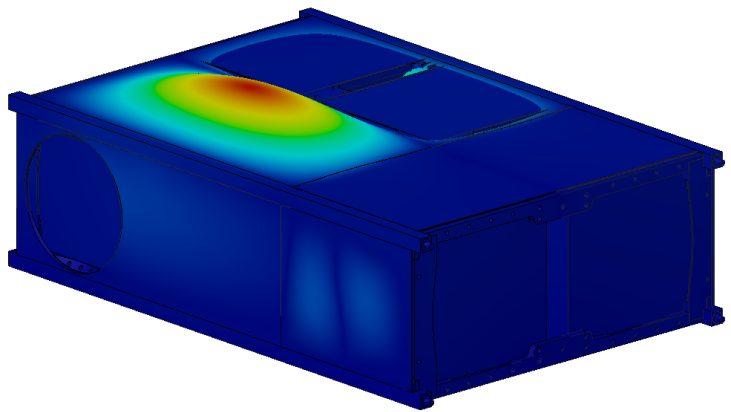


Mode 6: 584.9 Hz Total Modal Displacement
0 1



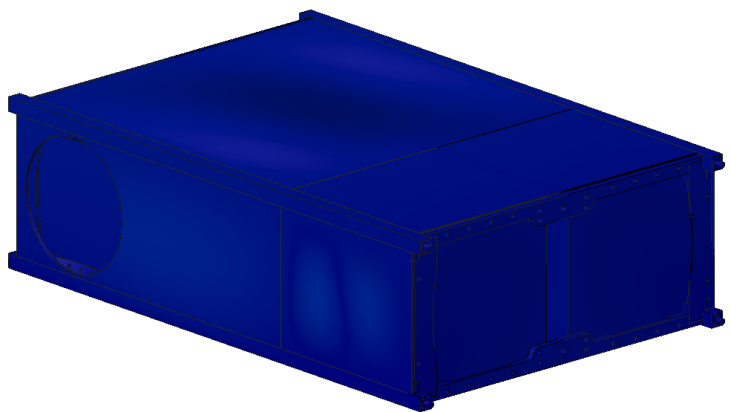


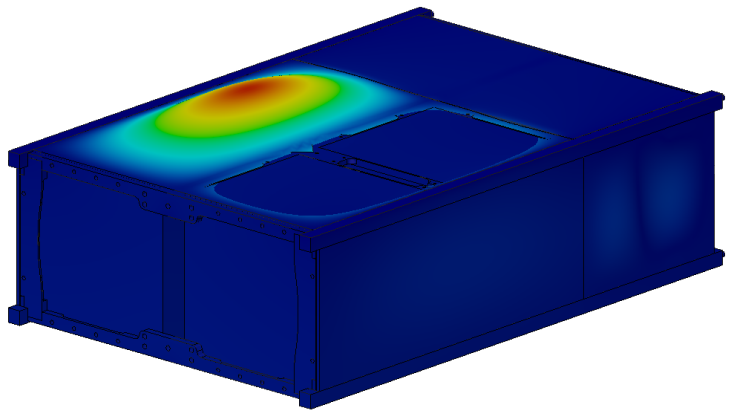
Mode 7: 592.4 Hz Total Modal Displacement
0 1





Mode 8: 627.3 Hz Total Modal Displacement
0 1





B.2 Stress Analysis

Summary

Name	Minimum	Maximum
Safety Factor		
Safety Factor (Per Body)	12.17	15
Stress		
Von Mises	4.28E-05 MPa	45.86 MPa
1st Principal	-9.476 MPa	54.14 MPa
3rd Principal	-47.28 MPa	6.362 MPa
Normal XX	-17.78 MPa	20.47 MPa
Normal YY	-13.88 MPa	16.73 MPa
Normal ZZ	-40.15 MPa	46.88 MPa
Shear XY	-5.804 MPa	5.876 MPa
Shear YZ	-5.397 MPa	25.96 MPa
Shear ZX	-3.658 MPa	4.746 MPa
Displacement		
Total	0 mm	0.05327 mm
X	-0.001023 mm	0.001023 mm
Y	-0.05327 mm	1.079E-04 mm
Z	-0.001306 mm	0.001083 mm

Figure B.2: Axial Static Stress Analysis Results

Study Report

Simulation Model 2:1

Static Stress

Study Properties

Study Type	Static Stress
Last Modification Date	2018-05-07, 04:06:17

Load Case1

Loads

Gravity

Type	Gravity
Magnitude	98.07 m / s^2
X Value	0 m / s^2
Y Value	-98.07 m / s^2
Z Value	0 m / s^2

Results

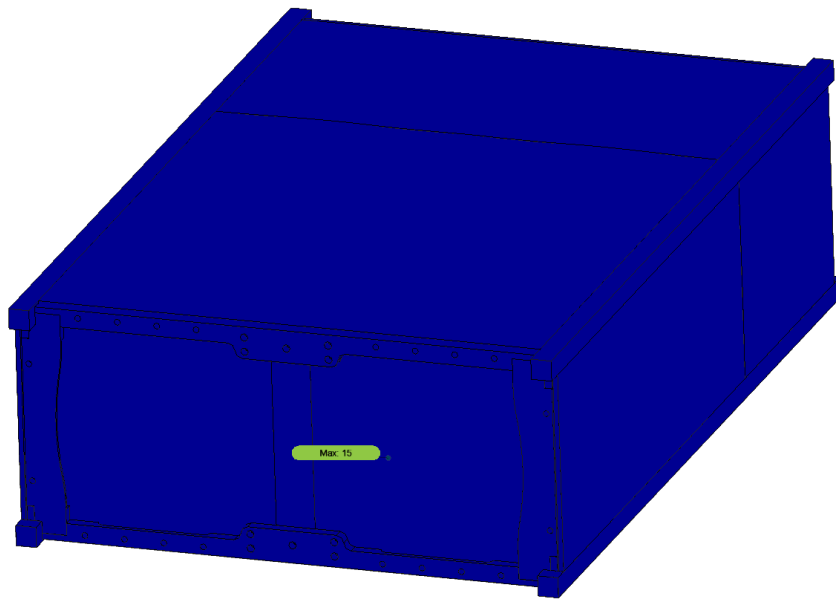
Result Summary

Name	Minimum	Maximum
Safety Factor		
Safety Factor (Per Body)	12.17	15
Stress		
Von Mises	4.28E-05 MPa	45.86 MPa
1st Principal	-9.476 MPa	54.14 MPa
3rd Principal	-47.28 MPa	6.362 MPa
Normal XX	-17.78 MPa	20.47 MPa
Normal YY	-13.88 MPa	16.73 MPa
Normal ZZ	-40.15 MPa	46.88 MPa
Shear XY	-5.804 MPa	5.876 MPa
Shear YZ	-5.397 MPa	25.96 MPa
Shear ZX	-3.658 MPa	4.746 MPa
Displacement		
Total	0 mm	0.05327 mm
X	-0.001023 mm	0.001023 mm
Y	-0.05327 mm	1.079E-04 mm
Z	-0.001306 mm	0.001083 mm
Reaction Force		
Total	0 N	34.11 N
X	-30.64 N	21.5 N
Y	-4.8 N	18.36 N
Z	-3.568 N	2.501 N
Strain		
Equivalent	1.01E-09	4.347E-04
1st Principal	-1.364E-06	3.99E-04
3rd Principal	-4.002E-04	2.305E-07
Normal XX	-1.476E-04	1.253E-04
Normal YY	-9.114E-05	9.587E-05
Normal ZZ	-1.699E-04	1.938E-04
Shear XY	-2.153E-04	2.18E-04
Shear YZ	-1.988E-04	3.74E-04
Shear ZX	-7.484E-05	1.761E-04
Contact Pressure		
Total	0 MPa	50 MPa
X	-15.04 MPa	14.43 MPa
Y	-11.85 MPa	18.54 MPa
Z	-40.05 MPa	46.88 MPa

Safety Factor

Safety Factor (Per Body)

0  8

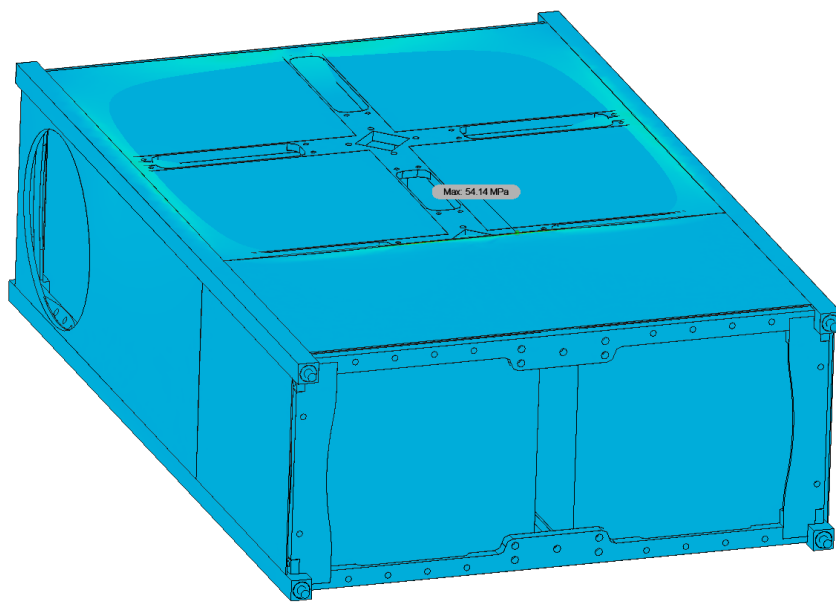


■ Stress

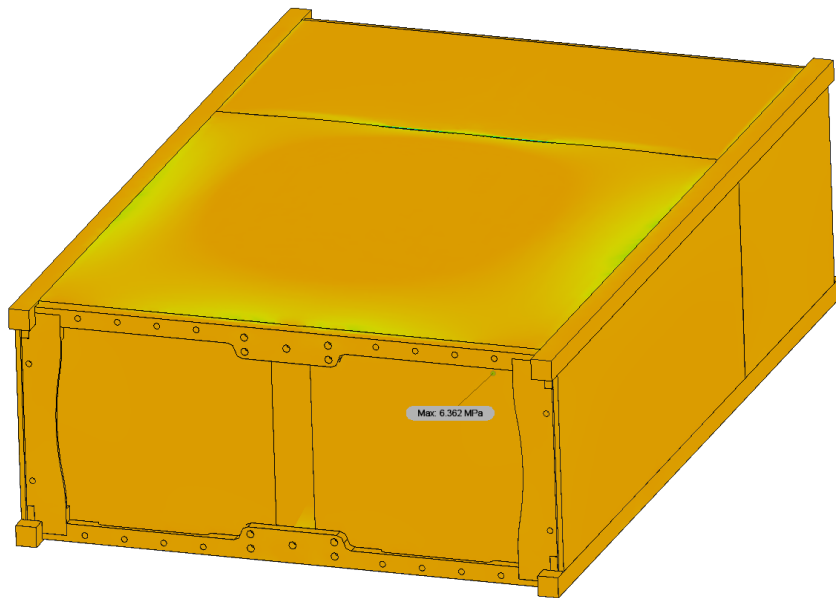
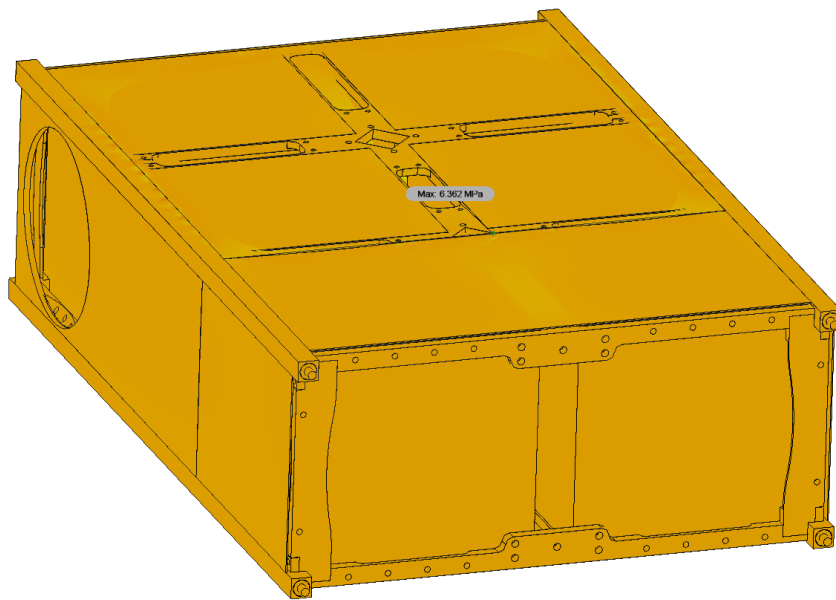
■ Von Mises
[MPa] 0 45.86



■ 1st Principal
[MPa] -9.48 54.14

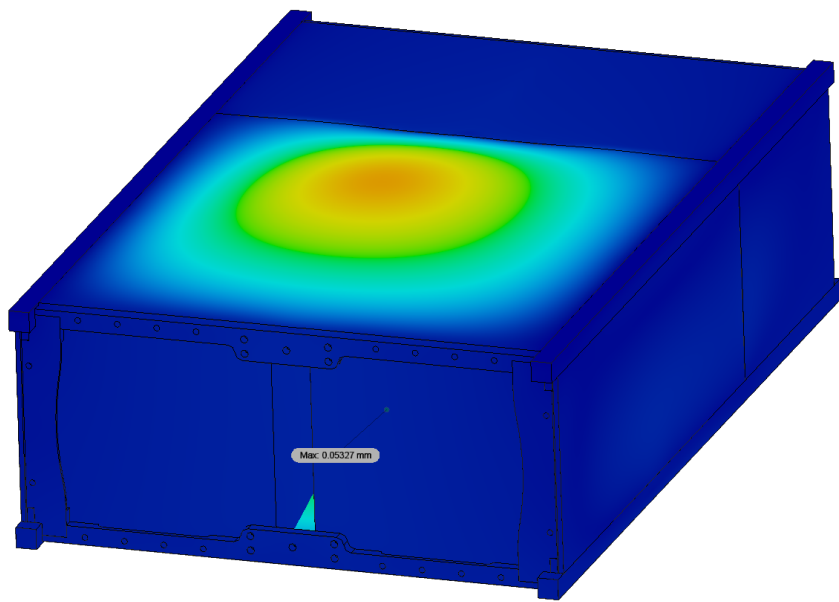


3rd Principal
[MPa] -47.28 6.36



Displacement

Total
[mm] 0  0.05327



Study Report

■ Simulation Model 2:1

■ Static Stress

■ Study Properties

Study Type	Static Stress
Last Modification Date	2018-05-12, 14:48:25

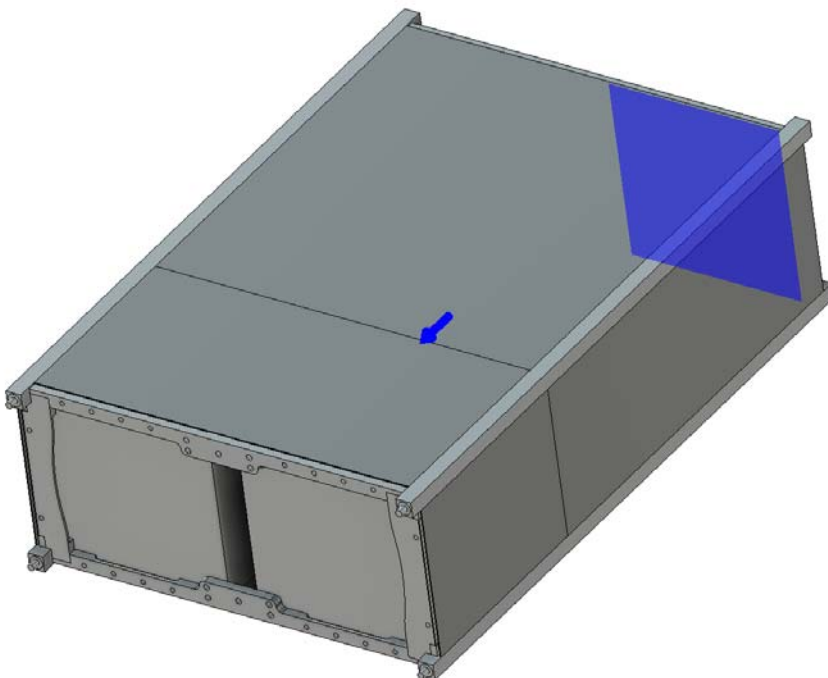
■ Load Case1

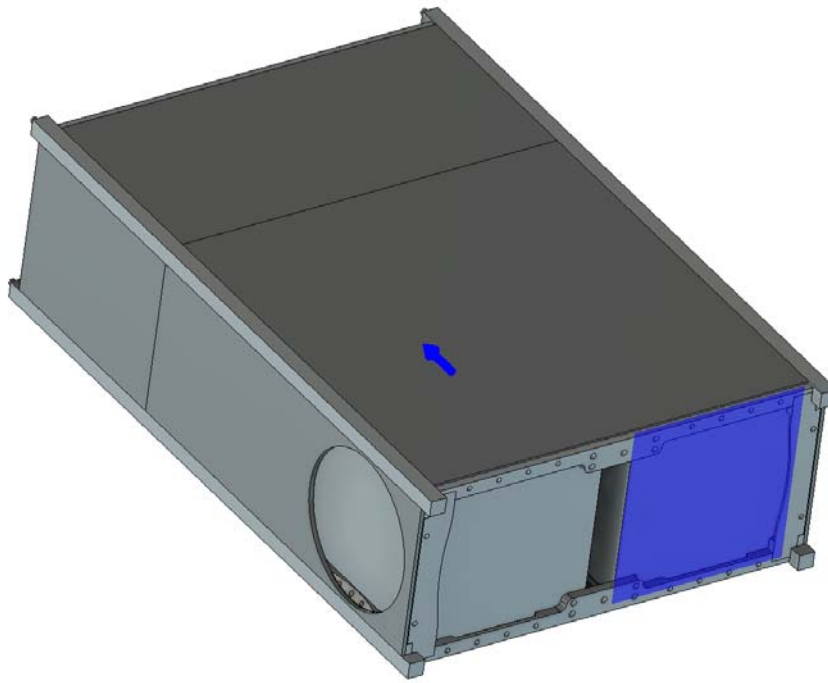
■ Loads

■ Gravity

Type	Gravity
Magnitude	29.43 m / s ²
X Value	0 m / s ²
Y Value	-0 m / s ²
Z Value	-29.43 m / s ²

■ Selected Entities





Results

Result Summary

Name	Minimum	Maximum
Safety Factor		
Safety Factor (Per Body)	15	15
Stress		
Von Mises	1.742E-05 MPa	2.669 MPa
1st Principal	-1.705 MPa	3.751 MPa
3rd Principal	-4.019 MPa	1.761 MPa
Normal XX	-3.293 MPa	2.09 MPa
Normal YY	-1.782 MPa	1.812 MPa
Normal ZZ	-3.615 MPa	3.602 MPa
Shear XY	-1.074 MPa	1.046 MPa
Shear YZ	-0.7062 MPa	0.3947 MPa
Shear ZX	-0.7428 MPa	0.6578 MPa
Displacement		
Total	0 mm	1.794E-04 mm
X	-4.269E-05 mm	4.954E-05 mm
Y	-6.278E-05 mm	5.685E-05 mm
Z	-1.713E-04 mm	2.479E-07 mm
Reaction Force		
Ttotal	0 N	4.506 N
X	-2.343 N	2.631 N
Y	-2.752 N	3.102 N
Z	-0.1766 N	2.773 N
Strain		
Equivalent	2.78E-10	3.591E-05
1st Principal	-1.264E-08	4.307E-05
3rd Principal	-3.797E-05	2.341E-08
Normal XX	-1.144E-05	8.395E-06
Normal YY	-7.798E-06	4.637E-06
Normal ZZ	-3.435E-05	3.367E-05
Shear XY	-2.141E-05	1.774E-05
Shear YZ	-2.057E-05	1.464E-05
Shear ZX	-1.535E-05	1.592E-05
Contact Pressure		
Total	0 MPa	3.498 MPa
X	-2.741 MPa	3.293 MPa
Y	-1.812 MPa	0.9162 MPa
Z	-1.677 MPa	1.9 MPa

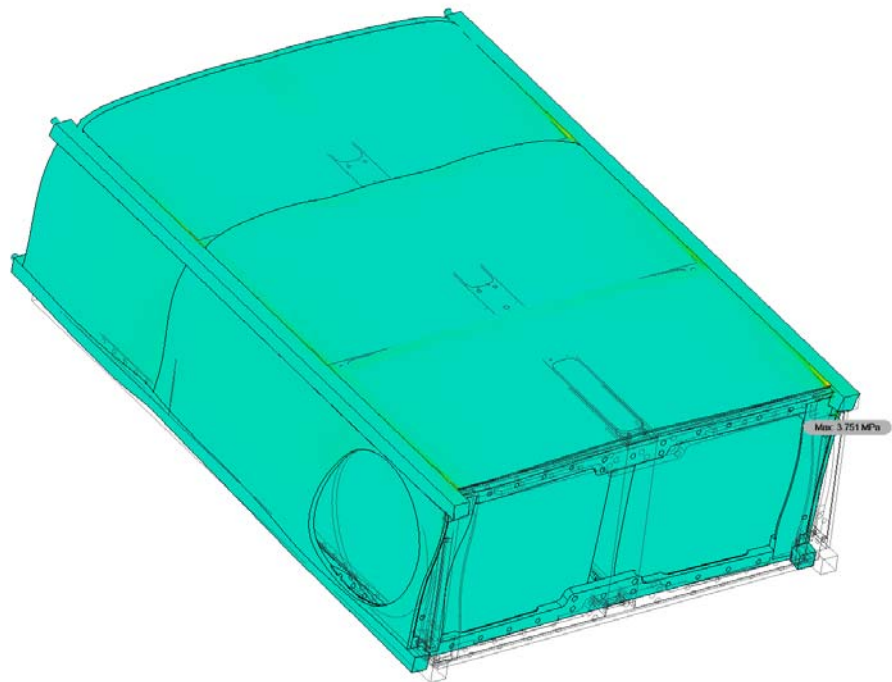
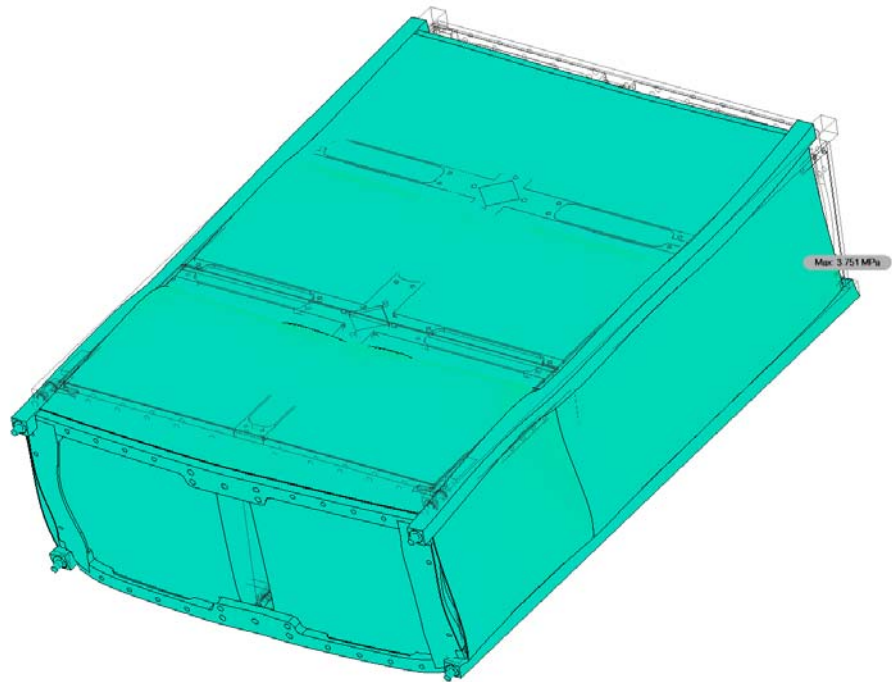
Stress

Von Mises

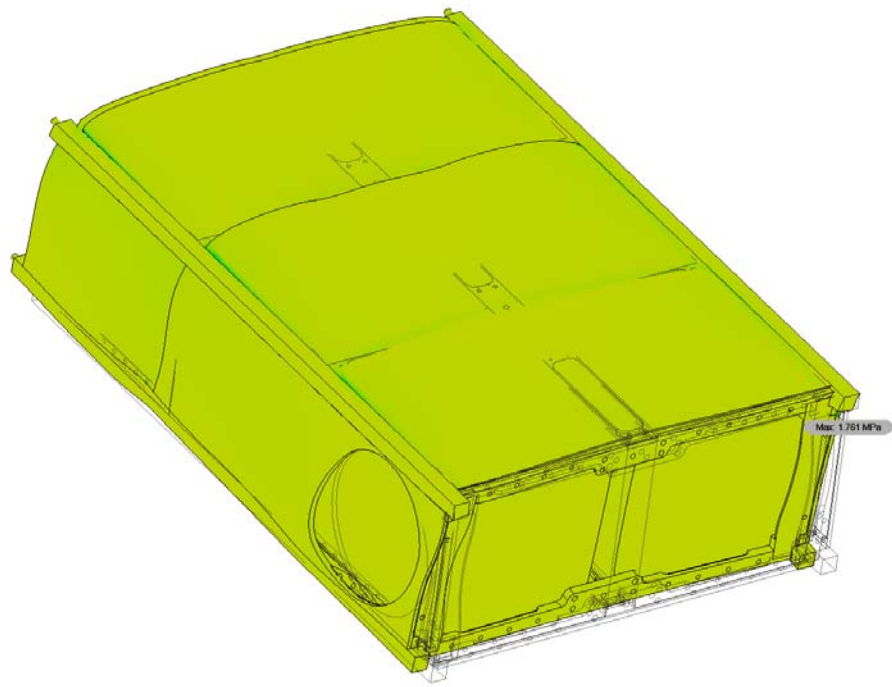
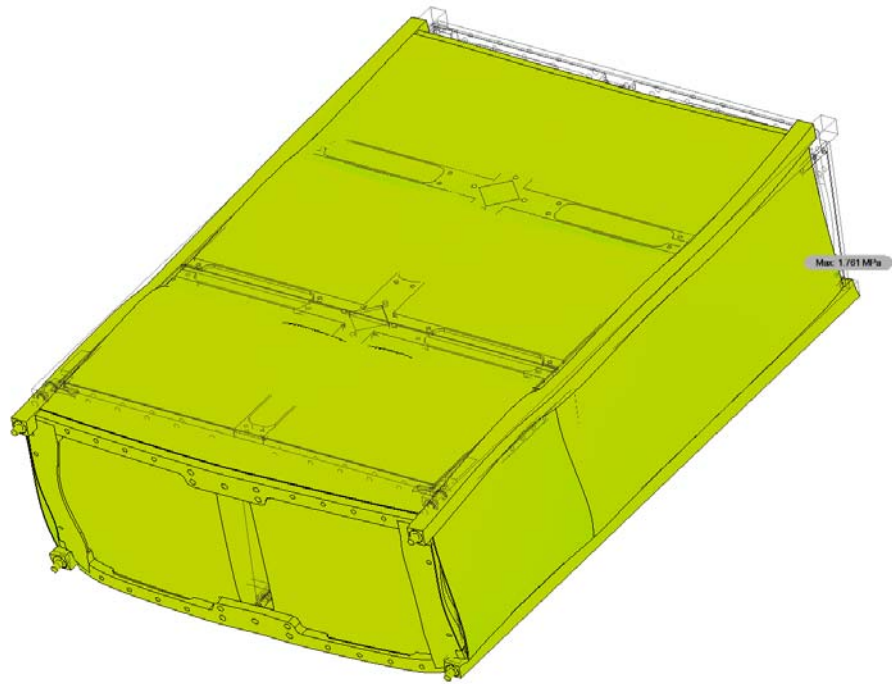
[MPa] 0 2.669



■ 1st Principal
[MPa] -1.705 3.751

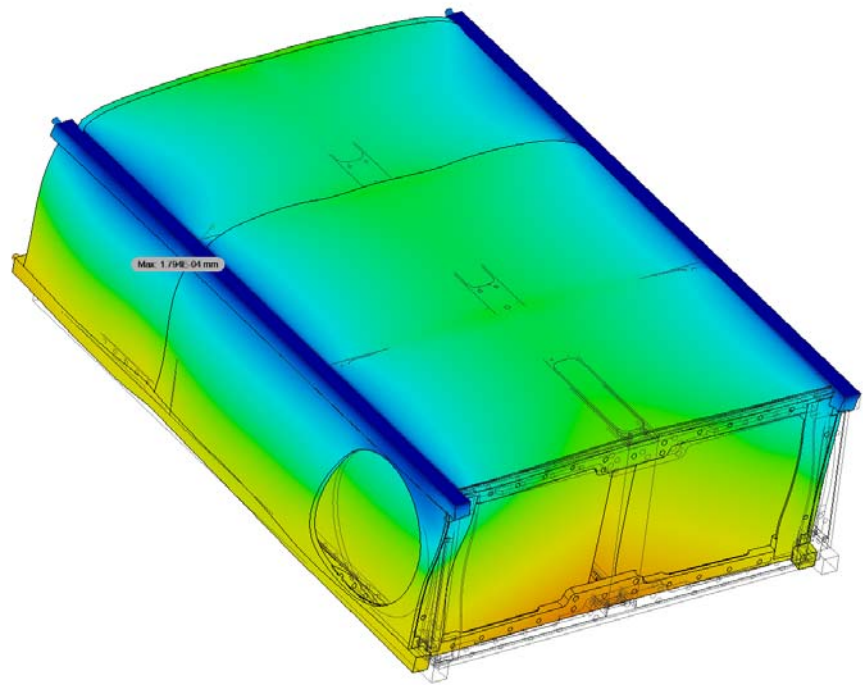
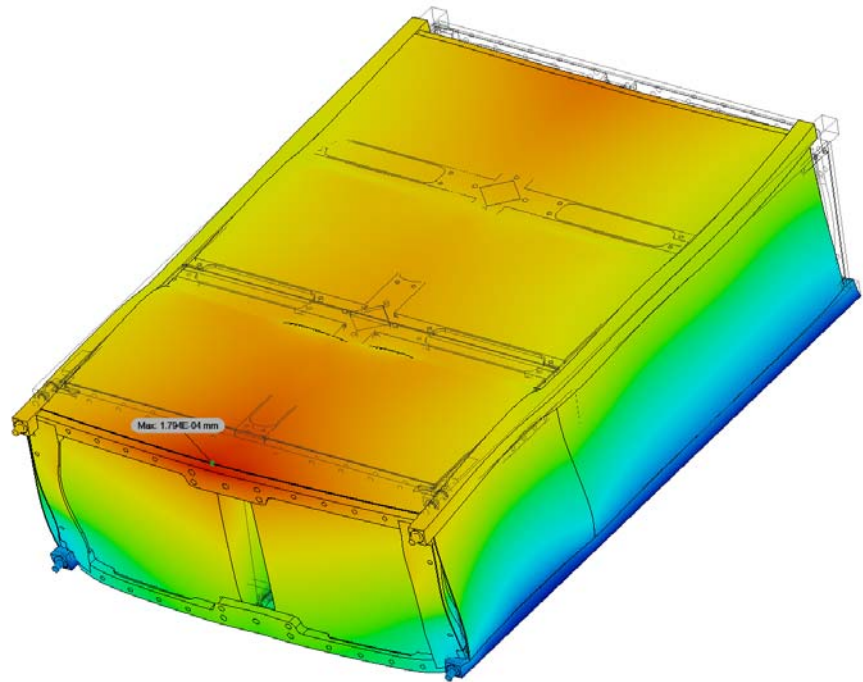


■ 3rd Principal
[MPa] -4.019 1.761



Displacement

Total
[mm] 0
1.794E-04



Study Report

□ Simulation Model 2:1

□ Static Stress

□ Study Properties

Study Type	Static Stress
Last Modification Date	2018-05-12, 15:48:40

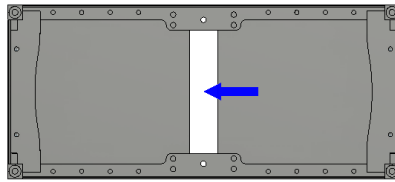
□ Load Case1

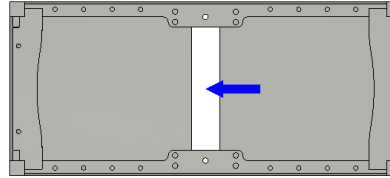
□ Loads

□ Gravity

Type	Gravity
Magnitude	29.43 m / s ²
X Value	29.43 m / s ²
Y Value	-0 m / s ²
Z Value	-0 m / s ²

□ Selected Entities





Results

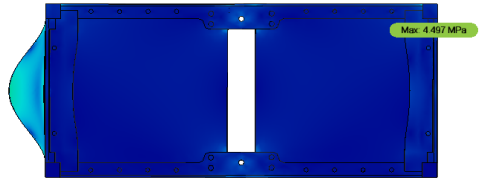
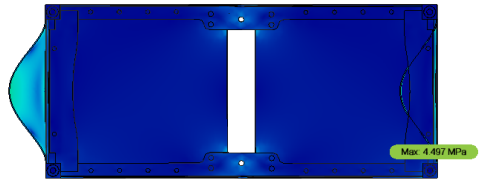
Result Summary

Name	Minimum	Maximum
Safety Factor		
Safety Factor (Per Body)	15	15
Stress		
Von Mises		
Von Mises	1.89E-05 MPa	4.497 MPa
1st Principal	-1.957 MPa	4.29 MPa
3rd Principal	-3.988 MPa	2.051 MPa
Normal XX	-1.973 MPa	2.06 MPa
Normal YY	-3.986 MPa	4.282 MPa
Normal ZZ	-2.175 MPa	2.303 MPa
Shear XY	-0.9346 MPa	1.174 MPa
Shear YZ	-0.4179 MPa	0.7579 MPa
Shear ZX	-2.484 MPa	1.61 MPa
Displacement		
Total	0 mm	0.01571 mm
X	-6.294E-06 mm	0.01571 mm
Y	-1.493E-04 mm	1.501E-04 mm
Z	-9.13E-05 mm	9.129E-05 mm
Reaction Force		
Total	0 N	3.899 N
X	-3.838 N	0.5556 N
Y	-1.451 N	1.459 N
Z	-0.511 N	0.5326 N
Strain		
Equivalent		
Equivalent	3.043E-10	1.111E-04
1st Principal	-1.259E-07	9.395E-05
3rd Principal	-9.852E-05	1.183E-07
Normal XX	-8.542E-06	8.054E-06
Normal YY	-1.606E-05	1.614E-05
Normal ZZ	-1.76E-05	1.602E-05
Shear XY	-1.347E-05	1.692E-05
Shear YZ	-1.451E-05	2.729E-05
Shear ZX	-9.217E-05	5.974E-05
Contact Pressure		
Total	0 MPa	3.93 MPa
X	-1.08 MPa	1.234 MPa
Y	-3.929 MPa	3.897 MPa
Z	-2.175 MPa	2.184 MPa

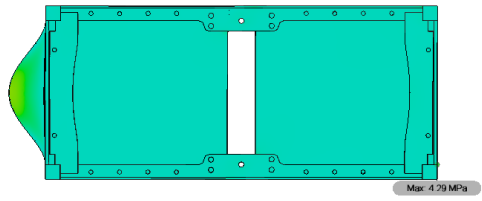
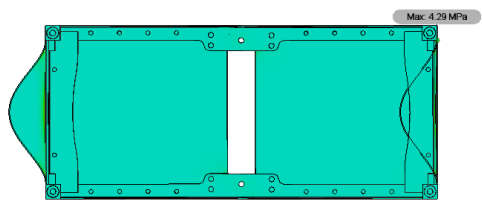
Stress

Von Mises

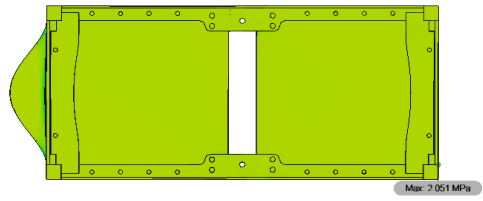
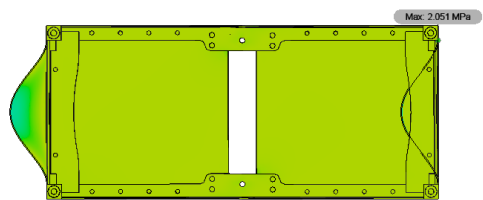
[MPa] 0 4.497



◻ 1st Principal
[MPa] -1.957 4.29

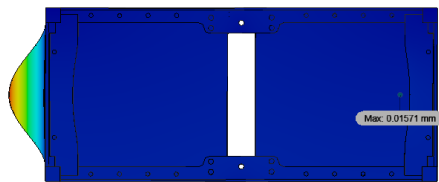
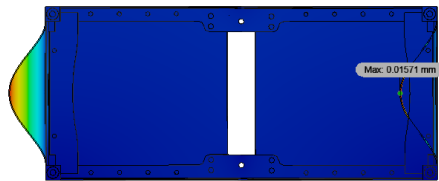


3rd Principal
[MPa] -3.988 2.051



Displacement

Total
[mm] 0  0.01571



Name	Minimum	Maximum
Safety Factor		
Safety Factor (Per Body)	15	15
Stress		
Von Mises	1.742E-05 MPa	2.669 MPa
1st Principal	-1.705 MPa	3.751 MPa
3rd Principal	-4.019 MPa	1.761 MPa
Normal XX	-3.293 MPa	2.09 MPa
Normal YY	-1.782 MPa	1.812 MPa
Normal ZZ	-3.615 MPa	3.602 MPa
Shear XY	-1.074 MPa	1.046 MPa
Shear YZ	-0.7062 MPa	0.3947 MPa
Shear ZX	-0.7428 MPa	0.6578 MPa
Displacement		
Total	0 mm	1.794E-04 mm
X	-4.269E-05 mm	4.954E-05 mm
Y	-6.278E-05 mm	5.685E-05 mm
Z	-1.713E-04 mm	2.479E-07 mm

Figure B.3: Lateral Static Stress Analysis Results

Name	Minimum	Maximum
Safety Factor		
Safety Factor (Per Body)	15	15
Stress		
Von Mises	1.89E-05 MPa	4.497 MPa
1st Principal	-1.957 MPa	4.29 MPa
3rd Principal	-3.988 MPa	2.051 MPa
Normal XX	-1.973 MPa	2.06 MPa
Normal YY	-3.986 MPa	4.282 MPa
Normal ZZ	-2.175 MPa	2.303 MPa
Shear XY	-0.9346 MPa	1.174 MPa
Shear YZ	-0.4179 MPa	0.7579 MPa
Shear ZX	-2.484 MPa	1.61 MPa
Displacement		
Total	0 mm	0.01571 mm
X	-6.294E-06 mm	0.01571 mm
Y	-1.493E-04 mm	1.501E-04 mm
Z	-9.13E-05 mm	9.129E-05 mm

Figure B.4: Lateral Static Stress Analysis Results